

DELETING OBSERVATIONS FROM A LEAST SQUARES SOLUTION

Charles A. Hall
Technical Services Division, Data Analysis Directorate,
White Sands Missile Range, New Mexico

ABSTRACT. In this paper we give a matrix treatment of the classical least squares theory and determine each observation's contribution to the least squares solution. If each observation's (or observer's) contribution is known, then it may be possible to delete certain observations (or observers), (1) to improve the least squares solution or (2) to minimize the number of observations (or observers) entering the least squares solution. It should be emphasized that redundancy is necessary to obtain a statistically sound least squares solution, however it may be advantageously limited without significantly changing the solution.

Although we present a general least squares theory for uncorrelated observations, special emphasis is given to the least squares missile position problem generated by a set of observed azimuths, elevations and slant ranges from a system of missile tracking systems such as Radar. The above treatment is used to develop a geometric ordering of available tracking stations, which is then combined with station ability and reliability to determine pre-flight minimal station participation. That is, given an approximate trajectory and n available tracking stations we predict the minimum station combination for an adequate coverage of a flight along this trajectory.

1.0 INTRODUCTION. In this paper we give a matrix treatment of the classical least squares theory and determine each observation's contribution to the least squares solution. If each observation's (or observer's) contribution is known, then it may be possible to delete certain observations (or observers), (1) to improve the least squares solution or (2) to minimize the number of observations (or observers) entering a least squares solution. It should be emphasized that redundancy is necessary to obtain a statistically sound least squares solution, however it may be advantageously limited.

The following procedure has been applied successfully in [4, 5, 6] to the following problem:

GIVEN: An approximate missile trajectory and the co-ordinates of n tracking stations (Cinetheodolite, Radars or Dovap receivers) along with various other pre-flight data;

DETERMINE: The best minimal station combination (how many? and which ones?) for an adequate coverage of a flight along this trajectory.

We will use the n-station radar position solution presented in [5] as an example of the general theory which follows.

2.0 LEAST SQUARES THEORY. A brief outline of a least squares method following the notation of D. Brown [1] will now be given. The model under consideration is assumed to be non-linear. There are obvious simplifications if the model is linear.

Let $\{X_i\}$ be a set of random variates ($i = 1, 2, \dots, q$)

$\{X_i^o\}$ be a set of uncorrelated observations of the set $\{X_i\}$,

For example: $\{A_i^o, E_i^o, R_i^o\}$, the set of azimuth, elevation and range readings from a system of n radar stations to a missile ($i = 1, 2, \dots, n$).

Let $\{Y_j\}$ be a set of variates (parameters) dependent on the X_i ,

$$Y_j = Y_j(X_1, X_2, \dots, X_q), \quad (j = 1, 2, \dots, p).$$

We note that the explicit form the for Y_j as functions of the X_i may not exist, in which case only an implicit form for this dependence is available.

For example: (x, y, z) , the missile co-ordinates are dependent on A_i^o, E_i^o, R_i^o .

If the set $\{X_i\}$ is such that not all the X_i are necessary to determine the entire set of $\{X_i\}$, or what is of more importance here and in [5], to determine the derived set $\{Y_j\}$, then the set $\{X_i\}$ is said to be over-determined. A least squares solution is in order. We need to find $\{Y'_j\}$ a set of approximations to $\{Y_j\}$ such that the sum of the squares of the residuals of the observed set $\{X_i^o\}$ is a minimum.

For example: In the n-station radar case [5], each radar determines a missile position $(x(j), y(j), z(j))$, ($j = 1, 2, \dots, n$). These points will coincide with probability zero. We use the least squares method below to determine the "true" missile position.

We have $X_i' = X_i^0 + \gamma_i$ ($i = 1, 2, \dots, q$)

$$Y_j' = Y_j^0 + \delta_j \quad (j = 1, 2, \dots, p)$$

where $\{Y_j^0\}$ is a first approximation to $\{Y_j\}$, $\{X_i'\}$ and $\{Y_j'\}$ are least squares approximations and the γ_i and δ_j are undetermined residuals.

Suppose the minimum number of $\{X_i\}$ required to determine the entire set of $\{X_i\}$ is q_0 , then the number of independent conditional equations relating the $\{X_i\}$ and $\{Y_j\}$ is $m = (q - q_0) + p$. Let these m equations be given by

$$(2.1) \quad f_i(X_1, \dots, X_q, Y_1, \dots, Y_p) = 0 \quad (i = 1, 2, \dots, m).$$

For example: In the radar case if 3 observations are known (azimuth, elevation and range readings from one station) then the others can be determined, thus $m = (3m - 3) + 3 = 3m$. In this example

$$f_{3i-2} = A_i - \tan^{-1} \left[\frac{y - y_i}{x - x_i} \right] = 0$$

$$f_{3i-1} = E_i - \tan^{-1} \left[\frac{z - z_i}{[(x - x_i)^2 + (y - y_i)^2]^{1/2}} \right] = 0$$

$$f_{3i} = R_i - \sqrt{(x - x_i)^2 + (y - y_i)^2 + (z - z_i)^2} = 0$$

($i = 1, 2, \dots, n$). Note that here (x_i, y_i, z_i) are the co-ordinates of the i^{th} radar station.

Assume that the f_i can be expanded in a Taylor series about the point $t = (X_1^0, X_2^0, \dots, X_n^0, Y_1^0, \dots, Y_p^0)$. Approximate the f_i by the constant and linear terms of these Taylor expansions and replace X_i by $X_i^0 + \gamma_i$. Equation (2.1) becomes (in matrix notation)

$$(2.2) \quad AV + BD + E = 0 \quad \text{where}$$

A is the m by q matrix (A_{ij}) with $A_{ij} = [\partial f_i / \partial X_j](t)$,

B is the m by p matrix (B_{ik}) with $B_{ik} = [\partial f_i / \partial Y_k](t)$,

E is the m by 1 matrix E_i with $E_i = f_i(t)$

$$V = (\gamma_1, \gamma_2, \dots, \gamma_q)^t \quad \text{and} \quad D = (\delta_1, \delta_2, \dots, \delta_p)^t.$$

For example: Note that $A = I$ in the Radar and Cinetheodolite cases, and A is a scalar matrix in the Dovap case.

Assuming uncorrelated observations, the least squares solution is that which results in minimizing the weighted sum of the squares of the residuals

$$(2.3) \quad S = V^t(\sigma)^{-1} V \quad \text{where}$$

(σ) is the relative variance matrix of the observations $\{X_i^0\}$. The element $(\sigma)^{-1}_{ii} = W_i$ is the weight of the i^{th} observation.

For example: In the radar case the weight $(\sigma)^{-1}_{jj} = W_j$ can be determined as follows. Compute

$$\begin{aligned} \bar{x}_j &= \frac{\sum_{i \neq j} x(i)}{n - 1} \\ \bar{y}_j &= \frac{\sum_{i \neq j} y(i)}{n - 1} \\ \bar{z}_j &= \frac{\sum_{i \neq j} z(i)}{n - 1} \quad (j = 1, 2, \dots, n). \end{aligned}$$

Compute the back azimuth: $\bar{A}_j = \tan^{-1} \left[\frac{\bar{y}_j - y_j}{\bar{x}_j - x_j} \right]$

the back elevation: $\bar{E}_j = \tan^{-1} \left[\frac{\bar{z}_j - z_j}{[(\bar{x}_j - x_j)^2 + (\bar{y}_j - y_j)^2]^{1/2}} \right]$

the back range: $\bar{R}_j = \sqrt{(\bar{x}_j - x_j)^2 + (\bar{y}_j - y_j)^2 + (\bar{z}_j - z_j)^2}$.

Let: $w_{3j-2} = 1 / (\bar{A}_j - A_j^o)^2$

$w_{3j-1} = 1 / (\bar{E}_j - E_j^o)^2$

$w_{3j} = 1 / (\bar{R}_j - R_j^o)^2 , \quad (j = 1, 2, \dots, n).$

In the terminology of matrix algebra the problem of least squares as considered by Brown [1, 2] and Hall [4, 5, 6] consists of determining of all possible vectors V and D satisfying (2.2), those which minimize (2.3).

We solve the constrained minima problem with the aid of Lagrange multipliers. Let $\lambda = (\lambda_1, \lambda_2, \dots, \lambda_q)^t$, from (2.2) and (2.3) we have

$$(2.4) \quad S = V^t (\sigma)^{-1} V - 2\lambda^t (AV + BD + E).$$

To determine the minimum value of S , equate to zero the partial derivatives of S with respect to the γ_i and δ_i .

Differentiation of S with respect to the residuals γ_i yields

$$(2.5) \quad (\sigma)^{-1} V - A^t \lambda = 0 \quad \text{or} \quad V = (\sigma) A^t \lambda .$$

Differentiation of S with respect to the residuals δ_i yields

$$(2.6) \quad B^t \lambda = 0.$$

Substitution of (2.5) into (2.2) yields

$$(2.7) \quad (A(\sigma) A^t) \lambda + BD + E = 0.$$

If $(A(\sigma) A^t)$ is nonsingular then the least squares solution results from (1.) Solve (2.7) for $\lambda = - (A(\sigma) A^t)^{-1} (BD + E)$

(2.) Substitute λ into (2.6) and derive the Reduced Normal Equation

$$(2.8) \quad ND + C = 0 \quad \text{where}$$

$$N = B^t (A(\sigma) A^t)^{-1} B \text{ and } C = B^t (A(\sigma) A^t)^{-1} E.$$

(3.) Solve (2.8) for D .

(4.) Solve (2.5) for V .

In most cases the matrix $A(\sigma) A^t$ is nonsingular and (2.8) is valid. In the few cases where this is not true, it is possible to remove the difficulty by manipulating the conditional equations, [2].

We have computed a least squares approximation to the parameters $\{Y_i\}$ using an initial approximation. We now repeat this procedure using $\{Y_i^0\}$ instead of $\{Y_i^0\}$ as an approximation and compute a new residual matrix D . The iteration continues until $\|D\|$ is sufficiently small.

Since we want to delete observations (or observers), we need some basis for determining which observations are the most likely candidates for deletion. We use the partial derivatives $\frac{\partial(\delta_1, \delta_2, \dots, \delta_q)}{\partial(x_1, x_2, \dots, x_p)}$ evaluated at t to aid in this determination.

3.0 DERIVATION OF D_U. As pointed out in the introduction there are two distinct motives for deleting observations. In general if we are trying

(a.) TO IMPROVE THE SOLUTION

WANT: $\frac{\partial \delta_j}{\partial X_i^0}$ small, so that errors in X_i^0 will have little effect on δ_j .

DELETE: $\frac{\partial \delta_j}{\partial X_i^0}$ large, since a small error in X_i^0 will result in a large error in the δ_j .

(b.) TO MINIMIZE PARTICIPATION

WANT: $\frac{\partial \delta_j}{\partial X_i^0}$ large, since this observation (X_i^0) has a great effect on the solution.

DELETE: $\frac{\partial \delta_j}{\partial X_i^0}$ small, since this observation (X_i^0) has little effect on the solution.

Let $U = (X_1, \dots, X_q)$ and define the p by q matrix

$$D_U = [\frac{\partial}{\partial U}] [D] = \begin{bmatrix} \left[\begin{array}{c} \frac{\partial}{\partial X_1^0} \\ \vdots \\ \frac{\partial}{\partial X_q^0} \end{array} \right] & [\delta_1, \delta_2, \dots, \delta_p] \end{bmatrix}^t = \begin{bmatrix} \frac{\partial \delta_1}{\partial X_1^0}, \dots, \frac{\partial \delta_1}{\partial X_q^0} \\ \vdots \\ \frac{\partial \delta_p}{\partial X_1^0}, \dots, \frac{\partial \delta_p}{\partial X_q^0} \end{bmatrix}$$

where $\frac{\partial \delta_i}{\partial X_j^0} = \frac{\partial \delta_i}{\partial X_j}$ (t).

One of the objectives of this paper is the derivation of D_U . Note that $(D_U)_{ji}$ is the rate of change of δ_j (the correction in the dependent variable Y_j) with respect to the observation X_i^o .

For example: In the radar case $(D_U)_{ij}$ is the rate of change of the correction in one of the missile position co-ordinates with respect to a change in azimuth, elevation or range at the j^{th} station.

From (2.8) we have

$$D = -N^{-1} C = -[B^t (A(\sigma) A^t)^{-1} B]^{-1} [B (A(\sigma) A^t)^{-1}] E.$$

Since observational errors have no significant effect on the matrices A , B and (σ) , they may be regarded as constants in the propagation of error under consideration. The vector E however is affected by the observational errors. Thus the error in D arises primarily from errors in E , which in turn are caused by errors in the observational vector U . Therefore

$$D_U = -N^{-1} R E_U \text{ where } R = B^t (A(\sigma) A^t)^{-1} \text{ and } E_U = \left[\frac{\partial}{\partial U} \right] [E].$$

But $E_U = A$ and thus

$$(3.1) \quad D_U = -N^{-1} R A.$$

Note the simplification if $A = I$, as is the case in [4, 5].

4.0 VARIANCE - COVARIANCE MATRIX. A well known, [2.7], generalized law of covariance (in matrix notation) states that if $D = (\delta_1, \dots, \delta_p)$ is a vector of functions of the elements of the vector $U = (X_1^o, X_2^o, \dots, X_q^o)$ which has the variance matrix $\sigma_o^2 (\sigma)$, then the variance-covariance matrix of the vector D is given by

$$(\sigma_D) = \sigma_o^2 D_U (\sigma) D_U^t.$$

In our discussion this reduces to

$$(4.1) \quad (\sigma_D) = \sigma_o^2 N^{-1} .$$

Note that σ_o^2 is the population variance and (σ) is a relative variance matrix of the observations.

$$\text{In the radar case } \sigma_o^2 = \frac{\sum_{i=1}^n (\gamma_{i1}^2 w_{i1} + \gamma_{i2}^2 w_{i2} + \gamma_{i3}^2 w_{i3})}{3n - 3} .$$

5.0 VARIABILITY ESTIMATE. For each correction δ_i of the derived quantities Y_i , a "variability estimate" will now be associated with each observation.

In the radar case, for each co-ordinate residual a variability estimate is associated with each tracking station.

Consider the matrix $H = \sigma_o D_U (\sigma)^{1/2}$. Note that

$$H_{ij} = \frac{\sigma_o}{w_j} \frac{\partial \delta_i}{\partial X_j}, \quad (i = 1, 2, \dots, p; j = 1, 2, \dots, q),$$

and

$$HH^t = (\sigma_D) .$$

It follows that the variance in the derived quantity Y_i

$$(5.1) \quad \sigma_{Y_i}^2 = \sum_{j=1}^q H_{ij}^2 = \sum_{j=1}^q \frac{\sigma_o^2}{w_j^2} \left[\frac{\partial \delta_i}{\partial X_j} \right]^2, \quad (i = 1, 2, \dots, p).$$

Since H_{ij}^2 is the j^{th} observation's contribution to the variance in Y_i , we will refer to H_{ij}^2 as the "variability estimate" in δ_i for the j^{th} observation, ($i = 1, 2, \dots, p; j = 1, 2, \dots, q$).

In the radar case there are three observations per station (azimuth, elevation and range) and thus the variability estimate "for the j^{th} station" is defined as the sum of the variability estimates (as defined above) for the azimuth, elevation and range readings at the j^{th} station. We are interested in eliminating stations and thus observations three at a time.

$$C_{ij}^2 = H_{i,3j-2}^2 + H_{i,3j-1}^2 + H_{i,3j}^2$$

is the variability estimate for the j^{th} station, where

$$X_{3j-2} = A_j, X_{3j-1} = E_j \text{ and } X_{3j} = R_j \quad (j = 1, 2, \dots, 3n).$$

6.0 MOTIVES FOR DELETING OBSERVATIONS. We will now discuss motives or reasons why one might want to delete observations before computing a least squares solution.

6.1 TO IMPROVE LEAST SQUARES SOLUTION. In this case we are interested in deleting observations which are "extremely" poor, that is, observations which contribute greatly to the variances. Certainly if all of the H_{ij}^2 ($j = 1, 2, \dots, q$) are relatively close to being equal then no observation is predominately worse than the others and no observation should be deleted as a result of investigating the variability estimates. One should remember that usually the variances increase with a decrease in observations. However, if one (or more) observation's variability estimate is quite large in comparison to the others, then this observation would be considered a predominate contributor to the variances $\sigma_{Y_i}^2$ (or least squares solution) and would definitely be a candidate for deletion. One must consider an observation's contribution to each variance $\sigma_{Y_i}^2$ ($i = 1, 2, \dots, p$) when deciding if an observation should be deleted. There are various ways one might want to combine these contributions to the variances $\sigma_{Y_i}^2$ so as to be able to order the observations (or observers). In the radar case we have three variances $\sigma_x^2, \sigma_y^2, \sigma_z^2$ ($p=3$) to consider and define station constants

$$D_j = \sqrt{C_{1j}^2 + C_{2j}^2 + C_{3j}^2} \quad (j = 1, 2, \dots, n)$$

The stations are then ordered according to the magnitude of their station constants. $(D_{i_1} \geq D_{i_2} \geq \dots \geq D_{i_n})$.

To improve a least squares solution the station corresponding to the largest station constant is designated the most likely to be deleted.

This case of improving solution, not being our main motive for the study, has not yet been thoroughly investigated.

6.2 TO MINIMIZE THE NUMBER OF OBSERVATIONS. In this case we are not primarily interested in an improved solution, but rather deleting observations which contribute "very little" to the solution, so as to minimize the data that we must consider for a solution. The observations (or observers) that contribute least to the variances of those with the smallest variability estimates are the most likely candidates for deletion. Our motive here might be completely logistical.

In the radar case, it should be pointed out that the matrices needed to obtain the ordering of stations given above $(D_{i_1} \geq D_{i_2} \geq \dots \geq D_{i_n})$

can be determined (or at least approximated) before flight. To find the variability estimates we need to know:

(1) $B = (b_{ij}) = \frac{\partial(X, Y, Z)}{\partial(A_j, E_j, R_j)}(t)$. This matrix is readily computed given station co-ordinates and an approximate missile position.

(2) $(\sigma) = \text{dg}(\sigma_{11}, \sigma_{22}, \dots, \sigma_{3n}, \sigma_{3n})$ = variance-covariance matrix of the observation variables. If the standard deviations σ_{A_j} , σ_{E_j} , σ_{R_j} ($j = 1, 2, \dots, n$) are known from past histories then set:

$$(\sigma)_{3j-2, 3j-2} = \sigma_{Aj}^2 / \cos^2 E_j / \sigma_o^2$$

$$(\sigma)_{3j-1, 3j-1} = \sigma_{Ej}^2 / \sigma_o^2$$

$$(\sigma)_{3j, 3j} = \sigma_{Rj}^2 / \sigma_o^2 \quad (j = 1, 2, \dots, n)$$

$$\text{where } \sigma_o^2 = \frac{\sum_{j=1}^n (\sigma_{Aj}^2 + \sigma_{Ej}^2 + \sigma_{Rj}^2 / R_j^2)}{3n}$$

In the Cinetheodolite Study, DR-Q has estimates of σ_{Aj} and σ_{Ej} and plans are being made to keep records for the Radar and Dovap systems.

If the standard deviations are not available, then the present weighting scheme at WSMR may be used setting

$$(\sigma)_{3j-2, 3j-2} = 1/R_j^2 \cos^2 E_j$$

$$(\sigma)_{3j-1, 3j-1} = 1/R_j^2$$

$$(\sigma)_{3j, 3j} = 1 \quad (j = 1, 2, \dots, n).$$

In this latter case an approximation of σ_o^2 is used instead of the above calculated values. (If neither of these weighting schemes are acceptable, then one can simply set $(\sigma) = I$.)

$$(3.) D_U = -[B^t (\sigma)^{-1} B]^{-1} [B^t (\sigma)^{-1}] \text{ since } A = I.$$

$$(4.) H = \sigma_o D_U (\sigma)^{1/2}, \text{ and thus the variability estimates and station constants are available before flight.}$$

Thus before flight we can order the stations geometrically by inducing "observational" errors, with the standard deviations σ_{Aj} , σ_{Ej} and σ_{Rj} in a simulated least squares solution.

It should be pointed out here that this ordering determines the best k station combination ($k \leq n$) as the stations (i_1, i_2, \dots, i_k) . Otherwise one would have to consider $nC_k = \frac{n!}{k!(n-k)!}$ possible combinations of k station solutions to arrive at this stage.

In the final stage the Minimal Station Participation problem [4, 5, 6] takes the form:

GIVEN: (1) A geometric ordering of n stations ($D_{i_1} \geq \dots \geq D_{i_n}$),

(2) A reliability factor P_j for each station - the probability of successful operation if scheduled,

(3) Data precision factors for each variable (A, E, R) per station - σ_{Aj} , σ_{Ej} , σ_{Rj} ,

(4) Necessary data to determine tracking capabilities such as tracking rates (focal lengths and object size in the case of Cinetheodolite), etc.

FIND: A subsystem of k stations ($k \leq n$), k a minimum, such that for this particular point and missile we have:

(1.) Each station in the subsystem is able to track,

(2.) The probability of two or more (three or more in Cinetheodolite case) of the k stations will operate successfully is greater than P ,

(3.) The geometric ordering given above is such that the stations deleted are insignificant contributors to the solution.

Thus we consider station ability, reliability and geometry in determining the Minimal Station Participation Before Flight (MSPARB) System.

The RADAR and DOVAP programs are in the process of being written. Consider the following SLIDE of the MSPARB Cinetheodolite program [4], as of 13 August 1965.

The input includes

- (1) (x_j, y_j, z_j) ----- ($j = 1, 2, \dots, n$), WSCS co-ordinates of the j^{th} station,
- (2) (x, y, z) ----- an approximate missile position,
- (3) $(\dot{x}, \dot{y}, \dot{z})$ ----- approximate velocity components,
- (4) $(\ddot{x}, \ddot{y}, \ddot{z})$ ----- approximate acceleration components,
- (5) σ_{A_j} ----- ($j = 1, 2, \dots, n$), the standard deviation in azimuth readings at the j^{th} station,
- (6) σ_{E_j} ----- ($j = 1, 2, \dots, n$), the standard deviation in elevation readings at the j^{th} station,
- (7) k_{1j} ----- ($j = 1, 2, \dots, n$), the angular velocity limit in azimuth for the j^{th} station,
- (8) k_{2j} ----- ($j = 1, 2, \dots, n$), the angular acceleration limit in azimuth for the j^{th} station,
- (9) k_{3j} ----- ($j = 1, 2, \dots, n$), the angular velocity limit in elevation for the j^{th} station,
- (10) k_{4j} ----- ($j = 1, 2, \dots, n$), the angular acceleration limit in elevation for the j^{th} station,
- (11) F_j ----- ($j = 1, 2, \dots, n$), effective focal length of the j^{th} camera,
- (12) O ----- object size
- (13) P_j ----- ($j = 1, 2, \dots, n$), the probability that station j will operate successfully if scheduled.

Notice that the criterion for deletion of stations contains three main considerations:

I. STATION ABILITY. All stations considered will first be tested as to inability to track for a certain interval for one or all of the following reasons:

- (1) Image size too small,
- (2) Tracking rates too large,
- (3) Elevation angle too small.

II. STATION RELIABILITY. The minimum number of stations is chosen so that the probability of three or more stations operating successfully at any one time is greater than a pre-determined number.

III. STATION GEOMETRY. The stations are ordered according to station geometry. Stations are deleted if their geometric contributions are "insignificant".

Program output includes:

- (1) Print out of all or part of input to program,
- (2) Computed azimuth and elevation angles from each station to the point under consideration,
- (3) Computed approximations to expected standard deviations in missile co-ordinates and angular standard deviation,
- (4) Geometric ordering of stations to include station numbers and geometric factors,
- (5) The probability that three or more of the stations in MSPARB will operate successfully if scheduled.

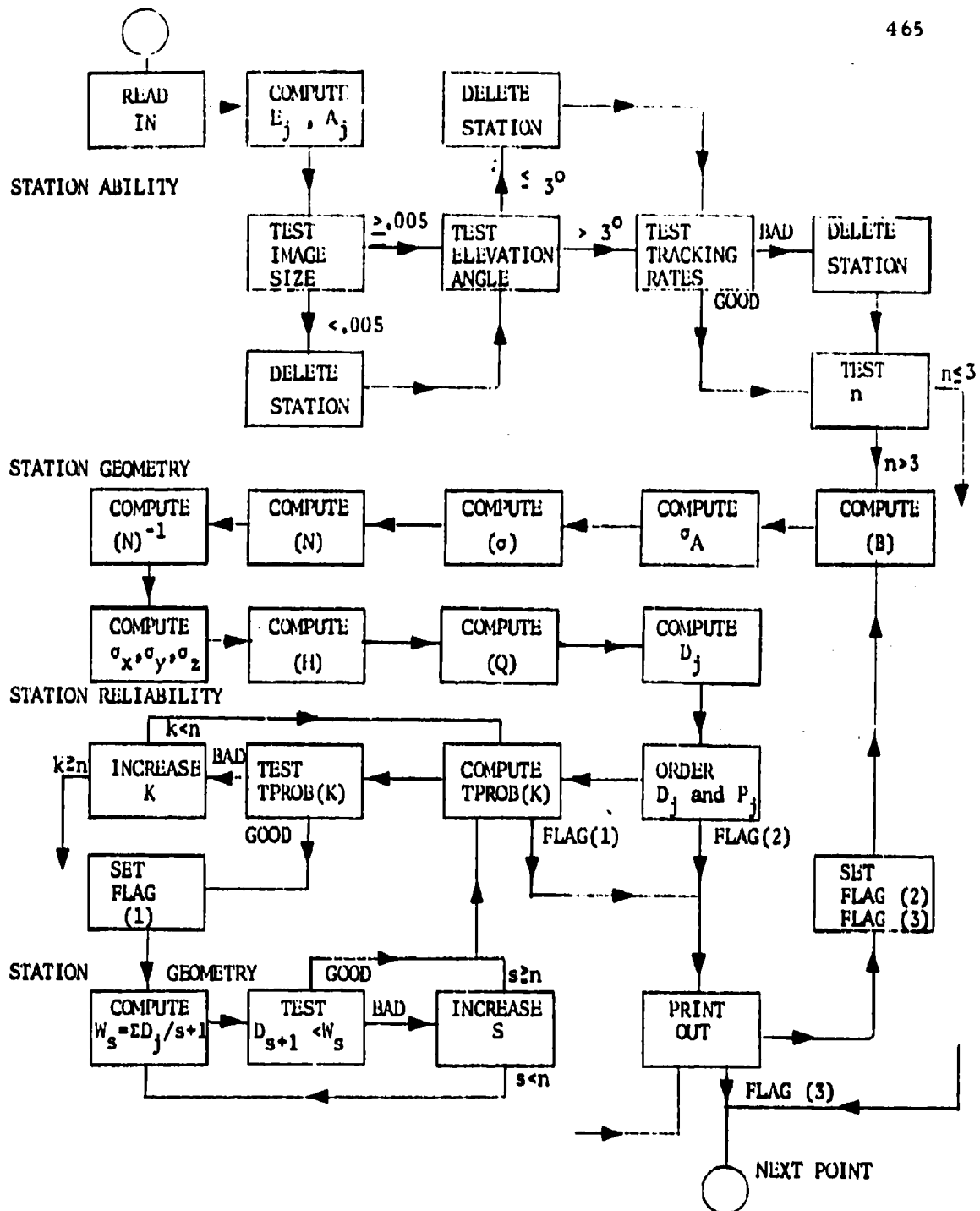
Modifications of the above MSPARB Cinetheodolite program since 13 Aug 65 include (1) a print out of error estimates for the system of the worst three stations in MSPARB as well as error estimates for MSPARB, (2) a print out of cumulative error estimates over the entire trajectory, (3) a print out

of how many times a station was used over the entire trajectory. (I have available here sample print outs for a few trajectories if anyone is interested.)

Areas where MSPARB can be used include:

- (1) Schedule determination.
- (2) Minimizing the current scheduling efforts.
- (3) Determination of best launch point (balloons).
- (4) Determination of best positioning of mobile units.
- (5) Determination of best positioning of future station sites.
- (6) Statement of expected system (MSPARB) errors - (confidence interval) - pre-flight.
- (7) Determination of which system (Cinetheodolites, Radar, or Dovap) or combination of systems will yield the best trajectory coverage-BET.
- (8) Pure error studies concerning geometry versus data precision.

Let us close by stating again that redundancy is necessary to obtain a statistically sound least squares solution, however, through the methods outlined here it can very definitely be advantageously limited.



MSPARB
CIN THEODOOLITES
as of 13 Aug 65

BIBLIOGRAPHY

1. BROWN, D. C., A Treatment of Analytical Photogrammetry, RCA Data Reduction Tech. Report No. 39, 1957.
2. BROWN, D. C., A Matrix Treatment of the General Problem of Least Squares Considering Correlated Observations, BRL Report No. 937, 1955.
3. COMSTOCK, WRIGHT, TIPTON, Handbook of Data Reduction Methods, Data Analysis Directorate (DR-T) Tech. Report, WSMR, 1964.
4. HALL, C. A., Minimal Station Participation Before Flight (MSPARB): Cinetheodolite Case, Data Analysis Directorate (DR-T) Tech. Report, WSMR, 1965.
5. HALL, C. A., Minimal Station Participation: Radar Case, DR-T Tech. Report, WSMR, 1965.
6. HALL, C. A., Minimal Station Participation: Dovap Case, DR-T Tech. Report, WSMR, 1965.
7. WORTHING and GEFFNER, Treatment of Experimental Data, New York, John Wiley and Son, 1948.

PRECISION AND BIAS ESTIMATES FOR DATA FROM
CINETHEODOLITE AND AN/FPS-16 RADAR
TRAJECTORY MEASURING SYSTEMS

Oliver L. Kingsley and Burton L. Williams
Range Instrumentation Systems Office
White Sands Missile Range, New Mexico

INTRODUCTION. A series of flight tests have been conducted at White Sands Missile Range in an effort to obtain a comparison of trajectory data derived from the measurements produced by different instrumentation systems. The instrumentation systems that have been used in some of these tests are Ballistic Camera, DOVAP, Cinetheodolite, and FPS-16 Radars. Interim reports were prepared, based on the data from the three earlier flights conducted on March 29, 1960, September 19, 1960, and January 29, 1962. Mr. Kingsley and Mr. Free presented a summary of the analysis and results of these earlier flights at the sixth, seventh and ninth annual meetings of this conference.

Purpose of Report

The fourth flight test was conducted on October 1, 1962 using a modified Nike Hercules Missile. The purpose of this report is to present an analysis of the bias and random error associated with some of the major range instrumentation systems used for this flight and to compare this data with the data from the earlier flight tests.

Comparability of Results and Earlier Flight Tests

The precision estimates are directly comparable but the bias estimates are not, because the comparison with trajectory data from the Ballistic Camera System was not available.

The earlier three flight tests were conducted at night so the Ballistic Camera System could be utilized to obtain trajectory data to be used as a standard for position bias error estimation. The Ballistic Camera, used on earlier tests, photographed a flashing light beacon on-board the missile against a star trail background. The light beacon flashes were controlled from the ground by a transponder aboard the missile.

Fourth Flight Test

The fourth flight test was conducted during the daylight hours utilizing two cinetheodolite systems and seven AN/FPS-16 radar systems, though only two of the radar systems are analyzed here. The Askania Cinetheodolite System was used as the reference standard for system position bias error estimation for the Contraves cinetheodolite and FPS-16 radar systems. No DOVAP or Ballistic Camera systems were used for this fourth flight test. The AN/FPS-16 radar systems were operated successfully in the beacon tracking mode for the first time during this fourth test of the series. Attempts were made to use the FPS-16 radar systems in the beacon tracking mode for the three earlier flight tests, but the on-board beacon did not operate properly.

Position, Velocity and Acceleration, Precision and Bias

In addition to the estimates of bias and precision for the position data as given in the earlier reports, estimates of the bias and precision given for the derived velocity, acceleration and smoothed trajectory position data are presented. These fourth flight test estimates of bias for position, velocity and acceleration are based on data taken from the Askania cinetheodolite system.

PRECISION ESTIMATES FOR TRAJECTORY DATA.Standard Deviation Estimate

Precision estimates were derived from trajectory data obtained from two cinetheodolite systems and two AN/FPS-16 radar systems in terms of standard deviations for the Cartesian component trajectory data. The standard deviation estimates were derived by the multi-instrument components of variance technique as given by Simon and Grubbs. [1,2]

Instrument Reduction for Position

The cinetheodolite trajectory position data were derived from a least squares reduction of angular measurements [3]. The Askania cinetheodolite system was a five instrument system making ten angular observations for each trajectory space point; the Contraves cinetheodolite system was a three instrument system for trajectory section one and a two instrument

system for trajectory section two, making six and four angular observations respectively for each trajectory space point. The radar trajectory position data were derived from the range, azimuth, and elevation observations that were reduced to the Cartesian coordinate system.

Mathematical Model

A mathematical model for the trajectory position data from the jth instrument system at the ith time may be written: $X_{ij} = X_i$ (true) + e_{ij} , where e_{ij} represents a composite random error for the jth instrument system at the ith time. Standard deviation estimates were determined for these position data, and also for sets of smoothed position, velocity, and acceleration data that were derived by fitting a set of component position data to an eleven point second degree polynomial in time, and evaluating at the midpoint for successive trajectory space points (50 per trajectory section). The polynomial equation for the smoothed X-component data for the ith time would be of the form:

$$(1) \quad X_{ij} \text{ (smoothed)} = a_{0j} + a_{1j}t_i + a_{2j}t_i^2$$

for the jth instrumentation system. An error would generally be associated with each of the coefficients for the jth instrumentation system. A composite random error for the jth system can be expressed in the mathematical model;

$$(2) \quad X_{ij} \text{ (smoothed)} = X_i \text{ (true)} + \bar{e}_{ij}$$

where \bar{e}_{ij} is the composite random error for the jth system at the ith time. The velocity equation is written:

$$(3) \quad \dot{X}_{ij} = a_{1j} + 2a_{2j}t_i$$

The composite random error for the velocity data can be expressed by the velocity equation:

$$(4) \quad \dot{X}_{ij} = X_i \text{ (true)} + \dot{e}_{ij}$$

where the composite random error in velocity (e_{ij}) arises in the two of the terms of the velocity equation. A similar pair of equations could be written for the derived acceleration data.

Discussion of Precision Estimates

The position standard deviation estimates presented in Table I represent essentially random error in position data from the particular system. The standard deviation estimates range from two to twenty-two feet with the exception of trajectory section two for the Contraves system where the system geometry is very poor. Generally, this would not be considered satisfactory coverage; it is included for the sake of continuity.

The position, velocity, and acceleration standard deviation estimates presented in Tables II, III, IV, and V represent the residual random error in the derived (or smoothed) position, derived velocity, and derived acceleration data respectively. The velocity standard deviations for the cinetheodolite data ranged from two feet per second to eleven feet per second except for the second trajectory section for the Contraves cinetheodolite. The velocity standard deviations for the radar data ranged from three feet per second to sixteen feet per second. Velocity data derived from the radar observations is as good as the velocity data derived from the cinetheodolites with respect to variability. The cinetheodolite systems and the radar systems are essentially equivalent in variability with respect to the acceleration data; the only exceptional values are the two large acceleration standard deviations due to the poor system geometry for the Contraves system.

BIAS ESTIMATES FOR TRAJECTORY DATA.

Standards Used In Computation.

All of the bias estimates for Flight Test Nr. 4 of the Operation Precise Program are based on trajectory data from the Askania cinetheodolite system with a mode of ten angular measurements. Earlier flight tests have used trajectory data from the Ballistic Camera System which was based on star trail background for calibration. The Askania system does very well in the determination of the horizontal trajectory position points but has some bias in the vertical determination as indicated by earlier flight tests [9, 11, 12].

Definition of Bias Errors and Discussion

The average bias estimates for position, velocity and acceleration are presented in Tables VI, VII, and VIII for the respective Contraves, Radar 112 and Radar 122 systems. A positive average bias means that the particular system trajectory data was on the average greater than that corresponding data from the Askania system.

The average absolute component position bias estimates ranged from a low of six feet to a high eighty-two feet. The velocity and acceleration average bias estimates were low. The largest velocity component bias was four feet per second; the largest acceleration component bias was only seven feet per second squared. The explanation for the large average position bias error and the much smaller average velocity and acceleration bias error is that the trajectories as determined by the instrumentation systems are parallel but differ by a constant amount in position. This means that the least squares fitting differ by essentially the constant term of the second degree polynomial in time.

A comparison of the unsmoothed position data from the Contraves and radar systems with the corresponding data from the Askania system reveals that the average bias does not differ from the corresponding bias estimates shown in Tables VI, VII, and VIII by more than one foot. This indicates that the smoothing process either moves the average bias estimate the same amount for all systems or that smoothing does not change the bias. A further study of the smoothed and unsmoothed trajectory data from the Askania system reveals that the smoothing process leaves the Askania trajectory data essentially unchanged.

SOME COMPARISONS OF PRECISION ESTIMATES WITH EARLIER FLIGHT TESTS. Comparison of earlier flight tests were possible for the Askania System and the two FPS-16 Radar Systems. The Contraves System was not operated on the earlier tests. Table IX shows the mode number of instruments that make up the Askania System for each flight test. Data from the first trajectory section were selected from the third flight test so as to approximate more closely the other tests. The standard deviation estimates for the Askania system are smaller for the X and Y component data for the later two flight tests.

Precision estimates for data from the earlier flight tests for radar systems 112 and 122 are shown in Table X. These standard deviation

estimates indicate that the best performance for the radar systems was during the fourth flight test. The FPS-16 radars were operated in the beacon tracking mode with a radar beacon aboard the tracked missile.

SUMMARY AND CONCLUSIONS. The standard deviation estimates for the position data ranged from two to nineteen feet for the cinetheodolite systems and ranged from five to twenty-two feet for the FPS-16 radar systems. This indicates that the radar system position data precision are as good as the cinetheodolite system position data precision for these flight test data. The velocity standard deviation estimates ranged from two to eleven feet per second for the cinetheodolite systems (exception Contraves section 2 data) and ranged from three to sixteen feet per second for the FPS-16 radar systems. Again, a precision equivalence for velocity data from these systems can be stated. The acceleration standard deviation estimates for all four tracking systems ranged from eight to forty feet per second squared (with the exception of Contraves section 2 data). Again an equivalence can be stated for precision of the acceleration data from these systems.

The position component average bias were based on the trajectory data from the Askania cinetheodolite system. The average bias for position data from the Contraves cinetheodolite ranged in absolute (component) value from six to seventeen feet (except for section 2 data). The average bias for position data from radar 122 ranged in absolute (component) value from eight to thirty-eight feet and from radar 112, the average bias range in absolute value from a low of 23 to 73 feet. Based on the Askania cinetheodolite position data, the radar systems did not do as well as the Contraves systems, with respect to bias error estimates. The average component bias for the derived velocity data ranged in absolute value from zero to four feet per second for the Contraves system and ranged in absolute value from zero to three feet per second for the FPS-16 radar systems. Essentially the average velocity bias errors are equal.

The acceleration component bias ranged in absolute value from zero to six feet per second squared for Contraves system and from zero to seven feet per second squared for the FPS-16 radar systems. These derived acceleration data for eleven point (two second) smoothed data are essentially equal in average component bias error.

TABLE I
PRECISION ESTIMATES FOR TRAJECTORY POSITION DATA
FROM FLIGHT TEST NUMBER FOUR

Instrumentation System	Trajectory System	Component Standard Deviation Estimate in Feet		
		North (X)	East (Y)	Up (Z)
Askania	1	5	8	10
Askania	2	7	3	17
Contraves	1	10	2	19
Contraves	2	45*	2	67*
Radar 112	1	12	8	16
Radar 112	2	12	5	7
Radar 122	1	9	5	22
Radar 122	2	9	8	22

*Very poor geometry for a two instrument (theodolite) system.

TABLE II
STANDARD DEVIATION ESTIMATES
FOR DERIVED (SMOOTHED) TRAJECTORY DATA
FROM ASKANIA CINETHEODOLITE SYSTEM
FOR FLIGHT TEST NUMBER FOUR

Trajectory Section	Derived Trajectory Element*	Dimensions	Component Estimates of Standard Deviation		
			North (X)	East (Y)	Up (Z)
1	position	feet	5	8	6
2	position	feet	5	2	13
1	velocity	ft/sec.	5	4	5
2	velocity	ft/sec.	6	3	11
1	acceleration	ft/sec. ²	11	8	25
2	acceleration	ft/sec. ²	15	8	40

*All data were derived from mid-point evaluation of a second degree least square polynomial fitted over a two second interval (11 points) with time as the independent variable.

TABLE III
STANDARD DEVIATION ESTIMATES
FOR DERIVED (SMOOTHED) TRAJECTORY DATA
FROM CONTRAVES CINETHEODOLITE SYSTEM
FOR FLIGHT TEST NUMBER FOUR

Trajectory Section	Derived Trajectory Element*	Dimensions	Component Estimates of Standard Deviation		
			North (X)	East (Y)	Up (Z)
1	position	feet	5	2	10
2**	position	feet	19	1	34
1	velocity	ft/sec.	5	2	4
2**	velocity	ft/sec.	25	4	43
1	acceleration	ft/sec. ²	16	3	38
2**	acceleration	ft/sec. ²	87	12	148

*All data were derived from mid-point evaluation of a second degree least squares polynomial fitted over a two second interval (11 points) with time as the independent variable.

**Poor geometry for a two cinetheodolite instrumentation system.

TABLE IV
 STANDARD DEVIATION ESTIMATES
 FOR DERIVED (SMOOTHED) TRAJECTORY DATA
 FROM RADAR (112) SYSTEM
 FOR FLIGHT TEST NUMBER FOUR

Trajectory Section	Derived Trajectory Element*	Dimensions	Component Estimates of Standard Deviation		
			North (X)	East (Y)	Up (Z)
1	position	feet	10	7	13
2	position	feet	12	4	7
1	velocity	ft/sec.	10	10	19
2	velocity	ft/sec.	6	4	6
1	acceleration	ft/sec. ²	32	26	40
2	acceleration	ft/sec. ²	30	8	20

*All data were derived from mid-point evaluation of a second degree least square polynomial fitted over two second interval (11 points) with time as the independent variable. The standard deviation estimates are based on a sample of fifty (50) trajectory points for each trajectory section.

TABLE V
 STANDARD DEVIATION ESTIMATES
 FOR DERIVED (SMOOTHED) TRAJECTORY DATA
 FROM RADAR (122) SYSTEM
 FOR FLIGHT TEST NUMBER FOUR

Trajectory Section	Derived Trajectory Element*	Dimensions	Component Estimates of Standard Deviation		
			North (X)	East (Y)	Up (Z)
1	position	feet	7	4	10
2	position	feet	6	2	9
1	velocity	ft/sec.	6	4	16
2	velocity	ft/sec.	4	3	9
1	acceleration	ft/sec. ²	10	16	44
2	acceleration	ft/sec. ²	10	12	30

*All data were derived from mid-point evaluation of a second degree least squares polynomial fitted over a two second interval (11 points) with time as the independent variable.

TABLE VI
BIAS ESTIMATES FOR DERIVED (ELEVEN POINT SMOOTHING) DATA
FROM CONTRAVES SYSTEM FOR FLIGHT TEST NUMBER FOUR

Trajectory Section	Derived Trajectory Element*	Bias Dimensions	Component Estimates of Average Bias**		
			North (X)	East (Y)	Up (Z)
1	position	feet	- 6	9	- 17
2	position	feet	-28	13	-82
1	velocity	ft/sec.	- 2	1	- 4
2	velocity	ft/sec.	0	0	- 2
1	acceleration	ft/sec. ²	0	- 1	- 1
2	acceleration	ft/sec. ²	- 4	0	- 6

*See note in Table II.

**The trajectory data at simultaneous times from the Askania System (chosen standard) were subtracted from corresponding data from the Contraves System to form an error set of data which were averaged for each trajectory section.

TABLE VII
 BIAS ESTIMATES FOR DERIVED (ELEVEN POINT SMOOTHING) DATA
 FROM RADAR 112 SYSTEM FOR FLIGHT TEST NUMBER FOUR

Trajectory Section	Derived Trajectory Element*	Bias Dimensions	Component Estimates of Average Bias**		
			North (X)	East (Y)	Up (Z)
1	position	feet	-55	-23	-52
2	position	feet	-73	-27	-41
1	velocity	ft/sec.	- 2	1	1
2	velocity	ft/sec.	- 2	- 1	0
1	acceleration	ft/sec. ²	- 1	0	2
2	acceleration	ft/sec. ²	- 1	- 1	- 3

*See note in Table II.

**The trajectory data at simultaneous times from the Askania System (chosen standard) were subtracted from corresponding data from Radar 112 System to form an error set of data which were averaged for each trajectory section.

TABLE VIII
BIAS ESTIMATES FOR DERIVED (ELEVEN POINT SMOOTHING) DATA
FROM RADAR 122 SYSTEM FOR FLIGHT TEST NUMBER FOUR

Trajectory Section	Derived Trajectory Element*	Bias Dimensions	Component Estimates of Average Bias**		
			North (X)	East (Y)	Up (Z)
1	position	feet	- .38	.11	.31
	position	feet	- .28	.8	.26
2	velocity	ft/sec.	0	1	0
	velocity	ft/sec.	3	0	- 2
1	acceleration	ft/sec. ²	1	1	.7
	acceleration	ft/sec. ²	0	0	- 2

*See note in Table II.

**The trajectory data at simultaneous times from the Askania System (chosen standard) were subtracted from corresponding data from Radar 122 System to form an error set of data which were averaged for each trajectory section.

TABLE IX
COMPARISON OF ASKANIA CINETHEODOLITE SYSTEM
BY FLIGHT TEST PERFORMANCE

Flight Test Number	Mode Number of Cinetheodolite	Component Standard Deviation Estimate in Feet		
		North (X)	East (Y)	Up (Z)
1	6	11	11	8
2	7	10	15	12
3*	7	7	4	10
4**	5	6	6	14

*Trajectory section one and mode number of instruments corresponding more closely to earlier tests. Average set for the three trajectory sections is 8, 8 and 12 respectively for Flight Test three.

**The first three flight tests were night tests with a point source of light for optical system tracking; whereas, the fourth flight test was conducted during daylight hours.

TABLE X
COMPARISON OF RADAR SYSTEMS
BY FLIGHT TEST PERFORMANCE

Flight Test Number	Radar Designation	Component Standard Deviation Estimation in Feet		
		North (X)	East (Y)	Up (Z)
1	R-112	18	46	34
2	R-112	25	68	92
3	R-112*	19	39	16
4	R-112**	12	7	12
1	R-122	29	29	21
2	R-122	21	18	20
3	R-122	26	34	31
4	R-122*	9	8	22

*Variate difference estimates for trajectory section 1; data sampled at 2 per second.

**These radars were operated in the beacon tracking mode; whereas, prior tests have utilized the skin tracking mode.

REFERENCES

- [1] Simmon, L. E., "On the Relation of Instrumentation of Quality Control," Instruments, Vol. 19, November 1946.
- [2] Grubbs, F. E., "On Estimating Precision of Measuring Instruments and Product Variability", American Statistical Assn. Vol. 43, pp 243-264.
- [3] Davis, R. C., "Techniques for the Statistical Analysis of Cinetheodolite Data, "NAVORAD Report 1299, China Lake, Calif. (March 22, 1951).
- [4] Pearson, K. E., "Evaluation of the AN/FPS-16 (System No. 1) at White Sands Missile Range," WSMR Technical Memorandum No. 606, February 1959.
- [5] Dibble, H. L., Carroll, C. L. Jr., "A Best Estimate of Trajectory using Reduced Data from Various Instruments at a Single Point in Time," AFMTC-TR-60-12, May 1960, Patrick Air Force Base, Florida.
- [6] Wine, L. R., "Statistics for Scientists and Engineers," Prentice-Hall Inc., Englewood Cliffs, N. J., 1964.
- [7] Duncan, David B., "On the Optimum Estimation of a Missile Trajectory from Several Tracking Systems", AMFTC-TR-60-16, 24 August 1960, Patrick Air Force Missile Test Center, Florida.
- [8] Kendall, M. G., "The Advanced Theory of Statistics," Vol. II, 3rd Ed. C. Griffin and Co. Ltd. London, 1951.
- [9] Kingsley, O. L., "Analysis of Some Trajectory Measuring Instrumentation Systems," Paper presented at the Sixth Conference on the Design of Experiments in Army Research, Development and Testing, October 1960, Aberdeen Proving Ground, Aberdeen, Maryland.
- [10] Weiss, J. E., Kingsley, O. L., "Study of Accuracy and Precision of Trajectory Measuring Systems," 30 June 1961 (U) ORDBS-IRM Task 5-4-2. WSMR, New Mexico.

- [11] Kingsley, O. L., "A Further Analysis of Missile Range Tracking Systems." Paper presented at the Seventh Conference on the Design of Experiments in Army Research, Development, and Testing, October 1961, Fort Monmouth, N. J.
- [12] Kingsley, O. L., Free, B. R., "Additional Analysis of Missile Trajectory Measuring Systems." Paper presented at the Ninth Conference on the Design of Experiments in Army Research, Development and Testing, October 1963, Redstone Arsenal, Alabama.
- [13] "Final Data Report No. 14775. AN/FPS-16 Radar R-112 for Nike Hercules RT-2 in Support of Accuracy and Precision of Trajectory Measuring System Launched 1 October 1962." (U) IRM-DRD WSMR, N. Mex. (16 November 1962) Classified Confidential.
- [14] "Final Data Report No. 14777. AN/FPS-16A Radar R-122 for Nike Hercules RT-2 In Support of Accuracy and Precision of Trajectory Measuring System Launched 1 October 1962" (U) IRM-DRD, WSMR, N. Mex. (16 November 1962) Classified Confidential.
- [15] "Final Data Report No. 14847. Contraves Trajectory Data for Nike Hercules RT-2 In Support of Accuracy and Precision of Trajectory Measuring Systems. Launched 1 October 1962." (U) IRM-DRD, WSMR, N. Mex. (3 December 1962) Classified Confidential.
- [16] "Final Data Report No. 14829. Askania Trajectory Data for Nike Hercules RT-2 In Support of Accuracy and Precision of Trajectory Measuring Systems." (U) IRM-LRD, WSMR, N. Mex. (28 November 1962) Classified Confidential.

THERMAL CYCLES IN WELDING

Mark M. D'Andrea, Jr.
U. S. Army Materials Research Agency
Watertown, Massachusetts

INTRODUCTION: The mechanical property integrity of weld heat-affected zones is an inherent and vital consideration in arc welding applications. A weld heat-affected zone, hereinafter termed "weld-HAZ", is defined as that volume of base material in a weldment that has been heated, as a result of welding, to a range of peak temperatures between the pre-heat temperature and the materials melting point.

Previous work conducted at the U. S. Army Materials Research Agency, concerning the welding of fully heat-treated high-strength steels for service in the as-welded condition, demonstrated that weld-HAZ areas characterized by peak temperatures at or about the lower critical temperature, suffered a marked loss of strength, thus reducing weld-joint efficiencies considerably. Other studies with high-strength and maraging steels have revealed deleterious mechanical property effects resulting from thermal cycles characterized by peak temperatures above the upper critical temperature. In addition, it is well known that an embrittling effect in alloy steels is generally associated with weld-HAZ structures characterized by peak temperatures between the lower and upper critical temperatures.

Recent work conducted at AMRA, established the general parameters necessary to define and reproduce the transformational behavior of weld-HAZ microstructures. These parameters included (but are not necessarily limited to) the following; (1) The time-temperature shape of a weld-HAZ thermal cycle, (2) the peak temperature of a thermal cycle, (3) the microstructure of the base material (defined by heat treatment, chemistry, working, etc.), prior to the imposition of a thermal cycle, and (4) factors affecting restraining stresses and strains produced in the base material as a result of the overall welding operation.

The gamut of microstructures produced in a weld-HAZ is the end result of the complex and varied transformations caused by welding thermal cycles. An important consideration which has been a pertinent reference point in the present investigation, was the fact that in any arc weld in a given material there will always be thermal cycles that have the same peak

temperature; these thermal cycles will differ only in that the shape and position of associated heating and cooling curves will be displaced somewhat in time and temperature. It is a well established metallurgical fact that the mechanical properties of a material depend primarily upon microstructure. In order to predict and perhaps control weld-HAZ microstructures resulting from welding thermal cycles, it is necessary first to investigate the effects of basic parameters of such structures.

OBJECT AND SCOPE:

Welding Metallurgy

The overall objective is to investigate and to establish basic metallurgical concepts to account for the phenomena of the attendant transformation behavior of weld-HAZ microstructures produced in 4340, H-11, and 18 1/2% Ni (300) maraging steels. The work is limited to a study of the effects of fundamental material and welding time-temperature parameters pertaining to single pass, arc welding situations. Realizing the potentially staggering number of general and sub-parameters that may significantly affect resultant microstructure, it was deemed advisable to initiate the investigation by studying only the effects of some of the general parameters, viz; the prior base material microstructure, the peak temperature of a thermal cycle, and the time-temperature shape of thermal cycles imposed by welding. The number and kind of stress-strain conditions that are applicable to welding were initially considered to be overwhelming; consequently the utilization of this general parameter in this initial investigation was abandoned in the sense that such conditions were kept constant.

Statistical Inference

The overall objective of the utilization of statistical inference techniques is to assist the metallurgical investigation by determining the significant factors (i.e., the more critical variables), affecting this phenomena, and to detect the specific significant differences that may exist among each set of significant factors. The transformational behavior and the resultant heat-affected zone microstructures produced will be evaluated metallurgically in terms of such specific significant differences obtained.

THE EXPERIMENT. A high-speed time-temperature controller is being used in this investigation to produce weld-HAZ synthetically.

The controller essentially is a simulating device which permits the duplication of welding thermal cycles experienced in weld-heat-affected zones. Each specimen is heated by its resistance to the passage of an A-C electric current furnished from a transformer, and is cooled by the removal of heat from the specimen by conduction through water-cooled copper clamps. A thermocouple percussion welded to the surface of the specimen, provides a signal which is balanced against a reference control signal designed to reproduce the desired thermal cycle. The resultant error signal is amplified and utilized by the controller to maintain temperature control during the cycle to within $\pm 5^{\circ}\text{F}$.

The basic experiment involves two of the general parameters as variables, viz., the prior base material microstructure (defined by various heat treated conditions of a given single heat of steel) and the time-temperature shape of various welding thermal cycles. The thermal cycle peak temperature parameter is a constant in each basic experiment, i.e., each basic experiment is conducted utilizing thermal cycles having the same peak temperature.

In each basic experiment, it is desired to determine the effects of prior base material microstructure (denoted factor code "H"), and the time-temperature shape of thermal cycles (denoted factor code "C"), on the notch toughness (quantitative response variable, measured in in.-lb/in.², indicative of microstructural change) of the resultant weld-HAZ microstructures.

In a given heat of steel, the interest lies in the effects of five particular prior base material microstructures and seven particular thermal cycles, i.e., factor "H" is a fixed factor at five fixed levels and factor "C" is a fixed factor at seven fixed levels.

There are three steels (one heat of each) involved in the investigation along with seven different peak temperatures per heat; therefore, there are three times seven or twenty-one basic experiments to be evaluated independently. Metallurgical considerations preclude statistical correlations between steel types and between peak temperatures per heat of steel.

THE DESIGN AND ANALYSIS: The number of observations (notch toughness values) to be taken is initially unknown; however it is desired

Design of Experiments

to design the statistical analysis to allow for the general situation of dealing with an uneven number of replications per cell, since some experimental observations are lost occasionally. A basic model appears to be a fixed, two-way analysis of variance; the suggested mathematical model for the sum of squares is:

$$\begin{array}{c}
 \text{Total} \qquad \qquad \qquad H \qquad \qquad \qquad C \\
 \left(\sum \sum_{ijk}^2 - \frac{T...^2}{npq} \right) - \left(\frac{T_{..j}^2}{nq} - \frac{T...^2}{npq} \right) + \left(\frac{T_{..k}^2}{np} - \frac{T...^2}{npq} \right) + \\
 \\
 \text{Interaction} \qquad \qquad \qquad \text{Residual} \\
 \\
 \left(\frac{T_{..j}^2}{n} - \frac{T_{..k}^2}{nq} - \frac{T_{..k}^2}{np} + \frac{T...^2}{npq} \right) + \left(\sum \sum_{ijk}^2 - \frac{T_{..k}^2}{n} \right)
 \end{array}$$

Once the individual ANOVA's are run for each basic experiment, one of the following techniques could be used to detect specific significant differences that may exist among each set of significant factors obtained.

(1) Use Duncan's Test of the means if, and only if, the cells have the same number of replications. The means used here are those of the columns, or rows as the case may be, of the cells pertaining to the significant factor; if both factors are significant, two such tests are made regardless of interaction effects. Perhaps this is not a proper technique, in that only the individual cell averages should be tested by Duncan's method.

(2) Use the following relationship to test the means of each cell if there are minor variations in the number of observations per cell.

$$\frac{S_x (\text{entry from studentized range})}{\sqrt{\text{no. observations/cell}}}$$

(3) Use the following relationship to test the means of each cell, if there are major variations in the number of observations per cell.

$$S \sqrt{\frac{1}{n_1} + \frac{1}{n_2}} \times \sqrt{(k-1) F(k-1, \gamma)} .$$

The foregoing is the author's suggested method of analysis. It is important to note that the author is merely a novice at this business of statistical analysis.

It has been suggested since the presentation of this paper that the use of regression analysis techniques may be a better approach to solving this statistical problem. Unfortunately, circumstances to date have not yet permitted a further investigation into the most efficient statistical procedures to be used in this problem.

STATISTICAL ANALYSIS OF TENSILE STRENGTH-HARDNESS
RELATIONSHIPS IN THERMOMECHANICALLY
TREATED STEELS*

Albert A. Anctil
U. S. Army Materials Research Agency
Watertown, Massachusetts 02172

INTRODUCTION. Generally speaking, statistical analysis finds limited applications in metallurgical problems. This is true because the sample size is usually quite small and in most cases, the variables are known and can be controlled. The clinical (statistical) problem described here is a segment of an investigation entitled, "Tensile Strength-Hardness Relationships in Thermomechanically Treated Steels." [1] The objective of the study was to determine metallurgically and statistically how well thermomechanically treated steels followed established tensile strength-hardness correlations.

The generally accepted tensile strength-hardness correlations are published by the American Society for Testing and Materials (ASTM) [2] and the Society of Automotive Engineers (SAE) [3]. These correlations specifically excluded cold worked, stainless steels and other thermomechanically treated steels. The ASTM and SAE correlations have been obtained from a particular steel quenched and tempered to various strength levels. Tensile specimens which contain hardness coupons were machined from each strength level condition. These specimens were distributed randomly to several laboratories participating in a standardized testing program. The assembled data were treated statistically to obtain a tensile strength-hardness correlation.

Thermomechanical treatments which are under consideration here, involve the introduction of cold work into the heat treatment cycle of steel to obtain higher strengths. There are three types of thermomechanical treatments based upon when in the heat treatment cycle the working cycle is performed. [4]

- Type I - Deformation of austenite followed by transformation
- Type II - Deformation of austenite during transformation
- Type III - Deformation after transformation of austenite

*Comments on this paper by one of the panelists can be found at the end of this article.

EXPERIMENTAL PROCEDURE. The experimental tensile strength-hardness data came from a literature survey of thermomechanically treated steels. Refer to Reference 1 for a more detailed explanation and data references for this presentation.

Figure 1 shows the ASTM (solid curve) and SAE (dashed curve) tensile strength-hardness correlations. There is some difference of opinion as to which is the better curve. A joint ASTM-SAE committee is presently working out a compromise curve. The ASTM curve has been extended beyond Rockwell C hardness 58 to encompass the very high strength steels. The data points are from Reference 1 and represent various steels having a quenched and tempered heat treatment. Such data could have been used to obtain these correlations. These same steels were then processed thermomechanically with Type I (open symbols) and Type III (closed symbols) treatments. Statistically the quenched and tempered data fits the ASTM correlation better than the SAE correlation. Accordingly, the ASTM correlation will be used for comparative purposes.

Tensile strength-hardness data for the Type I thermomechanical treatment are shown in Figure 2. The thermomechanical heat treatment cycle is shown schematically. The data follow the ASTM correlation (solid curve) reasonably well. Figure 3 illustrates Type II data. This thermomechanical treatment is usually performed on austenitic stainless steels at subzero temperatures. Meaningful comparisons of this data are difficult with such a small sample size. Type III data are shown in Figure 4. The cold work may be performed upon the asquenched martensite or upon tempered martensite that is subsequently aged. A positive deviation from the ASTM correlation is immediately apparent over the major portion of the hardness range for Type III data.

Selected data for Type III treatments where the percent reduction has been varied are shown in Figure 5. Consider the 5Cr-Mo steel where the lowest tensile strength plotted represents the quenched and tempered condition. Note, that as the amount of cold work is increased, the tensile strength increases at a faster rate than that shown by the ASTM correlation. This same trend can be seen for the majority of these steels. It is for this reason that a regression line was not drawn for this data. A tensile strength-hardness correlation for these steels would be dependent upon the amount of cold work.

DISCUSSION. Metallurgically the behavior was explained using Tabor's analysis [5] which relates hardness and tensile strength through an additional parameter, the strain hardening exponent n . The analysis is summarized in Figure 6. Quenched and tempered steels have strain hardening exponents in the range from 0.04 to 0.12. In this range the tensile strength-hardness ratio is nearly constant. It is for this reason that a unique tensile strength-hardness correlation exists. For Type I treatments the strain hardening exponents fall in the same range, therefore, the data fit the ASTM correlation. With Type III treatments the ratio starts at the minimum and increases as the exponent decreases to nearly zero with increasing amounts of cold work. This results in positive deviations from the ASTM correlation. Type II treatments are usually performed on austenitic stainless steels at subzero temperatures. These steels have very high exponents (0.3) in the annealed condition which decrease to nearly zero with increasing amounts of deformation. One would expect positive deviations from the high and low exponents and adherence to the correlation as the ratio passes through its minimum value. Cold-worked steel (Type III) and stainless steels (Type II) have been excluded from the ASTM correlation because of these drastic changes in strain hardening characteristics.

Statistical analysis of the data is summarized in Table I. The deviation d refers to the experimental tensile strength σ , minus the corresponding tensile strength σ_{ASTM} , from the ASTM correlation at a particular hardness. This deviation was determined for every data point. The arithmetic mean of the deviations $\bar{\Delta}\sigma$ was taken as the sum of the deviations divided by the sample size. It serves as an indication of how well the data for thermomechanically treated steels fit the ASTM correlation. This value would be zero for a regression line of the data. The absolute deviation $|\Delta\sigma|$ and the standard error of estimate S_y were calculated as measures of the dispersion of the data about the ASTM curve. These differ from the usually defined mean absolute deviation and standard error of estimate which measure the dispersion around a regression line.

Statistical results are shown in Table II. The mean of the deviations $\bar{\Delta}\sigma$, shows a better fit of the quenched and tempered data about the ASTM rather than the SAE correlation. Further, the data for the Type I treatment fit the ASTM correlation better than the Type III treatments.

Also, the predominantly positive deviation of the Type III data from the ASTM curve is obvious. Both measures of dispersion about the ASTM curve yield approximately the same results. They do not, however, reflect the positive deviation of data for the Type III treatments.

The problem before the panel is that of offering more descriptive statistical alternatives for comparing several populations of data (tensile strength-hardness values for thermomechanically treated steels) to a given regression line (the standard ASTM tensile strength-hardness correlation). Consider further that it may not be possible or meaningful to draw a regression line through each population of data.

REFERENCES

1. E. B. Kula and A. A. Anctil, Tensile Strength-Hardness Relationships in Thermomechanically Treated Steels, Proceedings, Am. Soc. Testing Mat'l's, Vol. 64, 1964, p. 719
2. Methods and Definitions for Mechanical Testing of Steel Products, 1965 Book of ASTM Standards, Part 1 (currently available as a separate reprint)
3. Hardness Tests and Hardness Number Conversions - SAE J417, SAE Handbook, 1964, p. 94
4. S. V. Radcliffe and E. B. Kula, Deformation, Transformation and Strength, Fundamentals of Deformation Processing, Syracuse University Press, Syracuse, N. Y., 1964, p. 321; also, E. B. Kula and S. V. Radcliffe, Thermomechanical Treatment of Steel, Journal of Metals, Vol. 16, 1963, p. 755.
5. D. Tabor, The Hardness of Metals, Oxford University Press, London, 1951

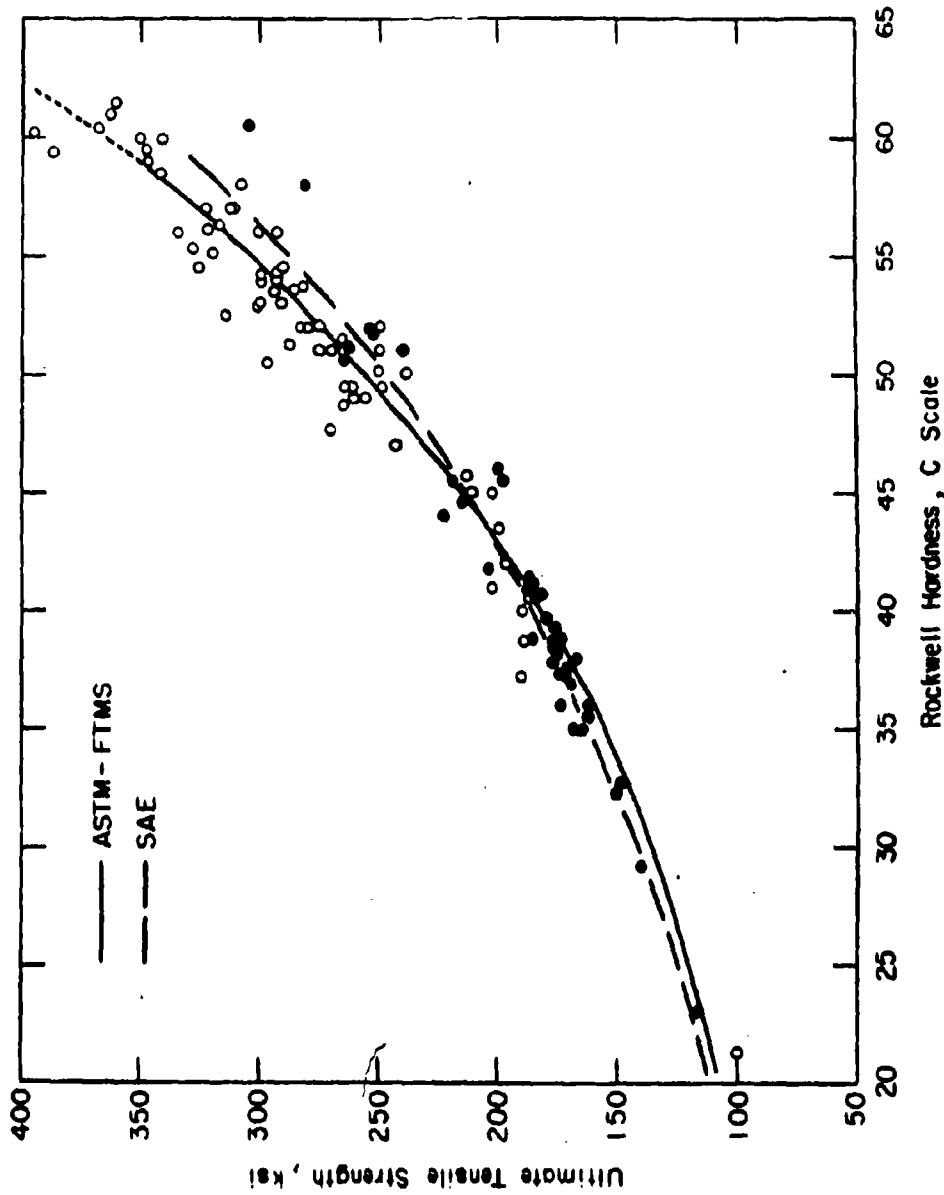


Figure 1. ULTIMATE TENSILE STRENGTH VERSUS ROCKWELL C HARDNESS FOR STEELS HAVING A CONVENTIONAL HEAT TREATMENT (QUENCHED AND TEMPERED). STEELS, ○ USED IN TYPE I, AND ● USED IN TYPE II THERMOECHANICAL TREATMENT.

U. S. ARMY MATERIALS RESEARCH AGENCY

19-066 525/AMC-6a

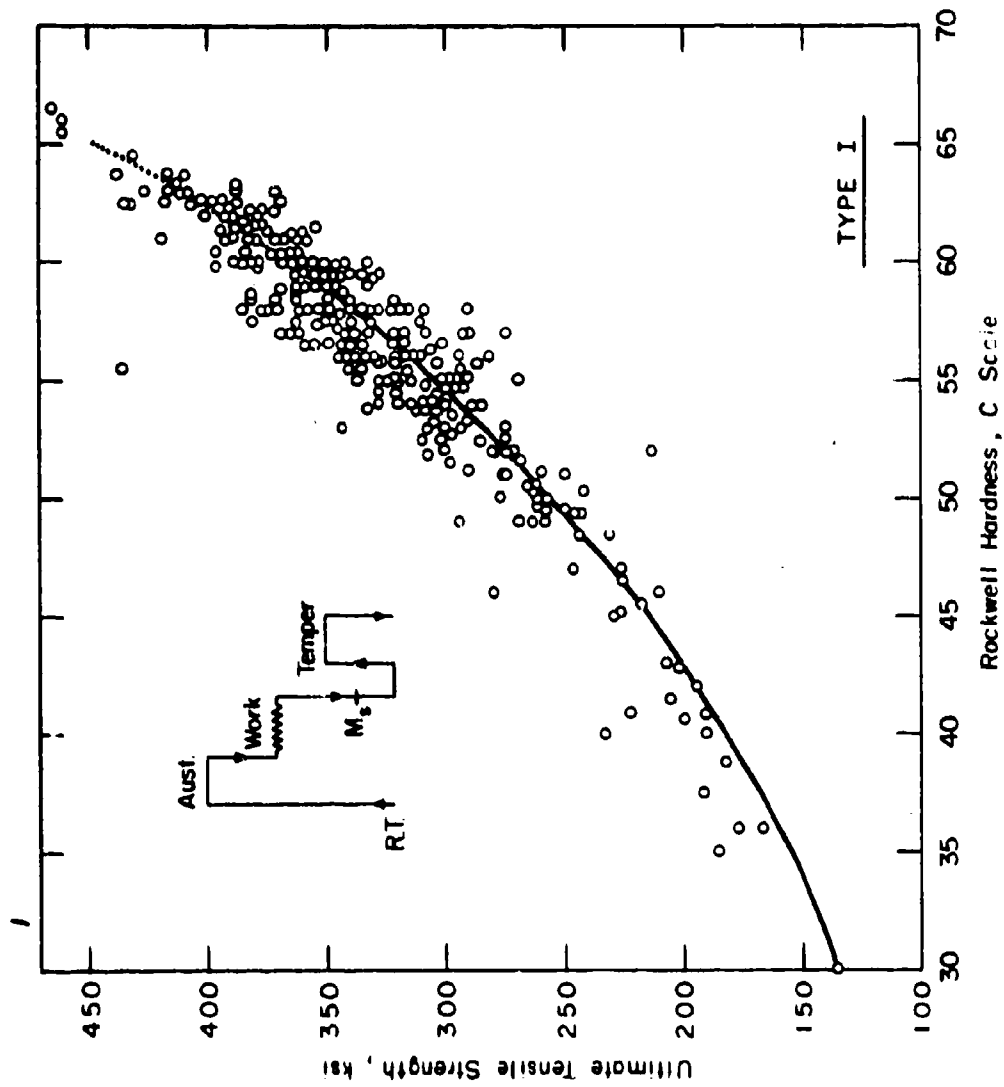


Figure 2. ULTIMATE TENSILE STRENGTH VERSUS ROCKWELL C HARDNESS FOR
TYPE I THERMOMECHANICALLY TREATED STEELS.

U. S. ARMY MATERIALS RESEARCH AGENCY

19-066-526/AMC-64

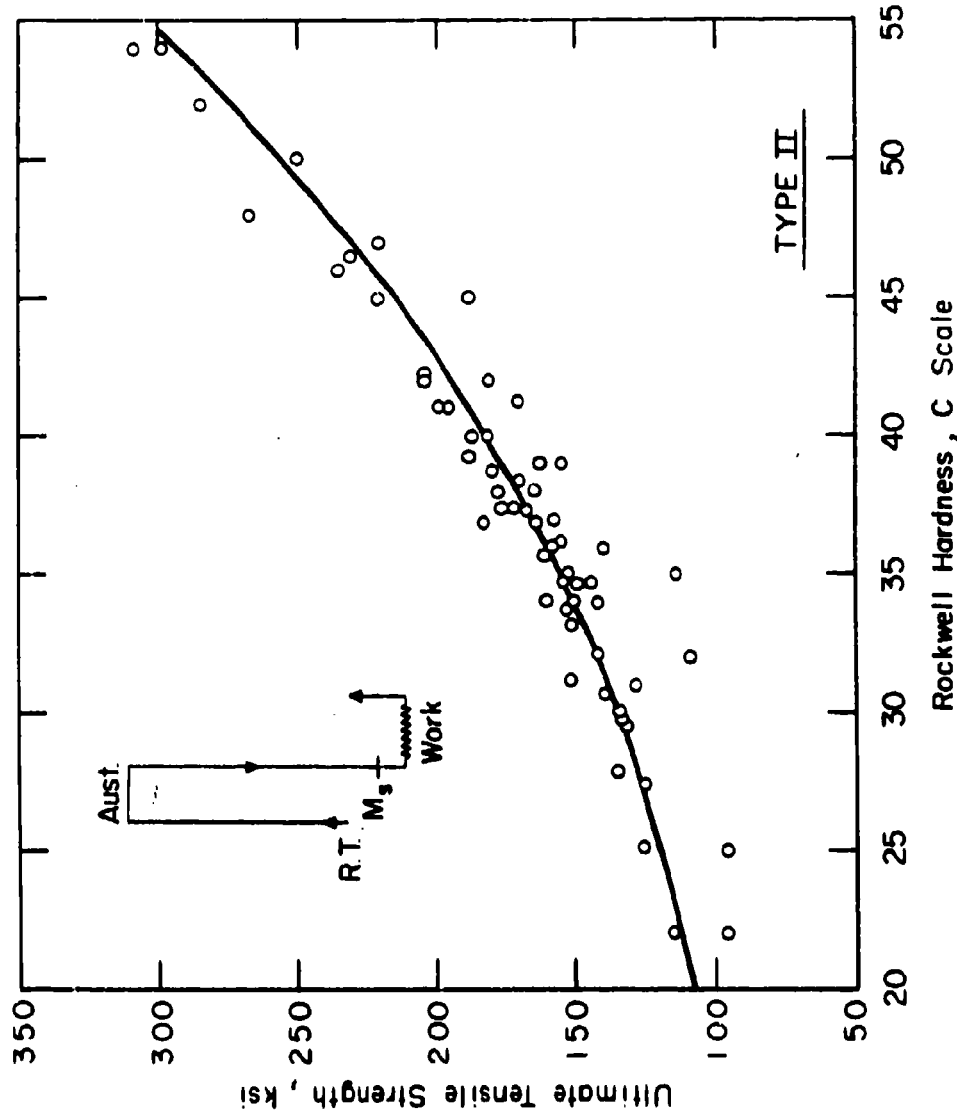


Figure 3. ULTIMATE TENSILE STRENGTH VERSUS ROCKWELL C HARDNESS FOR
TYPE II THERMOMECHANICALLY TREATED STEELS.

U. S. ARMY MATERIALS RESEARCH AGENCY

19-066-529/AMC-6a

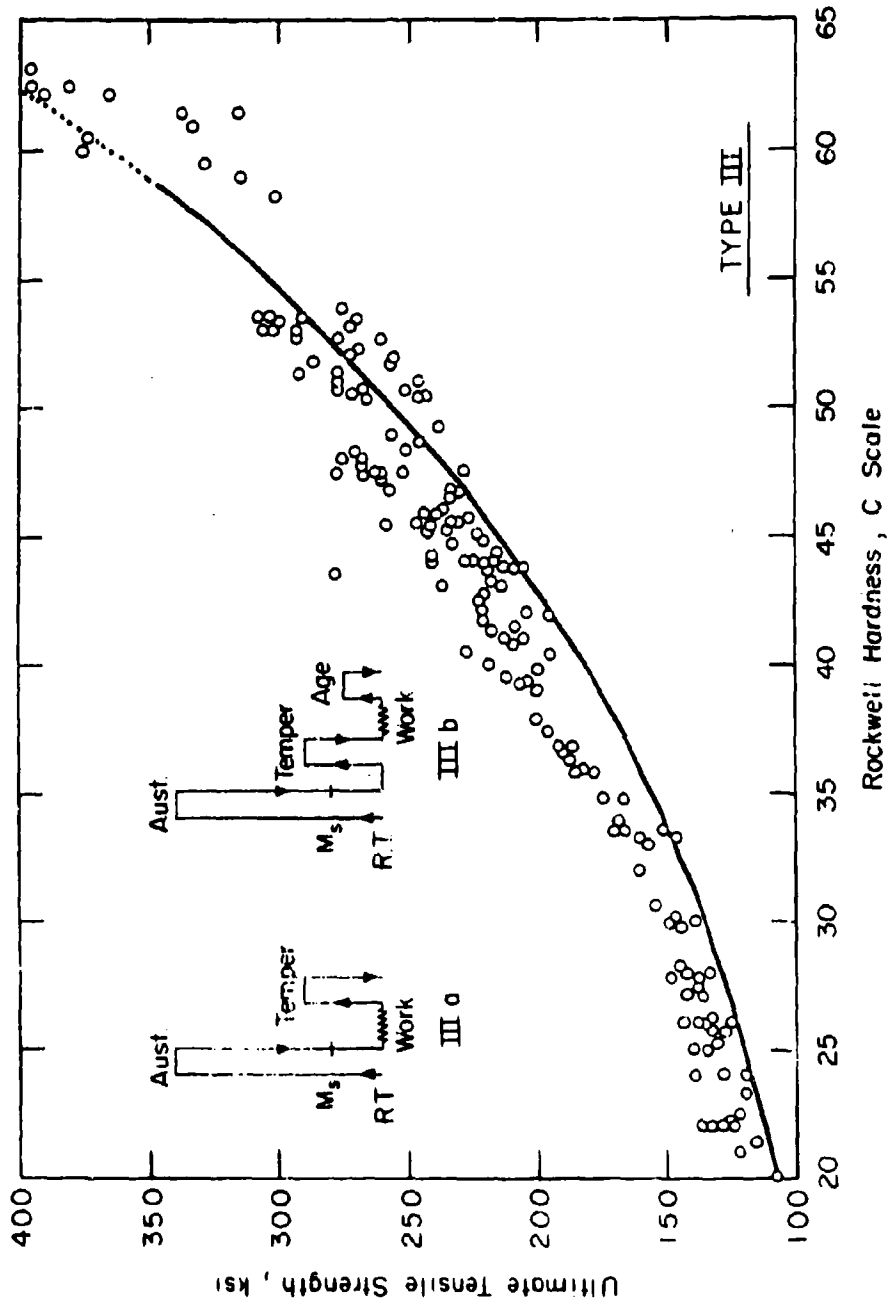


Figure A ULTIMATE TENSILE STRENGTH VERSUS ROCKWELL C HARDNESS FOR
TYPE III TERMOMECHANICALLY TREATED STEELS.
U. S. ARMY MATERIALS RESEARCH AGENCY

19-066 531/AMC-64

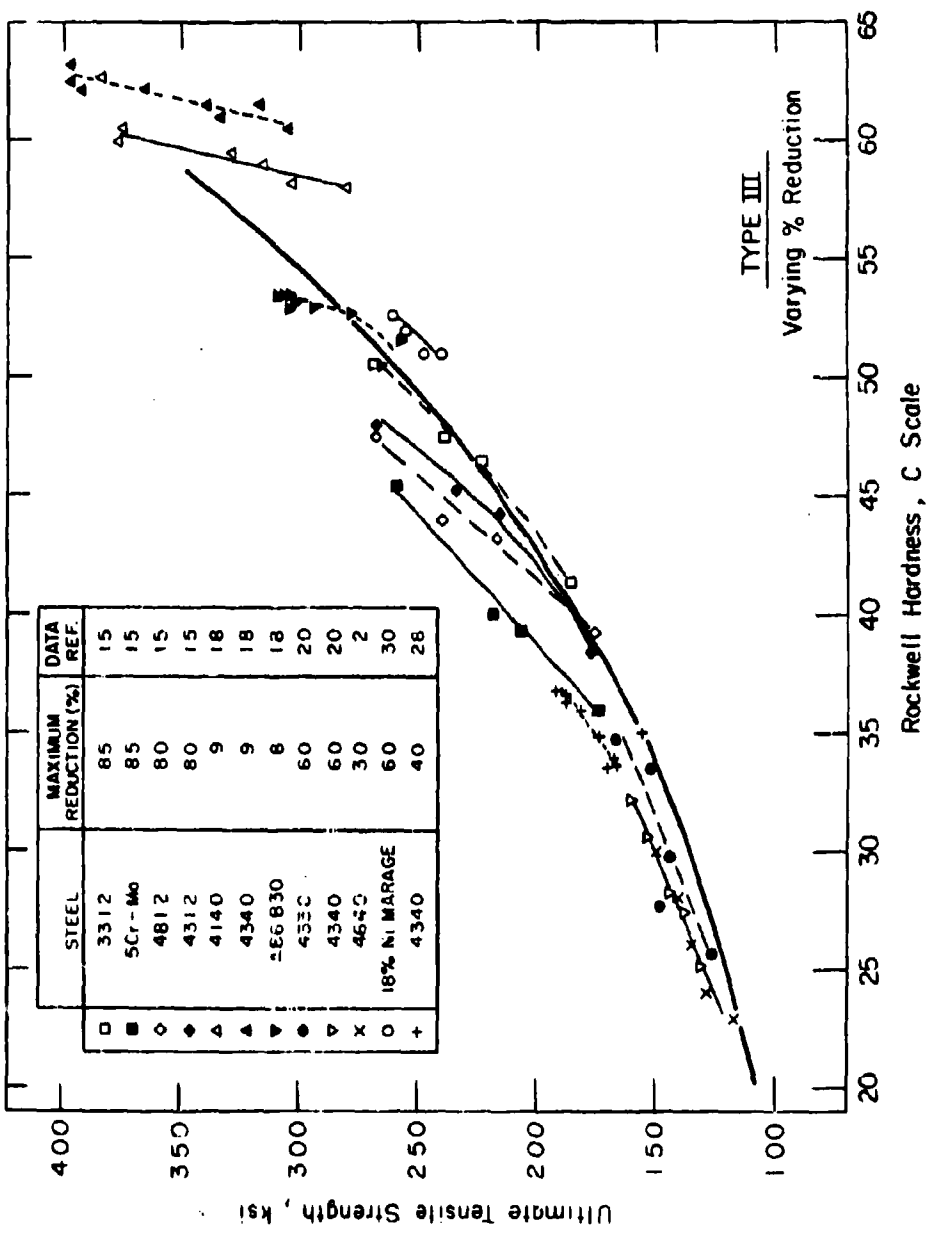


Figure 5 ULTIMATE TENSILE STRENGTH VERSUS ROCKWELL C HARDNESS FOR
TYPE III TREATMENTS WITH VARYING AMOUNTS OF REDUCTION AND CONSTANT
TEMPERING TEMPERATURE.

U. S. ARMY MATERIALS RESEARCH AGENCY

19-066-533/AMC-64

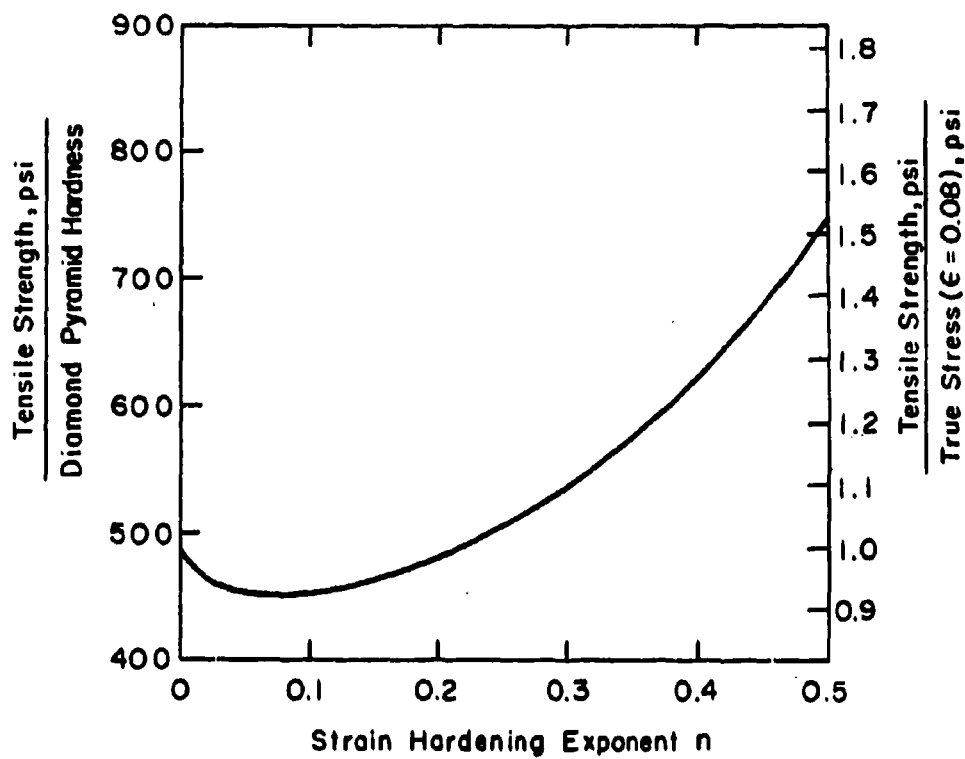


Figure 6. RATIO OF TENSILE STRENGTH TO DIAMOND PYRAMID HARDNESS AND TO TRUE STRESS ($\epsilon = 0.08$) AS A FUNCTION OF THE STRAIN-HARDENING EXPONENT
U. S. ARMY MATERIALS RESEARCH AGENCY

19-066-659/AMC-64

Table I. STATISTICAL ANALYSIS

$$\begin{aligned}d &= \sigma - \sigma_{\text{ASTM}} \\ \bar{\Delta\sigma} &= \frac{1}{n} \sum d \\ |\bar{\Delta\sigma}| &= \frac{1}{n} \sum |d| \\ S_y^* &= \left(\frac{\sum d^2}{n} \right)^{\frac{1}{2}}\end{aligned}$$

Table II. STATISTICAL RESULTS FOR QUENCHED AND TEMPERED AND THERMOMECHANICALLY TREATED STEELS

Condition	$\bar{\Delta\sigma}$ ksi	$ \bar{\Delta\sigma} $, ksi	S_y^* , ksi	n
Quenched and Tempered				
ASTM curve	0.23	11.7	17.7	112
SAE curve	7.33	14.1	19.4	112
Thermomechanically Treated				
Type I	3.70	15.4	20.6	319
Type II	1.45	9.3	12.8	60
Type III	11.00	17.2	20.8	176

COMMENTS ON PRESENTATION BY ALBERT A. ANCILL

Joan Raup Rosenblatt
Statistical Engineering Laboratory
National Bureau of Standards, Gaithersburg, Maryland

The evaluation of empirical relations of the kind you discussed is a difficult problem. The various functions of deviations from the ASTM curve that are presented in your Table II are extremely difficult to interpret: By themselves, they are nearly meaningless. Taken together with the data, as exhibited in your figures, they add very little and may be misleading.

For example, looking at Figure 1, I notice that the steels used in Type I and Type III thermomechanical treatments respectively seem to be grouped preponderantly in different hardness ranges. Is it possible that the ASTM curve fits better for Type I and the SAE curve for Type III? If this were so, an explanation would have to be sought in the metallurgical facts about the data used, and in the history of the two standard curves.

Table II gives overall measures of goodness-of-fit. Since these are well-defined functions of the data, they cannot be "wrong" in themselves. But if the deviations from the standard curves occur for different reasons if different types of steels and in different hardness ranges, the overall measures cannot be relied upon to describe the uncertainty of tensile strength estimates derived (using the curves) from hardness measurements. Furthermore, if the overall measures are used to select the "best-fitted" curve, there is great danger that the resulting curve will have systematic errors arising from the particular choice of data.

Of course, for many purposes a standard curve is entirely adequate. But your data seem to make it clear that one possible long-run goal would be the development of a collection of curves each applicable to specific circumstances. This development would probably require the performance of many new experiments. It could lead to the evolution of your qualitative explanation of the behavior of thermomechanically treated steels into a quantitative explanation.

The statistical measures quite properly play a very small role in your valuable summary of the published evidence on tensile-strength/

hardness relationships. I am sure that in future studies you will continue to be guided by the totality of scientific information available to you, and I hope you will often find that statistical techniques are helpful in data analysis.

SOME PROBLEMS IN STATISTICAL INFERENCE FOR GENERALIZED MULTINOMIAL POPULATIONS

Bernard Harris
Mathematics Research Center, U. S. Army
University of Wisconsin, Madison, Wisconsin

INTRODUCTION. Assume that a random sample of size N has been drawn from a "multinomial population" with an unknown and possibly countable infinite number of classes. That is, if X_i is the i th observation and M_j the j th class, then

$$P\{X_i \in M_j\} = p_j \geq 0, \quad j = 1, 2, \dots; \quad i = 1, 2, \dots, N,$$

and $\sum_{i=1}^{\infty} p_i = 1$. The classes are not assumed to have a natural ordering.

Let n_r be the number of classes occurring exactly r times in the sample. Then, we clearly have

$$\sum_{r=0}^{\infty} r n_r = N.$$

We will be concerned with estimating the following two quantities which are generally of interest to experimenters.

(1) The sample coverage, defined by

$$(1) \quad C = \sum p_i,$$

where the sum runs over all classes which have occurred at least once in the sample.

(2) The population entropy, defined by

$$(2) \quad H = - \sum_{i=1}^{\infty} p_i \log p_i$$

It will be convenient in our definition of entropy to violate the usual conventions and use natural logarithms rather than logarithms to base 2. This is equivalent to a scale change in units of measurement and will have no essential effect on any uses for which the entropy might be employed. Of course, we will assume throughout, that the series (2) converges, since otherwise the discussion will not be relevant.

In those problems which present difficulty, namely where too many of the p_i 's are too small, small sample inference appears to be virtually hopeless, hence, all results described herein will be asymptotic results, i.e. for large N .

Estimation of H and C. For the moment, we will restrict to the case of an ordinary multinomial population, that is, one with a finite number, k , of classes. Then the "natural estimator" of entropy H is defined by

$$(3) \quad \hat{H} = - \sum_{i=1}^N \frac{n_i}{N} \log \frac{n_i}{N} = - \sum_{i=1}^k \hat{p}_i \log \hat{p}_i$$

where \hat{p}_i is the maximum likelihood estimator of p_i .

Its properties has been discussed by G. P. Basharin [1] and we note them briefly. Basharin showed that

$$(4) \quad E(\hat{H}) = H - \frac{k-1}{2N} + O(N^{-2})$$

and

$$(5) \quad \sigma_{\hat{H}}^2 = \frac{1}{N} \sum_{i=1}^k [p_i \log^2 p_i - H^2] + O(N^{-2})$$

and $\sqrt{N}(\hat{H} - H)$ is asymptotically normally distributed. If we attempt to apply Basharin's results to the more general case described earlier, it is easily seen that the naive replacement of p_i by \hat{p}_i in (2) may not be successful. Essentially, Basharin's technique depends on the following sort of asymptotic behaviour,

as $N \rightarrow \infty$, $Np_i \rightarrow \infty$, $i = 1, 2, \dots, k$.

Consequently, if we have zero as a limit point of the p_i 's, or even, if we have the limiting behaviour associated with the Poisson approximation,

as $N \rightarrow \infty$, $p_i \rightarrow 0$, $Np_i \rightarrow \lambda_i$, $0 < \lambda_i < \infty$,

for a sufficiently large number of classes, then Basharin's estimator, \hat{H} , may be quite poor. The following illustration will exhibit this. Let $p_i = \frac{1}{N^2}$, $i = 1, 2, \dots, N^2$. Then $H = 2 \log N$. However, since the maximum of H occurs for $p_i = \frac{1}{k}$, when there are k classes, we have that $\hat{H} \leq \log N$. Hence, it is quite clear, that if there are "too many classes whose probabilities are too small", \hat{H} will not be a satisfactory estimator. One of the causes of the difficulty is that \hat{H} gives no weight to unobserved cells, so that if the total probability in unobserved cells is large, \hat{H} will not perform too well.

We can gain some insight in dealing with this, if we examine the second question we advanced, the estimation of the sample coverage. This problem is discussed in greater detail in B. Harris [3], but it is convenient at this time to make some intuitive observations concerning the estimation of C , so that we can resolve the difficulties noted above in the estimation of H .

First, note that if we were to proceed as Basharin did and set

$$\hat{C} = \sum \hat{p}_i$$

then we have that $\hat{C} = 1$ for all samples, which is clearly inappropriate. We can guide our intuition by first examining some extreme cases.

(1) If $n_1 = N$, then we readily reach the conclusion that C must be small. We can see this as follows. If we now take another observation, inasmuch as every past observation resulted in a new class being observed, it is apparent that with probability quite close to unity, the $N+1$ th observation will also result in a new class. In fact, the probability that the $N+1$ th observation will not result in a new class is C , which of course should be near 0, as noted.

(2) If, on the other hand, there is an integer t , substantially larger than one, such that $n_1 = n_2 = \dots = n_{t-1} = 0$, $n_t > 0$. Then, similar reasoning would lead us to conclude that most of the probability is concentrated in classes with high probability, and therefore C should be near unity.

(3) Let $p_i = \frac{1}{N}$, $i = 1, 2, \dots, N$. Then $E(n_1) \sim Ne^{-1}$ and $E(n_0) \sim Ne^{-1}$. Thus, we should have $C \sim 1 - e^{-1}$.

In short, as is shown in B. Harris [3], it is the low order occupancy numbers, such as n_1 , n_2 , and n_3 , which contain the principal information concerning the probability content of unobserved classes. A cursory examination of the three examples cited above suggest that an appropriate estimator for C is given by

$$(6) \quad \hat{C} = 1 - \frac{n_1}{N} .$$

In Harris [3], it is shown that \hat{C} is in fact an suitable estimator, in that it has good asymptotic properties.

In E. B. Cobb and B. Harris [2], a method for estimating entropy, when "all the sample information is contained in the low order occupancy numbers" was exhibited. In order to do this, we will show that we can represent entropy asymptotically by

$$(7) \quad H = \frac{1}{N} E(n_1) \int_{-\infty}^{\infty} e^x \log \left(\frac{N}{x} \right) dF^*(x)$$

where

$$(8) \quad F^*(x) = \sum_{Np_j \leq x} Np_j e^{-Np_j} / \sum_{j=1}^{\infty} Np_j e^{-Np_j} .$$

It is easily verified that $F^*(x)$ is a cumulative distribution function. Since

$$(9) \quad E(n_1) \sim \sum_{j=1}^{\infty} N p_j e^{-N p_j}$$

substitution of (8) and (9) into (7) produces

$$\frac{1}{N} \sum_{j=1}^{\infty} e^{N p_j} \log \left(\frac{1}{p_j} \right) N p_j e^{-N p_j} = - \sum_{j=1}^{\infty} p_j \log p_j = H$$

which verifies (7).

Under the assumptions stated above Cobb and Harris [3] suggested that the entropy be estimated by

$$(10) \quad \bar{H} = \frac{n_1}{N} \frac{(N-m_1)^2}{(N-m_1)^2 + (m_2-m_1)^2} e^{(Nm_1-m_2)/(N-m_1)} \log \left[\frac{N(N-m_1)}{Nm_1-m_2} \right]$$

where $m_1 = 2n_2/n_1$ and $m_2 = \max(m_1^2, 6n_3/n_1)$.

At this point it is worthwhile to present a numerical example, which will illustrate the behavior of \bar{H} .

Example $p_i = \frac{1}{N}$, $i = 1, 2, \dots, N$. Then $n_1 \sim Ne^{-1}$, $n_2 \sim \frac{N}{2} e^{-1}$, and

$n_3 \sim \frac{N}{6} e^{-1}$. Thus, $m_1 \sim 1$, $m_2 \sim 1$ and

$$F^*(x) = \begin{cases} 0 & x < 1 \\ 1 & x \geq 1 \end{cases}$$

Then

$$\bar{H} \sim \frac{Ne^{-1}}{N} \frac{(N-1)^2}{(N-1)^2} e^{-(N-1)/(N-1)} \log \left[\frac{N(N-1)}{N-1} \right] = \log N$$

and $H = \log N$, which is as it should be.

Clearly, it is principally the classes with small probabilities that contribute to n_0, n_1, n_2 , and n_3 . For those classes with large probabilities, we can estimate p_i by \hat{p}_i .

Then, the natural way of proceeding is to estimate the contribution to entropy from large classes by means of Basharin's method and the contribution of small classes by H , and we denote the final estimator by H^* . Recall that in order to use H , we have taken n_1, n_2 , and n_3 to determine H .

There is one last detail which must be taken into account. Part of the contribution to moderate order occupancy numbers, such as n_4, n_5 , and some of the succeeding occupancy numbers, will be due to classes with small probabilities and the effect of sample fluctuations. Therefore, we need to examine the following. What proportion of each n_j , $j = 4, 5, \dots, s$, s some sufficiently large integer, is due to a large deviation from a class with small probability? We can adopt a Theorem due to A. Wald [4] obtaining the following inequalities.

$$(11) \quad \text{if } m_2 > m_1^2, \quad E(n_{k+1}) \geq \frac{6(3^{k-2})n_3^{k-1}}{(k+1)!n_2^{k-2}}, \quad k = 3, 4, \dots,$$

$$(12) \quad \text{if } m_2 = m_1^2, \quad E(n_{k+1}) \geq \frac{2^k n_2^k}{n_1^{k-1}(k+1)!}, \quad k = 3, 4, \dots$$

The right hand side of each inequality gives the expected values of n_{k+1} , if "the sample information is contained in n_1, n_2 , and n_3 ". Thus the difference between the left and right hand sides of (11) and (12) gives an estimate of the contribution to n_{k+1} which is due to classes with larger probabilities. We apply Basharin's estimator (3) to these, upon replacing the expected values in the left hand sides of (11) and (12) by the observed values.

Thus, we finally write

$$(13) \quad H^* = \lambda \hat{H} + (1-\lambda) \bar{H}$$

where $0 \leq \lambda \leq 1$ is the proportion of the observations in n_1, n_2 , and n_3 and the parts of n_4, n_5, \dots, n_s determined by (11) and (12). For the parts of the sample allocated to small classes as noted above we use \hat{H} , and use \bar{H} on the part allocated to large classes.

The mathematical details will be given in a later publication.

REFERENCES

- [1] Basharin, G.P., (1959) On a statistical estimate for the entropy of a sequence of independent random variables. *Teoriya Verojatnostei i ee Primenija*, 333-336.
- [2] Cobb, E.B. and Harris, B. An asymptotic lower bound for the entropy of discrete populations with application to the estimation of the entropy of almost uniform populations. (Submitted for publication).
- [3] Harris, B. (1959) Determining bounds on integrals with applications to cataloging problems. *Annals of Mathematical Statistics*, 30, 521-548.
- [4] Wald, A. (1939) Limits of a distribution function determined by absolute moments and inequalities satisfied by absolute moments. *Transactions of the American Mathematical Society*, 46, 280-306.

APPLICATION OF NUMERICAL TECHNIQUES
TO
EXPERIMENTALLY MODEL AN AERODYNAMIC FUNCTION*

Andrew H. Jenkins

Physical Sciences Laboratory, Directorate of Research and Development
U. S. Army Missile Command, Redstone Arsenal, Alabama

ABSTRACT. This report describes the use of an aeroballistic range in the design and execution of an aerodynamic experiment, the analysis of the experimental data by numerical techniques to develop a model of a physical function, and the statistical testing of the data and the model. The report discusses the approach, the experimental design, and the testing of the data using several frequency distributions. It presents and describes a multivariate nonlinear regression analysis performed on the data, the physical model developed by the regression analysis, and the testing of the model. It also lists and presents the tests of hypotheses made and discusses the results of the tests.

SYMBOLS

a	Acoustic velocity in air
A	Pure constant of regression equation
b	First coefficient of regression equation
C	Counts per inch of photoreader = 3502
c	Second coefficient of regression equation
c_p	Coefficient of specific heat at constant pressure
c_v	Coefficient of specific heat at constant volume
d. f.	Statistical degrees of freedom
F	Frequency distribution
F_{sh}	Magnification factor of shadowgraph = 1.009
F_{sc}	Magnification factor of Schlieren = 0.855
K	Ratio of shock density ρ_s to free stream density ρ^∞
ln	Natural logarithm (base e)

*This article was initially issued as U. S. Army Missile Command Report No. RR-TR-65-11.

SYMBOLS (continued)

M	Mach number = V/a
M_1	Mach factor level = 1.1 to 1.5
M_2	Mach factor level = 2.5 to 2.9
M_3	Mach factor level = 3.9 to 4.3
M_i	Mach factor effect in statistical equation
M_ℓ	Mach factor linear effect
M_q	Mach factor quadratic effect
MR_{ij}	Main factor interaction effect
N	Total observation
P	Statistical probability
r	Regression correlation coefficient
R_o	Universal gas constant. = 1715 sq. ft./sq. sec./°R.
R	Radius
R_1	Model nose/base radius ratio = 1.0
R_2	Model nose/base radius ratio = 0.7
R_3	Model nose/base radius ratio = 0.4
R_b	Model base radius = 0.112 inch
R_j	Radius factor effect in statistical equation
R_n	Nose radius of model
R_r	Model nose to base radius ratio
R_ℓ	Radius factor linear effect
R_q	Radius factor quadratic effect
S	Surface roughness of model
S_e^2	Experimental sample variance
S_e	Experimental sample standard deviation

SYMBOLS (continued)

SS	Sum of squares
t	Value of students frequency distribution
T	Absolute temperature (°Rankine)
V	Flight model velocity
\bar{X}	Mean
\bar{X}_{aw}	Mean of Ambrosio-Wortman model
\bar{X}_e	Mean of experimental responses
X_i	i th response
\bar{X}_r	Mean of regression model responses
$X_{2, 3}$	Dependent variable of regression equation (computer language)
Y	Independent variable of regression equation (computer language)
Z	Normal frequency distribution
α	Type I error risk level
β	Type II error risk level
γ	Ratio of specific heats = c_p/c_v
δ_{sh}	Shock detachment distance from shadowgraph optical system
δ_{sc}	Shock detachment distance from Schlieren optical system
Δ	Shock detachment distance in photoreader counts (corrected)
$\epsilon_{k(ij)}$	Experimental error
σ_e^2	Variance of experimental responses
σ_r^2	Variance of regression model
σ_{aw}^2	Variance of Ambrosio-Wortman model
μ	Universal means
χ^2	Frequency distribution
ρ	Density

1. INTRODUCTION. A number of new aerodynamic problems have come into prominence in recent years. The source of the problems has been the very high flight velocities achieved by use of rockets. The characteristics of the problems of the very high flight velocities, referred to as supersonic or hypersonic flight, are those of a hydrodynamic nature. The Mach numbers are high and problems of a physical and chemical nature also exist because the energy of the flow is large. The gases are rarefied so that the mean free path is not negligibly small compared with an appropriate macroscopic scale of the flow field. Under such conditions, kinetic theory is included with the hydrodynamics.

The new features of a hydrodynamic nature allow the use of certain simplifying assumptions in developing theories for hypersonic flow. On the other hand, certain important features which appear introduce additional complications over those met within gas dynamics at more moderate speeds. The techniques of linearization of the flow equations and the use of mean-surface approximation for boundary conditions have a diminishing range of applicability. Also, entropy gradients produced by curved shock waves make the classical isentropic irrotational approach inapplicable.

The additional problems of a physical and/or chemical nature are associated with the high temperatures of the flow as the gases traverse the strong bow shock wave. The sudden shock heating of the gases excites the vibrational degrees of freedom of the molecules resulting in dissociation of the species into atoms, electrons, and ions which do not require treatment at lower velocities. Therefore, it must be recognized that physical phenomena rather than hydrodynamic phenomena may not only influence the flow but in many cases control it. In view of the complexities of the flow at high Mach numbers and the number of technical disciplines involved, many have resorted to experimental or empirical development of functional relationships.

The flow field originates at the bow shock. The shock wave characteristics are very important to the stagnation region characteristics. The volume of the stagnation region is dependent on the shock detachment distance. Therefore, much of the knowledge of the flow characteristics is dependent on the knowledge of the shock location. Experiments have been performed on wind tunnels to study the shock location. However, few experiments have been made to study this problem under free flight

conditions. Also, the studies which have been made and the derived relationships are lacking as tests have not been attempted to determine their reliability.

It is apparent that the community recognizes the need for improved hypersonic design theory. One of the important areas is the prediction of shock detachment distance. It is important to the computation of not only heat transfer but also pressure distributions and drag on the fore-part of the vehicle. This has been pointed out by Serbin [1], Ambrosio and Wortman [2], DiDonato and Zondek [3], Heberle, Wood, and Gooderum [4], and Love [5].

The lack of purely theoretical models for the prediction of shock detachment distance at transonic and supersonic velocities has led to the natural consequence of an experimental approach. This is to be expected and in addition the theoretical hypothesis is inevitable subject to experimental verification. For this reason, one can also expect to contribute to scientific progress by the inverted approach of formulating models of the mathematical relationships between physical variables by experimentation. However, the relationships derived are subject to experimental control, measurement accuracy, human error, and many other sources of unexplained or unaccounted for deviations from the true universal relationships.

In the direct approach (i.e., the a priori derivation of a mathematical model) quite often ideal physical conditions are assumed and simplifying mathematical assumptions are made which depart from the real case. Therefore, one cannot be sure of the theory nor can one be certain of the experimental data. Yet, in scientific endeavor, exacting conclusions are often drawn by the comparison of an idealized hypothesis and real case data. That is, both quantities are coupled to each other and not to an independent estimate of the deviation present.

Empirical models of the shock detachment distance for blunt bodies of revolution have been made by Serbin [1], Ambrosio and Wortman [2], and Heberle, Wood, and Gooderum [4]. The data were obtained by these authors using moving streams of air surrounding stationary spheres (i.e., radius nosed bodies) in such experimental devices as wind tunnels and jet nozzles. Both of these devices have two common disadvantages. The gaseous medium is in a state of expansion just prior to the shock

compression. Also, holding devices are present in the flow around the body which cause perturbations in the flow. The flow is often not uniform in cross section. The measurements, therefore, include these perturbations and do not represent the real case of a vehicle in free flight.

Serbin [1] derived the following relationship for a sphere:

$$(1) \quad \frac{\Delta}{R} = 2/3 (K - 1)^{-1},$$

Ambrosio and Wortman² derived the following relationship:

$$(2) \quad \frac{\Delta}{R} = 0.143e^{3.24/M^2},$$

and Heberle, Wood, and Gooderum⁴ derived this relationship:

$$(3) \quad \frac{\Delta}{R} = 4/3 (M - 1)^{-1/3}.$$

Each author stated that agreement between the model and the data was very satisfactory. However, the standard by which this was determine was not stated or explained. This type of unexplained, seemingly arbitrary, acceptance of a model and data appeared to be typical.

A machine literature search was made. In this search, over 100,000 documents were screened and matched by computer on the basis of key words and terms in aerodynamics and statistics. This was done to determine if, in the past, any use of statistics in testing aerodynamic experimental data had been done. Not one document was found during the search. However, this is not to imply that statistics have not been used. Apparently, it is either not a prevalent or accepted practice or possibly has not been reported.

Ambrosio and Wortman [6] did attempt the use of some simple statistical methods. This was done to the extent of computing the mean, the absolute mean, and the standard deviation. However, it was not for the purpose of testing the reliability of their data and model but to objectively establish the relative worth of their model as compared to Serbin[1].

This work has two objectives as follows:

- 1) To develop an empirical model of shock detachment distance as a function of Mach number and vehicle nose radius with experimental data obtained under free flight conditions
- 2) To subject this model and data to analysis by statistical methods to objectively define the level of confidence of such a model.

II. EXPERIMENTAL PROCEDURES.

1. Design

The shock detachment distance can be described aerodynamically for radius nosed bodies of revolution as:

$$(4) \quad \Delta = f(M, R).$$

Explicit models of several investigators were mentioned in the introduction.

Statistically, the model can be expressed as:

$$(5) \quad \Delta = \mu + M_i + R_j + MR_{ij} + \epsilon_{k(ij)}.$$

The model contains two independent factors, Mach number (M_i) and body radius (R_j). It also contains a second order effect, the MR_{ij} interaction.

The design of the experiment required consideration of both the aerodynamic and the statistical aspects. Past experience indicated that the shock detachment distance was a nonlinear function of Mach number (M) and a linear function of radius (R). The objectives of the experiment are to determine if the linear and quadratic effects of Mach number and radius contribute significantly to the shock detachment distance. Also, it was desired to determine if a second order or interaction effect between radius and Mach number contributes significantly to the shock location. The analysis of variance is a useful tool for this. In addition, it was also desired to develop an empirical model of the functional relationships between the independent and dependent variables. A regression analysis was planned for this.

The analysis of data by regression calculation can be simplified by the equal spacing of the independent variables which permits the use of orthogonal polynomials. This helps also in the subsequent adjustment arising from the discarding of insignificant variables or the addition of new terms. One objective of the experiment is to estimate the slope of the regression. The slope of a regression is estimated more precisely if the values of the independent variables are selected with equal spacing at the extremes of the quantified ranges of the variable. This is because interpolation is more reliable than extrapolation and the computations are simplified.

The effects of the main factors in this experiment could not be considered theoretically independent. Therefore, it is necessary to replicate the experiment within cells of all factor levels in order to test for interactions between factors and to estimate the experimental error. Since one objective is to statistically test for interaction, the analysis of variance will enable the test of interaction and estimates of error variance. The two best tests for statistical analysis of the aerodynamic experiment are the analysis of variance and the multivariate regression analysis. The experimental design most efficient for these methods is the factorial experiment with replication.

The factorial experiment enables one to test the effects of Mach number (M) and radius (R) on the shock location (Δ) over the ranges of interest of M and R at each factor level. It also promotes testing for the existence of interaction between M and R and the effect of interaction on Δ . One is also able to differentiate interaction effects from main effects. In addition, it allows the determination of confidence limits for the estimates of main and interaction effects based on the estimate of experimental error derived from replication.

Therefore, the experiment was designed as a fixed model 3^2 factorial. Both the radius and Mach number factors are equispaced three level, fixed and quantitative. The Mach number range of interest was 1.0 to 4.5. The levels selected were $M_1 = 1.1$ to 1.5, $M_2 = 2.5$ to 2.9, and $M_3 = 3.9$ to 4.3. The radii selected were nose to base radius ratios of $R_1 = 1.0$, $R_2 = 0.7$, and $R_3 = 0.4$. The experiment was replicated three times in each factor cell; therefore, a total of 27 observations was recorded ($N = 3 \times 3 \times 3 = 27$).

All 27 responses could not be obtained in 1 day. Therefore, to compensate for day-to-day variations in personnel, voltages, developing solutions, film batches, and printing, the firing sequence was randomized. All combinations of factors and replicates were listed and the experimental sequence was randomized by use of a random number generator [7] which was entered in a random manner. The results of the randomization are shown in Table I. The numbers shown without parentheses are the sequence of firing while the numbers in parentheses are the corresponding round identification numbers. Table I also shows the factor levels selected for the experiment.

Table I. Randomized Experimental Sequence

Nose/Base Radius Ratio	Replicate	Mach Number Levels		
		M ₁ 1.1 to 1.5	M ₂ 2.5 to 2.9	M ₃ 3.9 to 4.3
$R_1 = 1.0$	1	26 (75)	7 (56)	11 (60)
	2	22 (71)	8 (57)	6 (54)
	3	2 (49)	14 (63)	10 (59)
$R_2 = 0.7$	1	12 (61)	13 (62)	9 (58)
	2	23 (72)	27 (76)	25 (64)
	3	24 (73)	18 (67)	15 (66)
$R_3 = 0.4$	1	16 (65)	3 (50)	19 (68)
	2	1 (48)	17 (66)	5 (53)
	3	4 (52)	20 (69)	21 (70)

Notes:

1. Numbers without parentheses are randomly determined program firing sequence.
2. Numbers with parentheses are for experiment identification.

The radii of the models are discrete levels. The Mach number levels are discrete intervals as it is almost impossible to duplicate exact velocities by this method of experiment. This is due to variations in propellants, model material homogeneity, and model-launch tube interference. The Mach number levels chosen were fixed in selected ranges between Mach 1.0 and 4.5 which is the velocity regime of interest in this aerodynamic study. As a two factor fixed model experiment, it is assumed that μ is a fixed constant and the $\epsilon_{k(ij)}$'s are normally and independently distributed with a zero mean.

2. Procedure

The experimental data were obtained on the Physical Sciences Laboratory's free flight aeroballistic range. Figure 1 shows the experimental apparatus. It consists of a light gas gun for launching the models, and altitude simulation chamber, a shadowgraph and a Schlieren system for photographing the model and the flow around the model. Also, submicrosecond electronic counters to determine the model's time of flight are included.

The aerodynamic data required from this experiment are the radius of the model, the Mach number of the model, and the detachment distance of the shock. The radius of each model was known as the models were formed in accurately machined dies. Their geometries are shown in Figure 2. The models were made of copper coated lead. The Mach number is determined by taking the ratio of the model velocity to the acoustic velocity when the photographs are made. The acoustic velocity is computed as shown in Appendix A. It is seen that the acoustic velocity varies as the square root of the temperature and specific heat ratio. The temperature was recorded at the time of launching each model. The specific heat ratio was taken as 1.4. The model velocity was computed by taking the ratio of the distance between the shadowgraph and Schlieren stations to the time recorded on the counter. The distance between the shadowgraph and Schlieren stations is a constant of 5 feet. It was assumed that the deceleration of the model over 5 feet was linear; therefore, the velocity computed was the velocity of the model midpoint between the two stations.

Photographs of the model showing the shock detachment distance were taken by both the shadowgraph and Schlieren systems. The measure of the shock detachment distance from either one of these photos

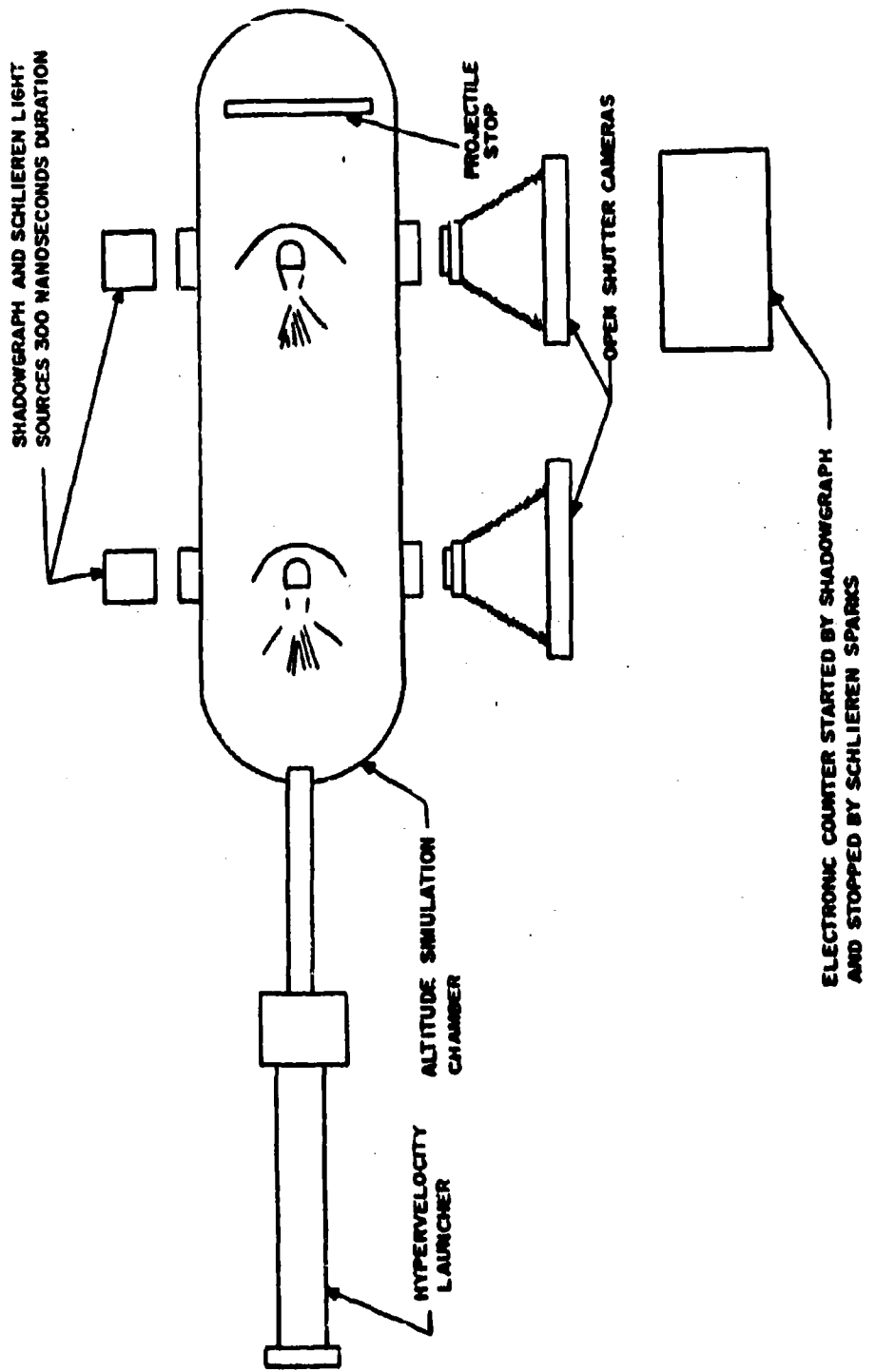


Figure 1. Arrangement of Experimental Apparatus

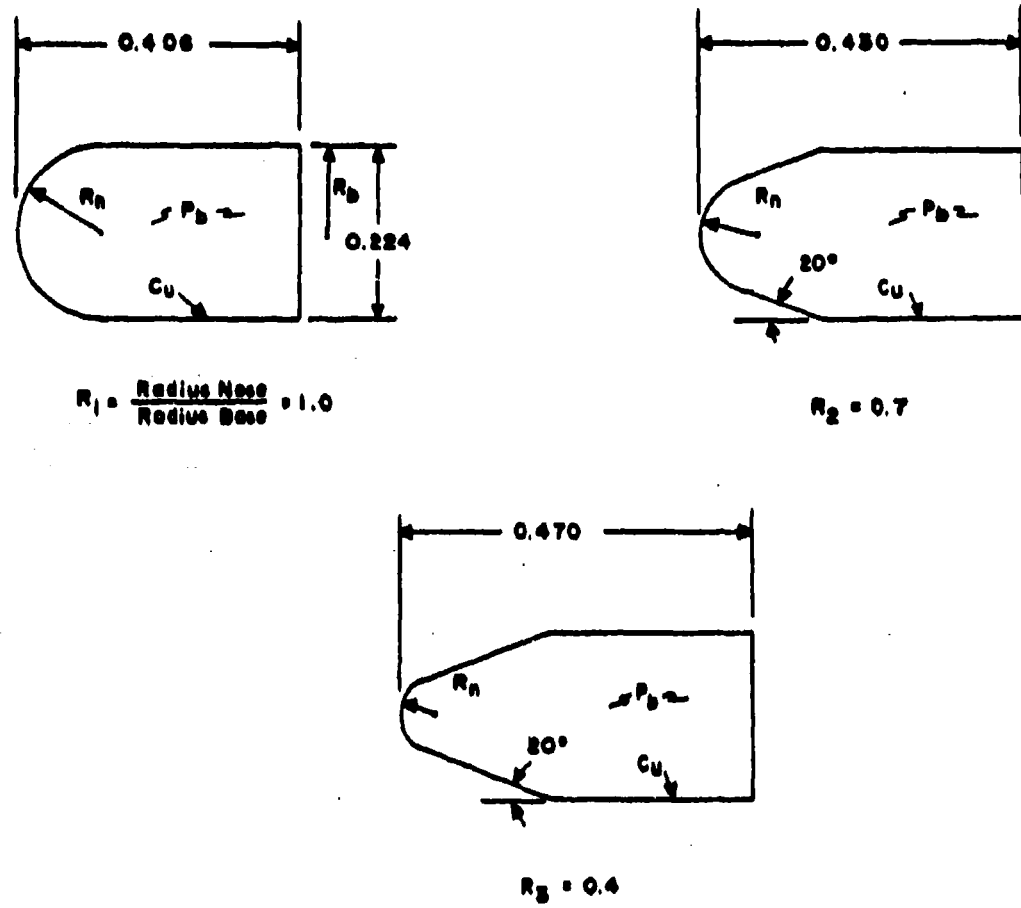


Figure 2. Sketch of Experimental Flight Models

would not coincide with the velocity of the model. Therefore, with the assumption of linearity, the shock detachment distance was corrected to the velocity computation. The correction of the detachment distance required the consideration of the magnification factors for the photographs. The magnification factor for the shadowgraph camera was 1.009 and the Schlieren camera was 0.855. The photo reader upon which the negatives were read was calibrated at 3502 electronic counts per inch in the plane of the negative on the photo reader. The shock detachment distance was read in counts from both the shadowgraph and Schlieren negatives. The detachment distance and radius of each type model was corrected to counts as follows:

$$(6) \quad \Delta = \delta_{sh} F_{sc} + \delta_{sc} F_{sh}$$

and

$$(7) \quad R = 2 \times C \times R_b \times F_{sh} \times F_{sc} \times R_r .$$

The values of Δ and R computed for each round are shown in Table II. A sketch of a typical shock detachment distance as taken by the shadowgraph and Schlieren is shown in Figure 3.

The experimental data obtained from the experimental program are compiled in Table II. The data are tabulated and identified by the round number assigned on the aeroballistic range. Computations of certain data presented in Table II are shown in Appendix A. The data from round number 75 were used to show a typical example of the computational procedures.

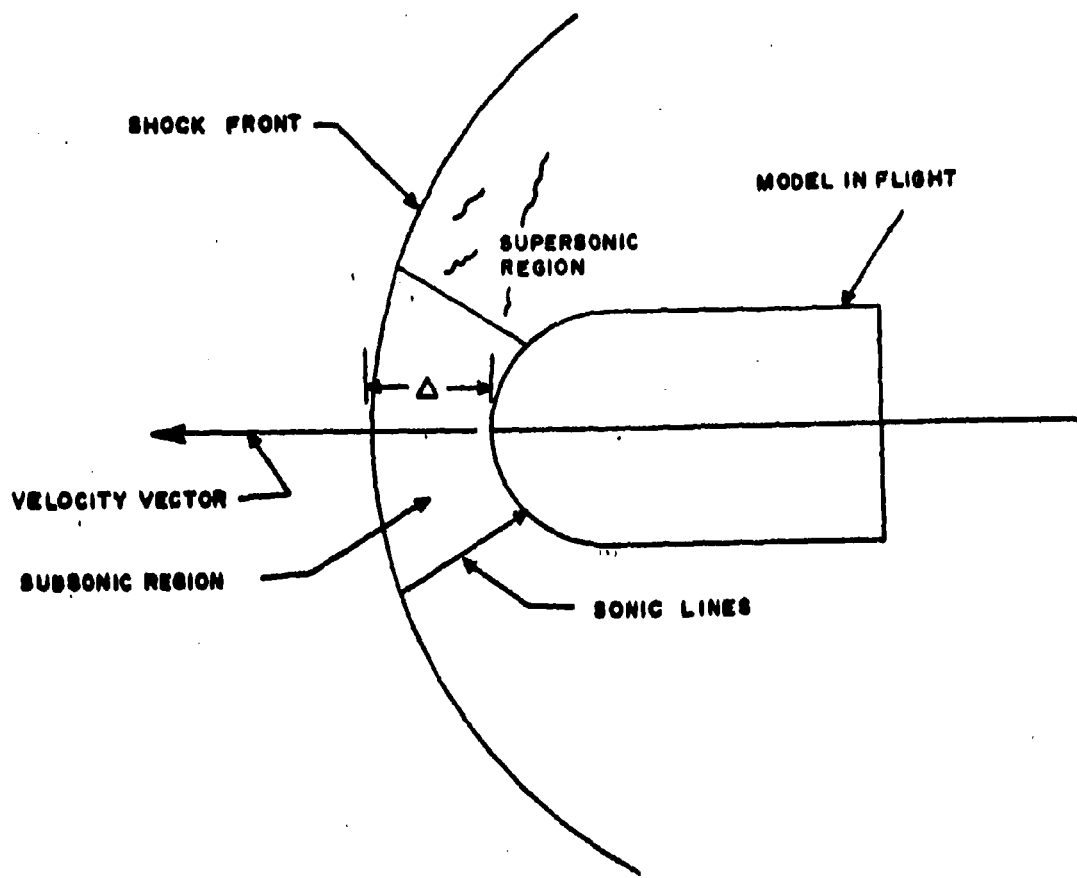


Figure 3. Sketch of Typical Shock Detachment

Table II. Compilation of Experimental Data

Row No.	Radius Ratio R_2/R_1	Nozzle Radius (Centimeters)	Mach Range	Temp. (°F)	Scale Vol. (fpo)	Mach No. V/A	Model Vol. (fpo)	Mach No. V/A	Shadow- Graph (Counts : 1)	Schlieren (Counts)	$\frac{A}{R}$	
75												
71	$R_1 = 1.0$	676.74	M_1 1.1 - 1.5	71	1131	1416	1.252	390	373	710	1.049	
69					73	1131	1303	1.152	540	543	1010	1.492
56					73	1133	1342	1.164	487	450	870	1.286
57	$R_1 = 1.0$	676.74	M_2 2.5 - 2.9	75	1135	3142	2.768	73	36	99	0.146	
63					73	1133	2969	2.620	78	32	99	0.146
60					72	1132	3215	2.840	92	49	124	0.189
34	$R_1 = 1.0$	676.74	M_2 3.9 - 4.3	72	1132	4541	4.011	162	63	151	0.223	
59					72	1132	4474	3.932	66	37	94	0.139
61					72	1132	4500	3.975	69	36	95	0.140
72	$R_1 = 0.7$	473.72	M_1 1.1 - 1.5	71	1131	1329	1.175	342	396	692	1.461	
73					71	1131	1156	1.022	1340	1438	2595	5.478
62					71	1131	1264	1.118	688	688	910	1.921
76	$R_1 = 0.7$	473.72	M_2 2.5 - 2.9	71	1131	3142	2.778	106	36	127	0.268	
67					71	1131	3069	2.714	56	41	89	0.188
58					74	1134	3259	2.874	91	42	120	0.253
74	$R_1 = 0.7$	473.72	M_2 3.9 - 4.3	72	1132	4464	3.943	61	24	86	0.182	
64					71	1131	4516	3.993	67	27	85	0.179
65					71	1131	4500	3.979	75	33	97	0.235
50					72	1132	1326	1.171	257	248	670	1.736
66	$R_1 = 0.4$	270.70	M_1 1.1 - 1.5	73	1133	1478	1.307	142	157	240	1.034	
52					72	1132	1284	1.133	332	320	607	2.243
53					73	1133	3306	2.908	50	18	61	0.226
67					71	1131	3242	2.866	64	21	76	0.280
68					70	1129	3589	3.179	72	23	87	0.321
53	$R_1 = 0.4$	270.70	M_2 3.9 - 4.3	70	1129	4730	4.190	53	27	95	0.203	
70					72	1132	4228	3.784	43	20	57	0.710
					70	1129	4662	4.112	64	22	59	0.217

III. ANALYSES. The data obtained from the experiment are presented in Table II. The observations taken as the dimensionless ratio of the standoff distance divided by the model radius are presented in the factorial design layout in Table III along with some computations in preparation for performing an analysis of variance. The statistical computations are presented in Appendix B.

The gathering of the data, the analysis, and derivation of the model of the functional relationships from the experimental observations are based on certain aerodynamic and statistical assumptions. These assumptions are:

- 1) Small angles of attack of the models (i.e., less than 2°) do not significantly effect the detachment distance.
- 2) The models were free from ablation products in the stagnation region.
- 3) The effects of gas constituent dissociation on the dynamics of flow was insignificant.
- 4) The effects of spin stabilization on the dynamics of flow was insignificant.
- 5) The effect of the conical section of two of the models on the dynamics of the flow was insignificant (i.e., all projectiles were hemispheres of various radii).
- 6) The experimental error is normally and independently distributed.
- 7) The experimental precision is essentially the same for all factor combinations.
- 8) The factors were fixed at discrete levels so, therefore, are not independent of each other.

Assumptions 1 through 5 are made concerning the aerodynamics of the experiment. These represent sources of variation which are considered negligible. They cannot be separated explicitly from the main

Table III. Data Layout for Shock Detachment Experiment

		Mach Number Region			ΣX_j	X_j	
		M_1	M_2	M_3			
Body Radius Ratio	$R_1 = 1.0$	1.049	0.146	0.223			
		1.492	0.146	0.139	4.810	0.5344	
		1.286	0.189	0.140			
		3.827	0.481	0.502			
	$R_2 = 0.7$	1.461	0.268	0.182			
		5.478	0.188	0.179	10.135	1.126	
		1.921	0.253	0.205			
		8.860	0.709	0.566			
	$R_3 = 0.4$	1.034	0.225	0.203			
		2.243	0.280	0.210	6.469	0.719	
		1.736	0.321	0.217			
		5.013	0.826	0.630			
ΣX_1		17.700	2.016	1.698	$\Sigma X_+ = 21.414$		
X_1		1.967	0.244	0.189	$X_+ = 0.793$		
						$\Sigma \Sigma \ddot{X}_+ = 50.7464$	

and interaction effects. It is important to note that, even though considered negligible, these variations are present and are statistically accounted for by summation into experimental error. The statistical assumptions 6 through 8 allude to these conditions.

1. Analysis of Variance

The experiment was described in Section II by the statistical model

$$(8) \quad \Delta = \mu + M_i + R_j + MR_{ij} + \epsilon_{k(ij)}$$

The theoretical model underlying the analysis of variance assumes that each experimental response of the shock detachment distance (Δ) is the algebraic sum of:

- 1) An overall mean of the detachment distance, μ (i.e. true standoff distance)
- 2) A Mach number effect on the standoff distance, M_i
- 3) A radius effect on the standoff distance, R_j
- 4) An interaction effect on the standoff distance, MR_{ij}
- 5) A random residual error (experimental), $\epsilon_{k(ij)}$

Since the model is a fixed model, none of the effects can be measured absolutely. They can be measured only as differential deviations, i.e., the M_i as deviations from μ , the R_j as deviations from μ , and the MR_{ij} as deviations from $M_i + R_j$.

The results of the analysis of variance are shown in Table IV. The computations are presented in Appendix B.

From Table IV, it can be seen that the main effects of radius have apparently no significant effect on the shock detachment distance at the 95 percent level of confidence. The linear and quadratic effects are also insignificant. The quadratic effects of radius seem to have the most effect on the standoff distance. They would be significant at the 80 percent level of confidence though still not significant at the 95 percent level.

Table IV. Analysis of Variance

Source of Variation	Degrees of Freedom (d.f.)	Sum of Squares (SS)	Mean Square (MS)	F Value (Computed)	Expected Mean Square	
					F Value (Tables) $\alpha = 0.05$ df source	EMSS
S. No. (R_i)	2	1.6499	0.8249	1.410	3.55	$e_q^2 + e_R^2$
R_i	1	0.1529	0.1529	0.261	4.41	$e_R^2 = 0.027$
R_q	1	1.4970	1.4970	2.560	4.41	
Mach No. (MR_1)	2	18.5583	9.2991	15.904	3.55*	$e_q^2 + e_M^2$
M_1	1	14.3146	14.3146	24.481	4.41*	$e_M^2 = 0.967$
M_q	1	4.2837	4.2837	7.478	4.41*	
Interaction (MR_{ij})	4	2.9985	0.7471	1.277	2.93	$e_q^2 + 3e_M^2$
$R_i M_i$	1	0.0855	0.0855	0.146	4.41	$e_M^2 = 0.054$
$R_i M_q$	1	2.1980	2.1980	3.759	4.41	
$R_q M_i$	1	0.0108	0.0108	0.018	4.41	
$R_q M_q$	1	0.6942	0.6942	1.187	4.41	
Error ($e_{ij(l)}$)	18	10.5261	0.567		e_q^2	$e_q^2 = 0.585$
Total	26	33.7628				35.10

*Significant

The Mach number is significant at the 95 percent level of confidence. The computed value in the F test is greater than the F distribution table value by a factor of about 5. The linear and quadratic effects are also significant. The linear effect of the Mach number factor was found to be more significant than the quadratic effect.

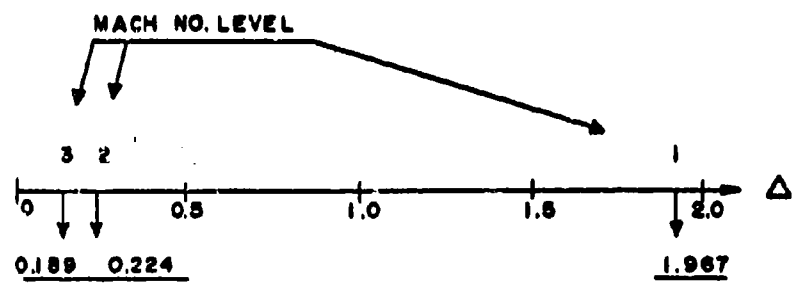
The analysis of variance also shows that there is apparently no significant effect of the MR_{ij} interaction on the standoff distance. It is interesting to note, however, that of all the combinations of linear and quadratic interactions between Mach numbers and radii, the quadratic radius and linear Mach number were most nearly significant at the 95 percent level of confidence. This is congruent with the fact that the test of the quadratic effects of radius and the linear effects of Mach number was highest in the main effects tests. Under the interaction effects tests, the computed value of 3.759 for the R_qM_1 combination would be significant at the 92 percent level as compared to 4.41 for the F value at the 95 percent level.

It is also noted in Table IV that the mean square for radius and radius-Mach number interactions were only slightly higher than the mean square for error. On the basis of the assumption that the experimental error is normally distributed between all factors and all levels, then radius and interaction effects do not significantly contribute to shock detachment distance within the limits of this experiment.

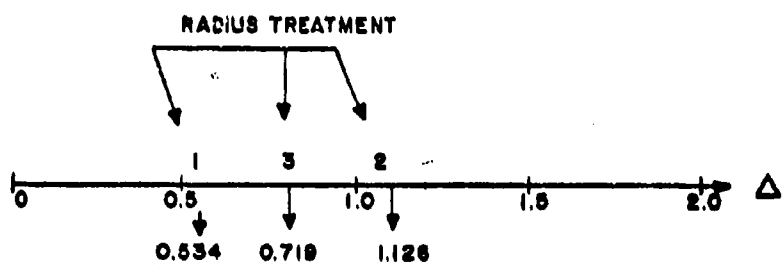
The results of the analysis of variance, as shown in Table IV, is further analyzed as shown in Figure 4. Figure 4 is the graphic display of the results of the Duncan range tests as computed in Appendix B. Figure 4(a), for the Mach number range significance test, shows that the M_1 level (1.1 to 1.5) is significantly different from the M_2 and M_3 levels of 2.5 to 2.9 and 3.9 to 4.3, respectively. The M_2 and M_3 levels were not found to be significantly different from each other. The radius factor range test as shown in Figure 4(b) shows the radius factor levels not significantly different from each other. The fact that the M_2 and M_3 levels are not significantly different from each other will be discussed later in this section.

2. Regression Analysis

The analysis of variance can be performed whether the factors are quantitative or qualitative. When the factors are quantitative, then



(a) MACH NUMBER RANGE SIGNIFICANCE TEST



(b) RADIUS RANGE SIGNIFICANCE TEST

(COMMONLY UNDERLINED MEANS ARE NOT SIGNIFICANTLY DIFFERENT
AND COULD HAVE COME FROM A COMMON POPULATION)

Figure 4. Graphic Display of Duncan Range Tests

a regression analysis can be performed on the data. This analysis is especially useful in the determination of the general functional relationships of the factors at other than the experimentally assigned levels. The analysis of variance has led to knowledge of the important factor considered in this experiment which contributes to the shock detachment distance. This was found to be the linear and quadratic effects of Mach number. This led to a bivariate regression analysis. The regression analysis used was the SNAP Multiple Regression Analysis for the IBM 7090 computer. It was the Army Missile Command SHARE 183 program.

As pointed out, it is realized that the shock detachment distance is not singularly a function of Mach number. There are other factors which were not included in this experiment. For the factors considered by the analysis of variance, some knowledge of the main significant factor (Mach number) is now available.

Before progressing with the regression analysis, the physical aspects of the shock detachment distance must be considered. The functional relationship must be consistent with the aerodynamic concepts of the detachment distance. The detachment distance is inversely proportional to Mach number. That is:

$$(9) \quad \Delta = \frac{1}{f(M)} = f\left(\frac{a}{V}\right)$$

The limits of the functional relationships are then

$$\lim_{a \rightarrow 0} f\left(\frac{a}{V}\right) = \lim_{M \rightarrow \infty} \frac{1}{f(M)} = \lim_{M \rightarrow \infty} \Delta = \infty$$

$$a \rightarrow 0 \quad M \rightarrow \infty$$

$$\lim_{a \rightarrow \infty} f\left(\frac{a}{V}\right) = \lim_{M \rightarrow 0} \frac{1}{f(M)} = \lim_{M \rightarrow 0} \Delta = 0$$

$$a \rightarrow \infty \quad M \rightarrow 0$$

$$\lim_{V \rightarrow 0} f\left(\frac{a}{V}\right) = \lim_{M \rightarrow \infty} \frac{1}{f(M)} = \lim_{M \rightarrow \infty} \Delta = 0$$

$$V \rightarrow 0 \quad M \rightarrow \infty$$

$$(10) \quad \lim_{V \rightarrow \infty} f\left(\frac{a}{V}\right) = \lim_{M \rightarrow 0} \frac{1}{f(M)} = \lim \Delta = \infty$$

$$\lim_{V \rightarrow a} f\left(\frac{a}{V}\right) = \lim_{M \rightarrow 1} \frac{1}{f(M)} = \lim \Delta = \text{constant.}$$

The functional relationship as determined by the regression analysis should be compatible with these bounds and pass the limit tests.

The computer program is a linear multiple regression analysis. However, the analysis of variance indicated that the linear and quadratic effects of Mach number are significant. Therefore, a transformation was required to make the computer program applicable to the hypothesized relationship. The relationship is hypothesized as

$$(11) \quad \Delta = AM^b M^c.$$

A physical limitation of the functional aspect of Δ is that

$$(12) \quad \frac{\Delta + R_n}{R_n} > 1$$

because as the free stream Mach number goes to infinity, the shock is no longer detached but attached and the standoff distance is zero. Therefore, the desired functional form of the equation is

$$(13) \quad \frac{\Delta}{R_n} = AM^b M^c,$$

which presents the detachment distance as a dimensionless ratio, which is a more usable form for design engineering purposes.

This is not to indicate the dependence of detachment distance on body nose radius but to account for differences in body geometry. That is, the equations of detachment distance for bodies with radius noses cannot be used for sharp pointed bodies such as cones or purely blunt bodies such as right circular cylinders. Therefore, this functional relationship is for a geometric class of bodies, i.e., radius nosed bodies.

Equation (11) was programmed for the regression analysis by using the natural logarithm transformation. The equation programmed was

$$(14) \quad \ln \frac{\Delta}{R} = \ln A + b \ln M + c \ln M.$$

In computer language, the equation was

$$(15) \quad \ln Y = \ln A + b \ln X_1 + c \ln X_2.$$

The values of Δ/R and M were taken from Table II and programmed into the computer, where

$$(16) \quad \begin{aligned} Y &= \frac{\Delta}{R} \\ X_1 &= M \\ X_2 &= M^2. \end{aligned}$$

The computer transformed the experimental data to the natural logarithm form.

The results of the computer regression analysis are shown in Table V. The computer made two runs. After the first run, the results are automatically tested for significance ($\alpha = 0.05$) and the insignificant variables are dropped. It can be seen that the X_2 term was dropped by the computer. The data for run 2 were taken as the final regression analysis values. The pure constant (A), the first coefficient (b), and the regression coefficient (r) were tested and found significant as shown in Table V and Table VI. The regression equation is therefore:

$$(17) \quad \begin{aligned} \ln Y &= \ln A + b \ln X_1 \\ \ln Y &= \ln 0.7512 - 1.911 \ln X_1. \end{aligned}$$

Taking the antilog the equation becomes

$$Y = 2.12 X_1^{-1.911}$$

(18)

$$Y = \frac{2.12}{X^{1.911}}$$

or

$$(19) \quad \frac{\Delta}{R} = \frac{2.12}{(M)^{1.911}}$$

with a standard error of estimate of 0.3933.

3. Testing the Model

Through the use of the analysis of variance, the effect of Mach number on the detachment distance was determined to be significant both linearly and quadratically. Based on this, a regression analysis was used to derive a general mathematical relationship between detachment distance and Mach number. Certain physical limits were prescribed for the form of the equation. These physical limits are tested as follows:

$$(20) \quad \begin{aligned} \text{if } M = 0, \quad \frac{\Delta}{R} &= -\frac{2.12}{0^{1.911}} \\ &= \frac{2.12}{0} \\ &= \infty \end{aligned}$$

Test of Significance of Regression Coefficients A, b hypothesis A = 0
 $b = 0$

$$t(\frac{a}{2} = 0.025, df = 25) = \pm 2.06$$

$$t = \frac{0.751177-0}{0.39033/\sqrt{27}} = 10.002 > 2.06 \quad \text{Test significant, reject hypothesis}$$

$$t = \frac{1.910723-0}{0.144127} = 13.25 > 2.06 \quad \text{Test significant, reject hypothesis}$$

Table V. Compilation of Regression Analysis Data

Model: $\ln Y = \ln A + b \ln X^1 + c \ln X^2$			
Type of Data		Run 1	Run 2
Pure Constant	(A)	0.748900	0.751177
First Coefficient	(b)	-27.610352	-1.910723
Second Coefficient	(c)	12.842773	(dropped)
Standard Deviation Y from Mean		1.084638	1.084638
Coefficient of Determination	(r^2)	0.878570	0.875469
Multiple Correlation Coefficient	(r)	-0.937321	-0.935665
Variance	$\sigma_{1.2}^2$	0.154759	0.152363
Standard Error of Estimate	$\sigma_{1.2}$	0.393394	0.390337
Standard Deviation of First Coefficient	σ_b	31.500086	0.144127
Standard Deviation of Second Coefficient	σ_c	15.740889	(dropped)
T Value for Coefficient Check after First Run ($\alpha = 0.05$)		2.60	-----

Test of Significance of Simple Correlation Coefficient r
 hypothesis $r = 0$

$$t = \frac{0.935665 - 0}{0.152363} = 6.14 > 2.06 \quad \text{Test significant, reject hypothesis}$$

$$(21) \quad \text{if } M = 1, \frac{\Delta}{R} = \frac{2.12}{(1) 1.911} \\ \approx 2.12$$

$$(22) \quad \begin{aligned} \text{if } M = \infty, \frac{\Delta}{R} &= \frac{2.12}{(\infty)^{1.911}} \\ &= \frac{2.12}{\infty} \\ &= 0. \end{aligned}$$

Therefore, the regression equation has the correct form for the physical limitations. Since Mach number is dimensionless, the inclusion of R gives dimension to Δ . R is not tested for limits of 0 and ∞ , as $R = 0$ implies a pointed body and $R = \infty$ a flat plate.

Table VI. Compilation of Test Hypotheses

Hypothesis	df	Frequency Distribution	α	Type Test	Significant	Hypothesis
$R = 0$	2, 18	F	0.05	1 Tail	No	Accept
$M = 0$	2, 18	F	0.05	1 Tail	Yes	Reject
$MR = 0$	4, 18	F	0.05	1 Tail	No	Accept
$\bar{X}_e = \bar{X}_r$	26	t	0.05	2 Tail	No	Accept
$\sigma_e^2 = \sigma_r^2$	26	χ^2	0.05	2 Tail	Yes	Reject
$\bar{X}_r = \bar{X}_{aw}$		Z	0.05	2 Tail	No	Accept
$\sigma_r^2 = \sigma_{aw}^2$	26	χ^2	0.05	2 Tail	No	Accept
$A = 0$	25	t	0.05	2 Tail	Yes	Reject
$b = 0$	25	t	0.05	2 Tail	Yes	Reject
$r = 0$	25	t	0.05	2 Tail	Yes	Reject

Next, the regression model was statistically tested against the experimental data and the Ambrosio-Wortman model mentioned in Section II. These computations are shown in Appendix B. The means and variances for the experimental data, the regression model, and the Ambrosio-Wortman model were computed based on responses computed for the experimental Mach numbers. Table VI shows a compilation of the hypotheses for testing the regression model means and variances. Table VII shows the computed 95 percent confidence limits of the means for the experiment, the regression model, and the Ambrosio-Wortman model. The hypothesis that there is no difference between the variance as experimentally determined and as determined by the regression model is the only hypotheses rejected. The hypothesis that there is no significant difference between the experimental mean and the regression model mean or between the regression model mean and the Ambrosio-Wortman model mean are accepted. The test of no significant difference between the regression model variance and the Ambrosio-Wortman model variance is also accepted.

Table VII. Compilation of 95 Percent Confidence
Limits on Means

Type Mean	Mean Δ/R	Increment	Limits
Experiment	0.793	\pm 0.451	1.244 to 0.342
Regression Model	0.726	\pm 0.249	0.975 to 0.477
Ambrosio-Wortman	0.687	\pm 0.293	0.981 to 0.395

The computation for the 95 percent confidence limits for the experimental responses, the regression model, and the Ambrosio-Wortman model are shown in Table VII. The regression model has the narrowest range of values for this level of confidence. However, the χ^2 test of the difference between the variances (the second statistical moment) is not significant nor is the difference in their means (the first statistical moment). Therefore, even though the limits of the regression model are narrower than the Ambrosio-Wortman model, they are not significantly different.

The fact that there is a significant difference between the variances of the regression model and the experimental responses is indicative of the insight into the functional relationship between detachment distance and Mach number obtained by the analysis of variance performed prior to the regression analysis. The fit of the equation by the method of least squares is approaching the true mean as evidenced by the high and significant correlation coefficient (r) of 0.94 (Table V).

In order to determine the power of the tests between the means of the two models (regression model and Ambrosio-Wortman model), an operating characteristics curve was computed. The calculations are in Appendix B and the plotted values are shown in Figure 5. From this plot, the probabilities of an acceptance of the hypothesis when it is actually false (type II error) can be determined for selected differences in the means of the two models. For example, the probability of acceptance when the difference between X_r and X_{aw} is $+0.30$ is about 65 percent, and the probability of rejecting the hypothesis is 35 percent.

Plots of the values of Δ/R computed for Mach numbers from 1 to 8 for the regression model and the Ambrosio-Wortman model are shown in Figure 6. The locus of the points for the regression model and the Ambrosio-Wortman model are shown for comparison. There is a region of high curvature or nonlinearity between Mach 1.5 and about Mach 2.5 with the curves becoming asymptotic beyond 2.5. The Ambrosio-Wortman model becomes asymptotic to a Δ/R value of 0.143, whereas the regression model has a zero asymptote, the ultimate physical limit. As mentioned earlier in this section, the Duncan range test indicated that the M_1 level was significantly different from the M_2 and M_3 level. Figure 6 shows the curve becoming essentially asymptotic at about Mach 2.5 or at about the beginning of the M_2 factor level.

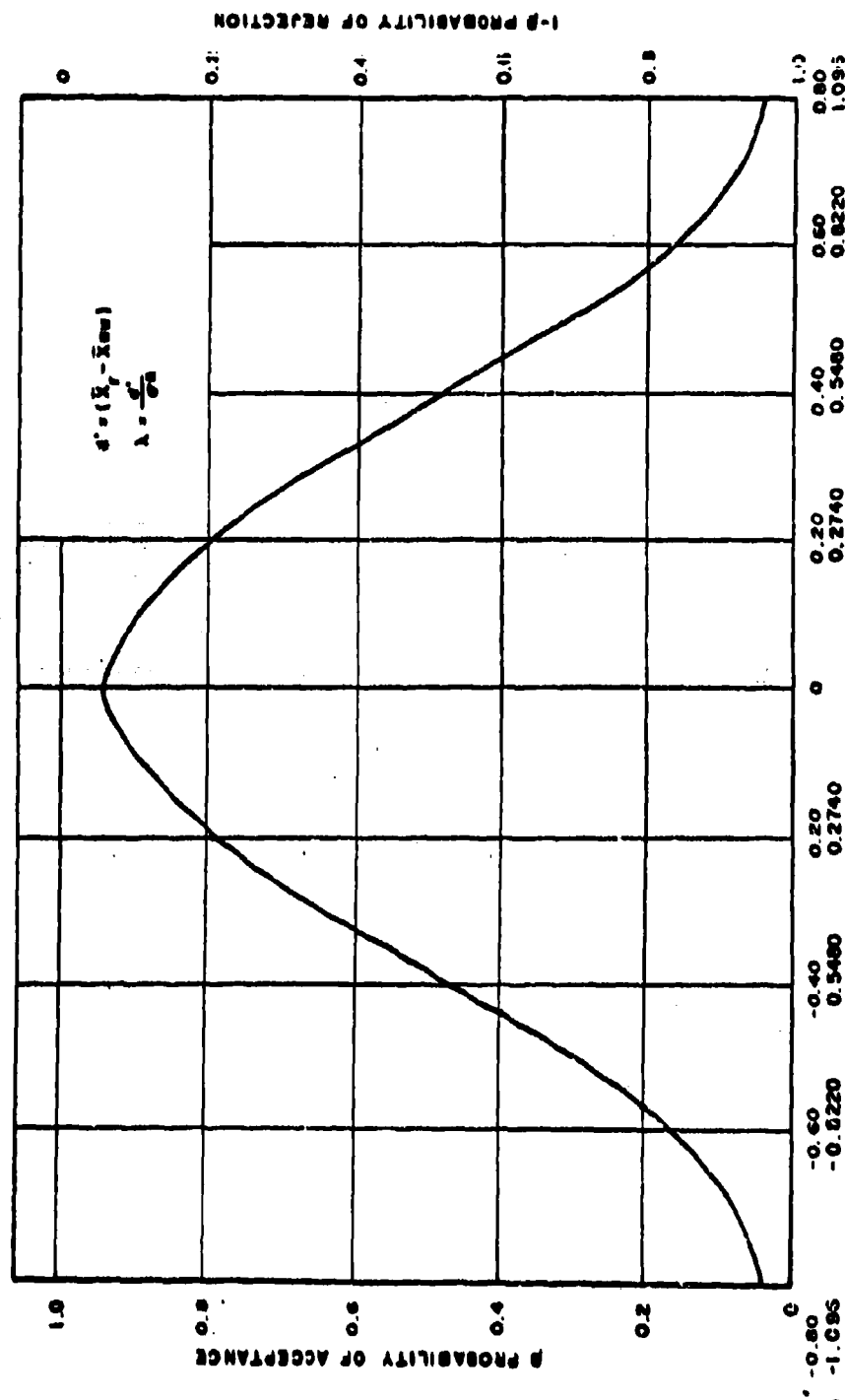


Figure 5. Operating Characteristics Curve for Two Tail
Test of Differences Between X_r and X_{aw}

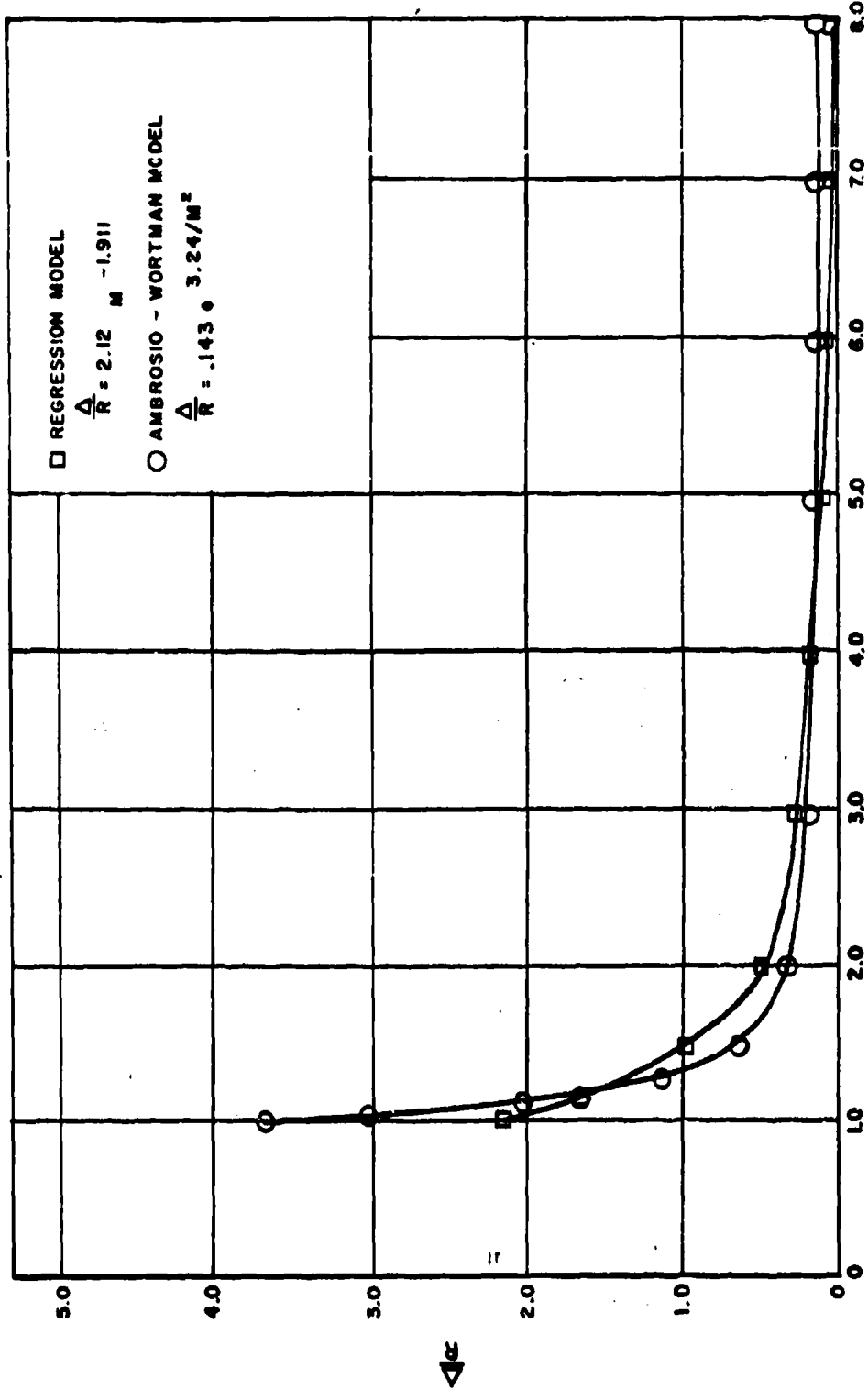


Figure 6. Plot of Δ/R Versus M for Derived Mathematical Model and Ambrosio-Wortman Model

IV. SUMMARY. This experimental and analytical exercise has led to the development of a mathematical model of shock detachment distance. This model has been statistically tested for significance on the basis of comparison with several universal frequency distributions. The hypotheses made and tested are compiled in Table VI.

The hypothesis that the radius has no effect on the detachment distance was accepted. This does not mean that radius has no effect on the shock detachment distance but that, within the limits of the tests, a significant effect cannot be detected. That is, one cannot reject the hypothesis.

The hypothesis that the Mach number has no effect on the detachment distance was rejected. Mach number is apparently a significant contributor to shock location. This means that within the limits of the test a significant variance associated with Mach number is detectable and cannot be attributed to experimental error.

The hypothesis that the MR interaction has no effect on detachment distance was also accepted. This hypothesis is accepted for similar reasons as the hypothesis on radius effects. From Table IV, the ANOVA table, it can be seen that the radius effect accounts for only 1.65 percent of the total expected mean square of the experiment. Mach number accounts for 59.25 percent, MR interaction accounts for 3.30 percent, and error accounts for 35.80 percent. It is pointed out that the variance attributable to variables not included in the experiment could be summed in the Mach number factor, which if separated would reduce the detectable effects of Mach number. For example, body surface roughness, free stream density, and humidity, possible sources not included in the experiment, may significantly effect shock location.

The hypothesis on the derived regression constants, coefficient, correlation coefficient were all rejected. This implies that these values were significantly different from the values one would derive from data where there was no correlation between the variables included in the analysis. The standard error of estimate of 0.390337 shows that the fit for the universe line of regression is good but not perfect. For a perfect fit, the standard error of estimate would be zero and the correlation coefficient 1.0 instead of 0.935665. This emphasizes the fact that all variables which affect the shock location are not included and all

variances present have not been accounted for. However, the model does account for the relative amount of variation in the dependent variable (Δ) that is "explained" by the independent variable (M).

The mean of the experimental data was not found to be significantly different from the mean of the regression model, whereas the variances were significantly different. However, since the variance test is a more sensitive test (i.e., the second statistical moments as compared to the first statistical moment), it is believed that this also attributes to the reliability of the model. The mean of the regression model was not found to be significantly different from the mean of the Ambrosio-Wortman model. This was also true for the variances of the two models. This indicates that within the limits of this investigation there is no significant difference between the model derived from wind tunnel data and free flight data. That is, the hypothesis that the perturbations of holding devices and expanding flow in wind tunnel tests increase the variance of main effects or experimental effects cannot be detected. This is not to say that they do not. It is indicated in Table VII that the regression model is to some degree more accurate than the Ambrosio-Wortman model as the 95 percent confidence limits on the means are more narrow but not significantly so.

Therefore, within the limits of the aerodynamic and statistical assumptions of this investigation, the following general observations are made:

- 1) The model derived is a reliable model for the prediction of shock detachment distance as a function of Mach number.
- 2) The model derived with free flight data is apparently not significantly better than models derived by data from wind tunnels.
- 3) The use of the statistical methods for the analysis of data can lead to increased knowledge of the functional relationships of physical variables.
- 4) The inferences that can be made through the analysis of data by statistical methods are more objective inferences than could otherwise be made.

5) The use of statistics is an extremely useful tool for the analysis of data which are functions of physical relationships and in many cases lead to increased confidence in the results of the analysis over mere visual inspection of experimental responses.

V. SUGGESTED FUTURE STUDIES. The results of this study indicate that the shock detachment distance for radius nosed bodies is strongly a function of Mach number between 1.0 and about 2.5. After 2.5, the detachment distance is practically independent of Mach number. This was established by the Duncan range test which shows that there is apparently no significant difference between the responses obtained at the M₂ (2.5 to 2.9) and the M₃ level (3.9 to 4.3). Therefore, it seems appropriate to perform future studies in the Mach range of 1.0 to 2.5 to obtain a better understanding of the function where the variation is most sensitive. This will provide a better estimate of the universe regression line of the shock detachment distance in this velocity range.

Another important point to consider for future experimental studies is to confound the daily variation with a selected interaction, since this study shows that there is apparently no significant effect of interaction on the shock detachment distance. In this study, the day effect was confounded with the experimental error and main effects through randomization of all factor levels and combinations with days. Another approach would be through design, to confound a priori the day effects with the interaction. This would separate the variance due to day effects from the experimental error and main effects and may result in a more sensitive test for main effects. However, this does not necessarily follow because the degrees of freedom for error would be reduced for the same number of responses. If the day effects are not large, the separation of the day effects may not be sufficient to offset the reduction in error degrees of freedom. This would require judgment in future designs. In this study, it is believed that it was advantageous to randomly distribute the day effects rather than confounding them with the main or secondary effects since one objective was to test for significance of interaction.

The very high significance of the Mach number factor indicated that further test should be initiated to include other factors as free stream density and some discrete levels of body surface roughness (density and body surface roughness effects were summed as experimental error in this study).

A suggested experiment of academic interest would be a 4^3 factorial with day effects confounded with the highest order interaction. The three factor, four level experiment is suggested in order to test for one degree higher order (cubic) effects. Models of constant radius, but with four levels of surface roughness, at four levels of free stream density and four levels of velocity would be flown in free flight.

This experiment would enable, through the analysis of variance the determination of cubic, surface roughness (S) and density (ρ) effects in addition to velocity effects. Since the first order interaction in this study $(MR)_{ij}$ was not significant, the day effects could be confounded with the second order interaction $(MS\rho)_{ijk}$.

LITERATURE CITED

1. H. Serbin, SUPERSONIC FLOW AROUND BLUNT BODIES, Journal of the Aeronautical Sciences, Vol 25, No. 1, January 1958.
2. A. Ambrosio, and A. Wortman, STAGNATION POINT SHOCK DETACHMENT DISTANCE FOR FLOW AROUND SPHERES AND CYLINDERS, ARS Journal, Vol 32, No. 2, February 1962.
3. DiDonato, and B. Zondek, CALCULATION OF THE TRANSONIC FLOW ABOUT A BLUNT-NOSED BODY WITH A REAR SKIRT, U. S. Naval Weapons Laboratory Unclassified Report (undated).
4. National Advisory Committee on Aeronautics, DATA ON SHAPE AND LOCATION OF DETACHED SHOCK WAVES ON CONES AND SPHERES by J. W. Heberle, G. P. Wood, and P. B. Gooderum, January 1950, TN 2000.
5. National Advisory Committee on Aeronautics, A RE-EXAMINATION OF THE USE OF SIMPLE CONCEPTS FOR PREDICTING THE SHAPE AND LOCATION OF DETACHED SHOCK WAVES by E. S. Love, December 1957, TN 4170.
6. A. Ambrosio, and A. Wortman, STAGNATION-POINT SHOCK-DETACHMENT DISTANCE FOR FLOW AROUND SPHERES AND CYLINDERS IN AIR, Journal of the Aerospace Sciences, Vol 29, No. 7, July 1962.
7. A. J. Duncan, QUALITY CONTROL AND INDUSTRIAL STATISTICS, Homewood, Illinois, Richard D. Irwin, Inc., 1959.

Appendix A
EXPERIMENTAL COMPUTATIONS

Sonic velocity was computed for each round from the following equation:

$$(A-1) \quad a = \sqrt{\gamma R_o T}$$

Model velocity was computed for each round from the following equation:

$$(A-2) \quad V = \frac{5 \text{ feet}}{t}$$

Mach number was computed for each round from the following equation:

$$(A-3) \quad M = \frac{V}{a}$$

The magnification factors for the shadowgraph (F_{sh}) and Schlieren (F_{sc}) systems were computed for all rounds from the following equation:

$$(A-4) \quad F_{sh} \text{ and } F_{sc} = \frac{\sum_{N=1}^8 \text{Film Model Diameter}/N}{\sum_{N=1}^8 \text{Model Diameter}/N}$$

The computed values are:

$$(A-5) \quad F_{sh} = \frac{0.226}{0.224} = 1.009$$

$$F_{sh} = \frac{0.1915}{0.224} = 0.855.$$

Shock detachment distance and model radius correcting for magnification and location was computed as follows:

$$(A-6) \quad \frac{\Delta}{R} = \frac{\frac{\delta_{sc}}{R_{sc}} + \frac{\delta_{sh}}{R_{sh}}}{2}$$

but

$$(A-7) \quad \begin{aligned} R_{sc}(\text{counts}) &= C \times R_b \times F_{sc} \times R_r \\ R_{sh}(\text{counts}) &= C \times R_b \times F_{sh} \times R_r \end{aligned}$$

therefore

$$(A-8) \quad \begin{aligned} \frac{\Delta}{R}(\text{counts}) &= \frac{\frac{\delta_{sc}}{C \times R_b \times F_{sc} \times R_r} + \frac{\delta_{sh}}{C \times R_b \times F_{sh} \times R_r}}{2} \\ &= \frac{\delta_{sc} F_{sh} + \delta_{sh} F_{sc}}{2(C \times R_b \times F_{sc} \times F_{sh} \times R_r)} \end{aligned}$$

Therefore,

$$(A-9) \quad \Delta(\text{counts corrected}) = \delta_{sc} F_{sh} \delta_{sh} F_{sc}$$

and

$$(A-9) \quad R(\text{counts corrected}) = 2(C \times R_b \times F_{sc} \times F_{sh} \times R_r)$$

Example computations for round 75 as shown in Table II.

$$\begin{aligned} a &= \sqrt{1.4 \times 1715 \times (460 + 71)} \\ &\approx 1131 \end{aligned}$$

$$V = \frac{5 \text{ ft}}{0.003531 \text{ sec}^*} = 1416$$

*This value for round 75 and all other rounds obtained from submicro-second electronic counters as recorded in aeroballistic data log.

$$(A-10) \quad M = \frac{1416}{1131} = 1.252$$

$$\Delta = 373(0.855) + 390(1.009) = 710.46(\text{counts})$$

$$R_1 = 2(3502 \times 0.112 \times 1.009 \times 0.855 \times 1.0) \\ = 676.74(\text{counts})$$

$$\frac{\Delta}{R} \frac{710.46}{676.74} = 1.049.$$

**Appendix B
STATISTICAL COMPUTATIONS**

1. Analysis of Variance

The computations for the analysis of variance was made from the data shown in Table III.

Sums of squares are listed below.

Total sum of squares

$$\begin{aligned}
 \text{SS}_t &= \sum_{ijk}^{abr} X^2 - \frac{(\sum X_{..})^2}{rab} \\
 (B-1) \quad &= 50.746 - \frac{(21.414)^2}{3.3.3} \\
 &\approx 33.7628.
 \end{aligned}$$

Sum of squares due to radius

$$\begin{aligned}
 \text{SS}_R &= \frac{\sum_j^b X_{j..}^2}{rab} - \frac{\sum X_{..}^2}{rab} \\
 (B-2) \quad &= \frac{(4.810)^2 + (10.135)^2 + (6.469)^2}{9} - \frac{(21.414)^2}{27} \\
 &= 18.6335 - 16.9836 \\
 &= 1.6499.
 \end{aligned}$$

Sum of squares due to Mach number.

$$\begin{aligned}
 SS_M &= \frac{\sum X_{i..}^2}{rab} - \frac{\sum X_{..}^2}{rab} \\
 (B-3) \quad &= \frac{(17.700)^2 + (0.481)^2 + (0.502)^2}{9} - \frac{(21.414)^2}{27} \\
 &= 35.5819 - 16.9836 \\
 &= 18.5983.
 \end{aligned}$$

Sum of squares due to MR interaction

$$\begin{aligned}
 (B-4) \quad SS_{MR} &= \frac{\sum \sum X_{...}^2}{r} - \frac{\sum X_{i..}^2}{rb} - \frac{\sum X_{..j}^2}{ra} + \frac{\sum X_{...}^2}{rab} \\
 &= \frac{(3.87)^2 + (0.481)^2 + (0.502)^2 +}{3} \\
 &\quad \frac{(8.860)^2 + (0.799)^2 + (0.566)^2 +}{3} \\
 &\quad \frac{(5.013)^2 + (0.826)^2 + (9.630)^2}{3} - 1.6499 - 18.5983 - 16.9836 \\
 &= 2.9885.
 \end{aligned}$$

Sum of squares due to error

$$\begin{aligned}
 (B-5) \quad SS_e &= SS_t - SS_R - SS_M - SS_{MR} \\
 &= 33.7628 - 1.6499 - 18.5983 - 2.9885 \\
 &= 10.5261.
 \end{aligned}$$

Sum of squares due to linear and quadratic effects within main and interaction effects. (Coefficients of orthogonal polynomials)¹

¹C. R. Hicks, Fundamental Concepts in the Design of Experiments, New York, New York, Holt, Rinehart and Winston, 1964

$$SS_{R\ell} = \frac{[-1(4.810) + 0(10.135) + 1(6.469)]^2}{3.3.2} = 0.1529$$

$$SS_{Rq} = \frac{[1(4.810) + -2(10.135) + 1(6.469)]^2}{3.3.6} = 1.4970$$

$$SS_{M\ell} = \frac{[-1(17.70) + 0(2.016) + 1(1.698)]^2}{1.3.2} = 14.3146$$

$$(B-6) \quad SS_{Mq} = \frac{[1(17.70) + -2(2.016) + 1(1.698)]^2}{3.3.6} = 4.2837$$

$$SS_{R\ell M\ell} = \frac{[1(3.827) + -1(0.502) + -1(5.013) + 1(0.630)]^2}{3.} = 0.08551$$

$$SS_{RqM\ell} = \frac{[-1(3.827) + 1(0.502) + 2(8.860) + -2(0.566) + -1(5.013) + 1(0.630)]^2}{3.12} = 2.198$$

$$SS_{R\ell Mq} = \frac{[-1(3.827) + 2(0.481) + -1(0.502) + 1(5.013) + -2(0.826) + 1(0.630)]^2}{3.12} = 0.0108$$

$$SS_{RqMq} = \frac{[+1(3.827) + -2(0.481) + 1(0.502) + -2(8.860) + 4(0.709) - 2(0.566) + +1(5.013) + -2(0.826) + 1(0.630)]^2}{3.36} = 0.6940.$$

2. Multiple Range Tests

Multiple range tests are listed below.

a. Mach Number Effects

$$(E-7) \quad \bar{X}_1, \text{ treatments } \frac{1.967 \quad 0.224 \quad 0.188}{1 \quad 2 \quad 3}$$

Error mean square = 0.5847 with 18 d. f.

Standard error of mean is

$$(B-8) \quad S_{\bar{X}_i} = \sqrt{\frac{\text{Error MS}}{\text{No. of Obs.}}} = \sqrt{\frac{0.5847}{9}} = 0.2545 .$$

From Table E,¹ ($\alpha = 0.05 n_2 = 18$) the significant ranges are

$$(B-9) \quad p_{\text{ranges}} = \frac{2}{2.97} \quad \frac{3}{3.12} .$$

Multiplying p values by $S_{\bar{X}_i}$, the least significant ranges are

$$(B-10) \quad LSR = \frac{p}{0.756} = \frac{2}{0.796} \quad \frac{3}{0.796} .$$

Largest versus smallest:

$$(B-11) \quad 1.967 - 0.224 = 1.743 > 0.796^* (\text{significant})$$

Largest versus second smallest:

$$(B-12) \quad 1.967 - 0.189 = 1.778 > 0.756^* (\text{significant})$$

Second largest versus smallest:

$$(B-13) \quad 0.224 - 0.189 = 0.035 < 0.756$$

(See Figure 4 for display of results).

b. Radius Effects

$$(B-14) \quad \bar{X}_{.j} \text{ treatments } \frac{1.126}{2} \quad \frac{0.719}{3} \quad \frac{0.534}{1}$$

Standard error of mean is

¹Hicks, loc. cit.

$$(B-15) \quad S_{\bar{X}_j} = \sqrt{\frac{\text{Error MS}}{\text{No. of Obs.}}} = \sqrt{\frac{0.5847}{9}} = 0.2545$$

From Table E,¹ ($\alpha = 0.05$ $n_2 = 18$) the significant ranges are

$$(B-16) \quad p_{\text{ranges}} = \frac{2}{2.97} \quad \frac{3}{3.12} .$$

Multiplying p values by $S_{\bar{X}_j}$, the least significant ranges are

$$(B-17) \quad p_{\text{LSR}} = \frac{2}{0.756} \quad \frac{3}{0.796} .$$

Largest versus smallest:

$$1.126 - 0.5344 = 0.5916 < 0.796 .$$

Largest versus second smallest:

$$1.126 - 0.719 = 0.407 < 0.756 .$$

Second largest versus smallest:

$$0.719 - 0.534 = 0.184 < 0.756 .$$

(See Figure 4 for display of results).

3. Computations for Testing the Model

a. Computation of Experiment Mean and Variance

¹Hicks, loc. cit.

Design of Experiments

\bar{x}_i	\bar{x}_e	$(x_i - \bar{x}_e)^2$	\bar{x}_i	\bar{x}_e	$(x_i - \bar{x}_e)^2$
1.049	0.793	0.0655	0.188		0.3660
1.492		0.4886	0.253		0.2916
1.286		0.2430	0.182		0.3732
0.146		0.4186	0.179		0.3769
0.146		0.4186	0.205		0.3457
0.189		0.3648	1.034		0.0580
0.223		0.3249	2.243		2.1025
0.139		0.4277	1.736		0.8892
0.140		0.4264	0.226		0.3226
1.461		0.4462	0.280		0.2631
5.478		21.9492	0.321		0.2227
1.921		1.2723	0.203		0.3481
0.268		0.2756	0.210		0.3398
			0.217		0.3317
			$\Sigma 21.414$		

$$\bar{x}_e = 21.414/27 = 0.793$$

$$s_e^2 = 33.752/27-1 = 1.298$$

$$s_e = \sqrt{1.298} = 1.139$$

b. Computation of Regression Model Mean and Variance

\bar{x}_i	\bar{x}_r	$(\bar{x}_i - \bar{x}_r)^2$	\bar{x}_i	\bar{x}_r	$(x_i - \bar{x}_r)^2$
1.382	0.726	0.4303	0.314		0.1697
1.618		0.7956	0.282		0.1971
1.535		0.6544	0.154		0.3271
0.303		0.1789	0.151		0.3306
0.336		0.1521	0.152		0.3294
0.288		0.1918	1.271		0.2970
0.149		0.3329	1.668		0.8873
0.154		0.3271	1.568		0.7089
0.152		0.3294	0.276		0.2025
1.557		0.6905	0.283		0.1962
2.035		1.7134	0.232		0.2440
1.714		0.9761	0.137		0.3469
0.299		0.1923	0.167		0.3124
			0.142		0.3410
			$\Sigma 19.597$		
			$\Sigma 11.8449$		

$$\bar{X}_r = 19.597/27 = 0.726$$

$$\sigma_r^2 = 11.8449/27 = 0.4387$$

$$\sigma_r = \sqrt{0.4387} = 0.6623$$

c. Computation of Mean and Variance of Ambrosio and Wortman's Model (Z) for the Experimental Conditions of this Study

$$\text{Model } \frac{\Delta}{R} = 0.143e^{3.24/M^2}$$

\underline{x}_i	\bar{x}_{aw}	$(x_i - \bar{x}_{aw})^2$	\underline{x}_i	\bar{x}_{aw}	$(x_i - \bar{x}_{aw})^2$
1.133	0.6875	0.1984	0.176		0.2616
1.642		0.9110	0.176		0.2616
1.444		0.5722	1.493		0.6568
0.218		0.2199	3.180		6.2125
0.229		0.2097	1.910		1.4945
0.214		0.2237	0.218		0.2204
0.175		0.2626	0.222		0.2166

\underline{x}_i	\bar{x}_{aw}	$(x_i - \bar{x}_r')^2$	\underline{x}_i	\bar{x}_{aw}	$(x_i - \bar{x}_r)^2$
0.212		0.2261	0.209		0.2289
0.176		0.2616	0.212		0.2261
0.175		0.2626	0.197		0.2411
0.176		0.2616	0.172		0.2657
0.951		0.0694	0.179		0.2636
1.783		1.2096	0.173		0.2647
1.519		0.6914	$\Sigma 18.564$		$\Sigma 16.3939$

$$\bar{x}_{aw} = 18.564/27 = 0.6875$$

$$(B-18) \quad \sigma_{aw}^2 = 16.3939/27 = 0.6072$$

$$\sigma_{aw} = \sqrt{0.6072} = 0.7792$$

95 percent confidence limits on experiment mean

$$(B-19) \bar{X}_e(0.95) = 0.793 \pm \frac{1.139}{\sqrt{n}} (2.06) = 0.793 \pm 0.451 = 1.244 \text{ to } 0.342$$

95 percent confidence limits on regression mean

$$(B-20) \bar{X}_r(0.95) = 0.726 \pm \frac{0.6623}{\sqrt{n}} (1.96) = 0.726 \pm 0.249 = 0.975 \text{ to } 0.477$$

95 percent confidence limits on Ambrosio-Wortman Model mean

(B-21)

$$\bar{X}_{aw}(0.95) = 0.6875 \pm \frac{0.7792}{\sqrt{27}} (1.96) = 0.6875 \pm 0.293 = 0.981 \text{ to } 0.395.$$

d. Tests of Means and Variances

$$\text{Hypothesis: } \bar{X}_e = \bar{X}_r$$

$$(B-22) t \left(\frac{\alpha}{2} = 0.025 \text{ d.f.} + 26 \right) = \pm 2.06$$

$$t = \frac{\bar{X} - \bar{X}'}{S_e/\sqrt{n}} = \frac{0.793 - 0.726}{1.139/\sqrt{27}} = \frac{0.067}{1.139/5.196} = 0.305.$$

Computed value less than table value. Test not significant. Accept hypothesis.

$$\text{Hypothesis: } S_e^2 = \sigma_r^2$$

$$(B-23) \chi^2 \left(\frac{\alpha}{2} = 0.025 \text{ d.f.} = 26 \right) = 13.8 \text{ to } 41.9$$

$$\chi^2 = n \frac{S_e^2}{\sigma_r^2} = 27 \left(\frac{1.298}{0.4387} \right) = 79.885.$$

Computed value exceeds table value. Test is significantly higher.
Reject hypothesis.

$$\text{Hypothesis: } \bar{X}_r = \bar{X}_{aw}$$

$$(B-24) \quad Z\left(\frac{\alpha}{2} = 0.025\right) = \pm 1.960$$

$$\sigma_{r-aw} = \sqrt{\frac{0.4387}{27} + \frac{0.6072}{27}} = \sqrt{0.01624 + 0.02248} = \sqrt{0.03872} = 0.1968$$

$$Z = \frac{0.726 - 0.687}{0.1968} = +0.1981.$$

Computed value less than table value. Test not significant. Accept hypothesis.

$$\text{Hypothesis: } \sigma_r^2 = \sigma_{aw}^2$$

$$(B-25) \quad \chi\left(\frac{\alpha}{2} = 0.025 \text{ d.f.} = 26\right) = 13.8 \text{ to } 41.9$$

$$\chi^2 = \frac{N\sigma_r^2}{\sigma_{aw}^2} = 27 \left(\frac{0.4387}{0.6072} \right) = 19.510.$$

Computed value between table values. Test not significant. Accept hypothesis.

- e. Computations for Operating Characteristics Curve for Two-Tail Test of Differences Between the Mean of the Regression Model (X_r) and the Mean of the Ambrosio-Wortman Model (X_{aw})

Assumption - the variances are known for both models.

$$\sigma^* = \sqrt{\frac{N_{aw} \sigma_r^2 + N_r \sigma_{aw}^2}{N_{aw} + N_r}} = \sqrt{\frac{27(0.4387) + 27(0.6072)}{27 + 27}}$$

(B-26)

$$= \sqrt{0.52277} = 0.7299$$

These data are plotted in Figure 5.

$(\bar{X}_r - \bar{X}_{aw})$	λ (d'/σ^*)	$\frac{d'}{\sigma_{r-aw}}$	$Z = 0.95 - d'/\sigma_{r-aw}$ $= 1.96 - d'/\sigma_{r-aw}$	Probability of Acceptance β	Probability of Rejection $1 - \beta$
0	0	0	1.96	0.95	0.05
0.0492	0.0680	0.25	1.71	0.93	0.07
0.0984	0.1360	0.50	1.46	0.90	0.10
0.1476	0.2040	0.75	1.21	0.86	0.14
0.1968	0.2720	1.00	0.96	0.81	0.19
0.2460	0.3400	1.25	0.71	0.74	0.26
0.2952	0.4080	1.50	0.46	0.65	0.35
0.3936	0.5440	2.00	-0.04	0.50	0.50
0.4920	0.6800	2.50	-0.54	0.32	0.68
0.5904	0.8160	3.00	-1.04	0.17	0.83
0.6888	0.5520	3.50	-1.54	0.09	0.91
0.7872	1.0880	4.00	-2.04	0.05	0.95

PRESENTATION OF THE FIRST
SAMUEL S. WILKS MEMORIAL MEDAL*

Frank E. Grubbs

ACCEPTANCE OF THE FIRST WILKS MEMORIAL AWARD

John W. Tukey

It is indeed a pleasure to have Mrs. Samuel S. Wilks with us this evening for the presentation of the first Samuel S. Wilks Memorial Medal Award.

The Samuel S. Wilks Memorial Award for statisticians was established and announced a year ago at the Tenth Conference on Design of Experiments in Army Research, Development and Testing. An account of the announcement of the Wilks Award is given in the American Statistician for December, 1964. The idea for the Award was due to Major General Leslie E. Simon (Ret.), who gave the opening paper at the Tenth Design of Experiments Conference entitled "The Stimulus of S. S. Wilks to Army Statistics". The Wilks Memorial Award is sponsored by the American Statistical Association through the generosity of Mr. Philip G. Rust, retired industrialist of the Winnstead Plantation, Thomasville, Georgia. The American Statistical Association accepted the obligation of administering the Award and funds in accordance with guidance and criteria which are consonant with law and with the wishes of the Army representatives, Mr. Rust, and the American Statistical Association. The name of the recipient of the Wilks Award is announced each year during the annual Conference on Design of Experiments in Army Research, Development and Testing.

With the approval of the President of the American Statistical Association the Wilks Award Committee for 1965 consisted of:

Dr. Francis G. Dressel, Duke University and the Army Research Office-Durham

Dr. Churchill Eisenhart, National Bureau of Standards

*After the dinner meeting at the Eleventh Conference on Design of Experiments in Army Research, Development and Testing, the chairman of the conference, Dr. Frank E. Grubbs, gave the above address. Professor John W. Tukey was presented the first Wilks Memorial Award. Following his acceptance of this honor he spoke to the group about his friend Sam Wilks.

Professor Oscar Kempthorne, Iowa State University
Dr. Alexander M. Mood, U. S. Office of Education
Major General Leslie E. Simon (Ret.), Winter Park, Florida
Dr. Frank E. Grubbs, Ballistic Research Laboratories, Aberdeen
Proving Ground, Maryland - Chairman

The Wilks Award Committee met during the annual meeting of the American Statistical Association in Philadelphia on 8-10 September 1965. Many candidates for the 1965 Wilks Award were considered based on nominations from individuals and also statisticians thought worthy of consideration by the committee.

The Wilks Award is not limited to contributors to design of experiments activities in connection with Army research, development and testing, but rather all statisticians who have made significant contributions to the general field of Army statistical endeavors, whether theoretical or applied, are eligible. Moreover, persons eligible for the award include not only government statisticians but also those from universities and industry. The annual programs of the Conference on Design of Experiments in Army Research, Development and Testing indicate rather broadly the nature of statistical endeavors of interest to the Army, but the achievements of those being considered for the award need not be restricted to these areas. Rather, as indicated earlier, the awardee is selected for the advancement of scientific or technical knowledge in statistical efforts which co-incidentally will have benefited the Army and government in one way or another.

As a result of the committee meeting, it is a great pleasure to announce that Professor John W. Tukey of Princeton University has been selected to receive the first Samuel S. Wilks Memorial Medal Award.

Professor Tukey has long been an authority on the statistical analysis of data and has received wide recognition for his many contributions to mathematical statistics and applied statistics in many different fields. Professor Tukey has contributed to the Army Design of Experiments Conferences from the beginning and gave freely of his time to promulgating the uses of statistics in Army applications, DOD applications, Government and industrial applications. The citation for the first Wilks medalist reads as follows:

To John W. Tukey for his contributions to the theory of statistical inference, his development of procedures for analyzing data, and his influence on applications of statistics in many fields.

Upon receiving the Wilks Medal, Professor Tukey responded as follows:

We are met to honor Sam Wilks' memory. All of us would have so much preferred to have had him here instead. Many of us knew him for ten or twenty years, some for thirty. No matter whether we knew him intimately as a close colleague and friend or only as someone met once a year at such a recurring event as this, we all respected him and all he stood for. In this we are but a small sample.

The memorial minute of the Princeton University faculty begins thus: "Samuel Stanley Wilks died in his sleep on March 7, 1964 at the peak of a distinguished career in teaching, research, and public service. His sudden death, without any warning leaves many friends and associates stunned by a sudden loss of a man upon whom they depended for advice on problems large and small, for a wise appraisal of proposals under consideration, for getting many jobs done---a man instinctively so friendly and fair that everyone responded to him with great affection. His death terminates a quiet, penetrating, and influential leadership in the work of many organizations---especially in mathematics, statistics, and social science---to which he brought wisdom, commitment, persistence, and a remarkable sense of the importance of new developments. His passing leaves an emptiness in so many plans, that one wonders how one man was so versatile and did so much".

The memorial notice of the American Philosophical Society approaches its end thus [1]: "In his service to our Society, Sam showed all the wonderful characteristics we have noticed elsewhere: quiet, modest diligence, deep wisdom, a technical skill that was always adequate to any demand; the ability to comprehend, and bring others to comprehend, the broader issues." The notice then ends: "Mosteller's memoir, written for statisticians, was fittingly entitled: "Samuel S. Wilks: Statesman of Statistics". As members of Benjamin Franklin's own society it is only right that we salute our departed colleague and friend as "Sam: A Quiet Contributor to Mankind".

On the afternoon of his death Sam told my wife: "Now that so many of our former graduate students are leading statistics departments of their own, it's time that John and I worked out something new to do." I never saw Sam again; what we are working out in Princeton today is not what it would have been under his leadership, but we can, and will, do our best to make the new Department of Statistics something of which Sam would have been proud.

For thirty years he kept Fine Hall statistics in balanced contact with mathematics on the one hand and with a wide variety of applications on the other, showing clearly by his example how it was best to combine both. His recognition of the dangers of tight Gaussian assumptions led him to pioneer with non-parametric methods. His recognition of the growing importance of computing came very early; the first punched card equipment on the Princeton campus occupied the room next to his office.

As a unified Princeton statistics comes into being and grows, we will do all we can to continue his tradition. We will emphasize the need for combining contact with mathematics and contact with applications. We will do all we can to bring statistics, computer science, and the use of computer facilities ever closer together. We will try to be ever more realistic in understanding the problems of the real world and in formulating those pale copies of real problems, whose solutions serve to guide us as we face reality. We can do no less if we are to follow his noble tradition.

REFERENCE

- [1] Samuel Stanley Wilks (1906-1964). 1964 Yearbook of the American Philosophical Society, 147-154.

TARGET COVERAGE PROBLEMS

William C. Guenther
University of Wyoming, Laramie, Wyoming

Much of the material contained in this paper is a review of literature which has appeared in many different publications. The definition of a single shot coverage problem which was given in a paper by Guenther and Terragno [1] is extended to a multiple shot case. The results which were reviewed in reference 1 appear here in abstracted form since they are useful for the new extension. Some models for the multiple shot case are considered in detail. The latter include some for which results have not been previously published. It is hoped that this paper will be a coordinating force for future research.

In recent years a large number of publications have appeared on probability problems arising from ballistic applications. Many of these papers and reports are concerned with topics which are often referred to as coverage problems. A definition of a coverage problem, which yields many interesting models as special cases, appears in a paper by Guenther and Terragno [1] and will be reproduced here. That definition was for the single shot case but only minor modifications are required to extend it to a multiple shot situation. Further modifications may be necessary if it is desired that the definition yield certain other problems, which have already been investigated or may be formulated in the future, as special cases.

Although most work in this field has been restricted to the two-dimensional case, some applications are meaningful in three dimensions. It is doubtful that the coverage problem has any useful interpretation in more than three dimensions. We will use n-dimensional notation not only because it includes the cases $n = 2$ and $n = 3$ but also because results one derives can occasionally be used in unexpected places where n dimensions are meaningful.

For brevity we will use the notation $X_i = (x_{i1}, x_{i2}, \dots, x_{in})$ and $\int dF(X_i)$ will represent an n -fold integral.

DEFINITION FOR THE SINGLE SHOT CASE. Before attempting to define a coverage problem, let us consider a special case which will help to introduce some of the essential ideas and language. Suppose that a point target is located at the origin of a two-dimensional coordinate system. A weapon with killing radius R is aimed at the origin with the intention of destroying the point target. When the weapon arrives at the target, the latter is located at $X_2 = (x_{21}, x_{22})$, a randomly selected position within or on a circle of radius D centered at the origin (see Figure 1). That

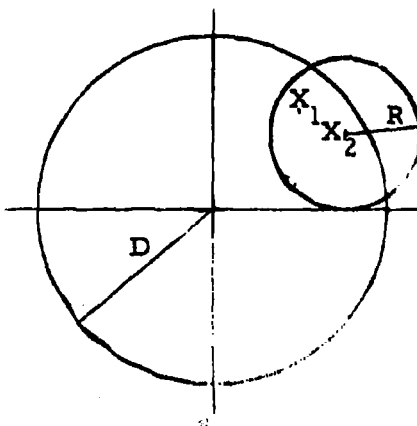


Fig. 1. X_2 is point target and weapon has killing radius R .

is, the probability density function of X_2 is

$$g(x_{21}, x_{22}) = \frac{1}{\pi D^2}, \quad 0 \leq x_{21}^2 + x_{22}^2 \leq D^2.$$

Assume that aiming errors are circularly normally distributed with unit variance so that the center of the lethal circle $X_1 = (x_{11}, x_{12})$ has p. d. f.

$$f(x_{11}, x_{12}) = \frac{1}{2\pi} \exp[-\frac{1}{2}(x_{11}^2 + x_{12}^2)].$$

Now a given point X_2 will be destroyed if the impact point of the weapon is within R units of X_2 . The probability that this happens is

$$h(x_{21}, x_{22}) = \int_{C_1} \int f(x_{11}, x_{12}) dx_{11} dx_{12}$$

where C_1 is the region $(x_{11}-x_{21})^2 + (x_{12}-x_{22})^2 \leq R^2$. The probability of destroying the target (that is, the probability that the impact point is within R units of the target given that the target is as likely to be at one point as at any other within the circle of radius D) is

$$P(R, D) = \int_{C_2} \int h(x_{21}, x_{22}) g(x_{21}, x_{22}) dx_{21} dx_{22}$$

where C_2 is the region $x_{21}^2 + x_{22}^2 \leq D^2$. The evaluation of $P(R, D)$ for any number of dimensions is discussed in Section 2 of reference 1 and is mentioned in the abstract of that paper which appears in the next section.

Now let us formulate the definition of a coverage problem for the single shot case. Let X_1 be the impact point of the weapon, X_2 be the position of the target at the time of impact, $P_1(X_1, X_2)$ = probability of destroying the target for given values of X_1 and X_2 (sometimes called the damage function), $F(X_1)$ = the distribution function of the impact point, $G(X_2)$ = the distribution function of X_2 . Then

$$\begin{aligned} P_2(X_2) &= \int_{-\infty}^{\infty} P_1(X_1, X_2) dF(X_1) \\ &= \text{probability a given } X_2 \text{ is destroyed} \end{aligned}$$

and

$$\begin{aligned} P(\cdot) &= \int_{-\infty}^{\infty} P_2(X_2) dG(X_2) \\ &= \text{probability of destroying a point target whose position is governed by } G(X_2). \end{aligned}$$

We will define a single shot coverage problem as the computation of a probability of the type $P(\cdot)$, that is, the evaluation of

$$(1) \quad P(\cdot) = \int_{-\infty}^{\infty} \int_{-\infty}^{\infty} P_1(X_1, X_2) dF(X_1) dG(X_2) .$$

All three functions $P_1(X_1, X_2)$, $F(X_1)$, and $G(X_2)$ (and consequently $P(\cdot)$) will in general depend upon parameters.

Although the order of integration in (1) has proven to be the most efficient in the majority of problems which have been studied, there is no reason why that order cannot be reversed if it is profitable to do so. This change gives

$$(2) \quad P(\cdot) = \int_{-\infty}^{\infty} \int_{-\infty}^{\infty} P_1(X_1, X_2) dG(X_2) dF(X_1) .$$

Several special cases are worthy of consideration. If

- (a) $P_1(X_1, X_2) = 1, \quad X_1 \in \text{region } C_1 \text{ (usually a sphere)}$
- (3) $\qquad\qquad\qquad = 0, \quad \text{otherwise}$
- (b) $g(X_2) = 1, \quad X_2 = B = (b_1, \dots, b_n)$
 $\qquad\qquad\qquad = 0, \quad \text{otherwise,}$

then (1) reduces to

$$(4) \quad P(\cdot) = \int_{C_1} dF(X_1)$$

which is the probability content of region C_1 under distribution $F(X_1)$.

If (a) of (3) is satisfied (sometimes called a zero-one damage function)

but $G(X_2)$ does not concentrate all the probability at one point, then (1) reduces to

$$(5) \quad P(\cdot) = \int_{-\infty}^{\infty} \int_{C_1} dF(X_1) dG(X_2),$$

where in general C_1 is defined in terms of both X_1 and X_2 .

If X_2 is uniformly distributed over a region C_2 , that is

$$(6) \quad g(X_2) = \frac{1}{V(C_2)}, \quad X_2 \in C_2$$

$$= 0, \quad \text{otherwise}$$

where $V(C_2)$ is the volume of C_2 , and the damage function is zero-one, then $P(\cdot)$ can be interpreted as the expected fraction of overlap of the region of total destruction and a target area C_2 . To see this integrate in reverse order. Given a value of X_1 (see Figure 2)

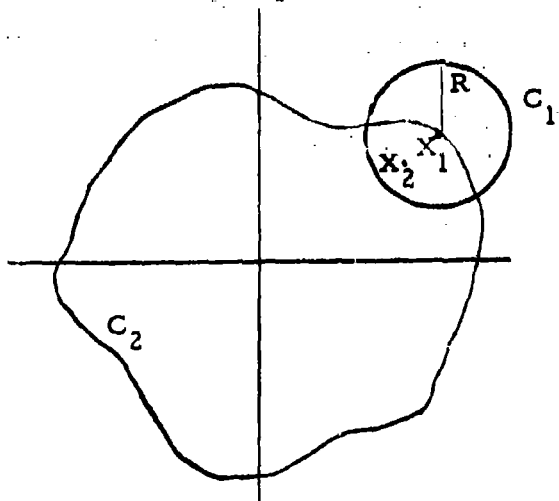


Fig. 2. Circular area of total destruction and target area C_2 .

X_2 is captured if it lies in the region common to C_1 and C_2 . The probability that happens is

$$\int_{C_1 \cap C_2} \frac{1}{V(C_2)} dX_2 = \frac{V(X_1)}{V(C_2)}$$

where $V(X_1)$ is the volume common to C_1 and C_2 for given X_1 . Then integrating over X_1 we get

$$\int_{-\infty}^{\infty} \frac{V(X_1)}{V(C_2)} dF(X_1) = E \left[\frac{V(X_1)}{V(C_2)} \right]$$

which is, by definition, the expected fraction overlap. Multiplying the latter result by $V(C_2)$ gives $E[V(X_1)]$ or the expected overlap.

When the damage function is not of the zero-one type and X_2 has the density (6), then $P(\cdot)$ can again be interpreted as the fraction of the target area destroyed. This is best seen by writing $P(\cdot)$ as

$$P(\cdot) = \int_{C_2} P_2(X_2) \frac{1}{V(C_2)} dX_2$$

and observing that since $P_2(X_2)$ can be interpreted as the fraction of the point X_2 destroyed, $E[P_2(X_2)]$ is the fraction of the target area C_2 which is destroyed. Morganthaler [2] has used this interpretation.

SOME SPECIFIC RESULTS FOR SINGLE SHOT CASE--GUENTHER-TERRAGNO PAPER. A comprehensive review of results for the single shot case has been published by Guenther and Terragno [1]. This paper lists 58 references of which about 30 deal directly with target coverage. A thorough knowledge of results for the single shot case is extremely helpful in the multiple shot situation. This section will be an abstract of that paper.

For most models discussed in the review it is assumed that X_1 has density

$$(7) \quad f(X_1) = f(x_{11}, \dots, x_{1n}) \\ = \left[(2\pi)^{\frac{1}{2}n} \prod_{i=1}^n \sigma_{1i} \right]^{-1} \exp \left[-\frac{1}{2} \sum_{i=1}^n (x_{1i}/\sigma_{1i})^2 \right].$$

Section 1 is devoted to probability content problems, special cases of (4) with the region C_1 being $\sum_{i=1}^n (x_{1i} - b_i)^2 \leq R^2$. Thus the point B is destroyed if the point of impact is within R units of the fixed point. If all $\sigma_{1i}^2 = \sigma^2$, then $P(\cdot)$ is the integral of a non-central chi-square density function with n degrees of freedom and non-centrality parameter $\sum_{i=1}^n b_i^2/\sigma^2$. Very extensive tables exist for $n=2$, adequate tables for $n = 3(1)30(2)50(5)100$. Results are less abundant if the variances are not equal. However, for $B = 0$, $n = 2, 3$ and $B \neq 0$, $n = 2$, existing tables seem to be quite adequate.

Section 2 describes some special cases of (5). The most interesting results are obtained by using (7) with equal variances for the density of X_1 and $\sum_{i=1}^n (x_{1i} - x_{2i})^2 \leq R^2$ for C_1 . Thus, if X_1 is within R units of X_2 , X_2 is destroyed. For these cases the probability can be expressed as the integral

$$(8) \quad P(\cdot) = \int_{-\infty}^{\infty} H\left(\frac{R^2}{\sigma^2}; n, \frac{r^2}{\sigma^2}\right) dG(X_2) = \int_{-\infty}^{\infty} H\left(\frac{R^2}{\sigma^2}; n, \frac{r^2}{\sigma^2}\right) dQ\left(\frac{r}{\sigma}\right)$$

where $H\left(\frac{R^2}{\sigma^2}; n, \frac{r^2}{\sigma^2}\right)$ is the non-central chi-square distribution function

with n degrees of freedom and non-centrality parameter $\sum_{i=1}^n \frac{x_{2i}^2}{\sigma^2} = r^2/\sigma^2$.

$Q(r/\sigma)$ is the distribution function of r/σ (which is, of course, determined by $G(X_2)$). The evaluation of the integral (8) is discussed for the cases:

- I. The distribution of X_2 gives equal weight to each point on $\sum_{i=1}^n x_{2i}^2 = D^2$, no weight elsewhere. That is, X_2 is uniformly distributed over the surface of a sphere of radius D centered at the origin.

- II. X_2 is uniformly distributed within or on a sphere of radius D centered at the origin. Thus,

$$g(X_2) = \begin{cases} \frac{1}{V(D)}, & \sum_{i=1}^n x_{2i}^2 \leq D^2 \\ 0, & \text{elsewhere} \end{cases}$$

where $V(D)$ is the volume of the sphere.

- III. X_2 has a density $g(X_2)$ taking on the form (in spherical coordinates)

$$p(r, a_1, \dots, a_{n-1}) = (2D\pi^{n-1})^{-1}, \quad \begin{aligned} 0 \leq r &\leq D \\ 0 \leq a_i &\leq \pi, i=1, \dots, n-2 \\ 0 \leq a_{n-1} &\leq 2\pi \end{aligned}$$

$$= 0, \quad \text{elsewhere}$$

so that the spherical coordinates are each independently and uniformly distributed.

- IV. r/σ has a gamma distribution.

- V. r^2/σ^2 has a gamma distribution.

- VI. r/σ has a beta distribution.

Finally, a case not falling under (8) in which X_1 and X_2 both have density (7) (but with different variances) is discussed. Perhaps II is the most interesting since it generalizes a well known result by Germond [3]. For this case

$$(9) \quad P(\cdot) = P\left(\frac{R}{\sigma}, \frac{D}{\sigma}\right) = H\left(\frac{R^2}{\sigma^2}; n+2, \frac{D^2}{\sigma^2}\right) + \left(\frac{R/\sigma}{D/\sigma}\right)^n H\left(\frac{D^2}{\sigma^2}; n, \frac{R^2}{\sigma^2}\right)$$

and evaluation is accomplished by using tables of the non-central chi-square distribution [4].

In Section 3 a few models with damage function

$$P_1(X_1, X_2) = \exp\left[-\sum_{i=1}^n (x_{2i} - x_{1i})^2 / 2 \lambda^2\right]$$

are discussed. Again X_1 is assumed to have density (7). Then $P(\cdot)$ is evaluated for

- I. Same as Case I of Section 2.
- II. Same as Case II of Section 2 except that unequal variances are permitted in (7).
- III. Same as Case III of Section 2.
- IV. Same as Case V of Section 2.
- V. Both X_1 and X_2 have density (7) but with different variances.

EXTENDING THE DEFINITION TO THE MULTIPLE SHOT CASE.

Again, having a special problem in mind will help in constructing the definition. Let us consider the following case discussed by Jarnagin

and Di Donato [5]. A big bomb is aimed at a point target located at the origin of a two-dimensional coordinate system. When the weapon arrives at the target, the latter is located at X_2 , a randomly selected position within or on a circle of radius D. Assume that aiming errors for the big bomb are circularly normally distributed with unit variance. That is, when the big bomb detonates its position X_3 is governed by the density

$$f_3(x_{31}, x_{32}) = \frac{1}{2\pi} \exp \left[-\frac{1}{2}(x_{31}^2 + x_{32}^2) \right].$$

At detonation the big bomb scatters N bomblets, each with lethal radius R, with impact points uniformly and independently distributed over a circle of radius A. Thus, the density of X_1 , the impact point of a bomblet, is for given X_3

$$\begin{aligned} f_{13}(X_1 | X_3) &= \frac{1}{\pi A^2}, & (x_{11}-x_{31})^2 + (x_{12}-x_{32})^2 \leq A^2 \\ &= 0, & \text{otherwise.} \end{aligned}$$

Now, given that the target is at X_2 and the big bomb detonates at X_3 , X_2 is captured by a bomblet if X_1 is within a distance R of X_2 (see Figure 3). The probability that this happens is

$$P_S = \int_{C_1} \frac{1}{\pi A^2} dX_1$$

where C_1 is the region $(x_{11}-x_{21})^2 + (x_{12}-x_{22})^2 \leq R^2$. The target will be captured if it is covered by at least one bomblet. This happens with probability $1-(1-P_S)^N$ because of the independence condition. The probability that the target will be captured regardless of where the big bomb detonates is

$$h(X_2) = \int_{-\infty}^{\infty} [1 - (1-P_S)^N] f_3(X_3) dX_3.$$

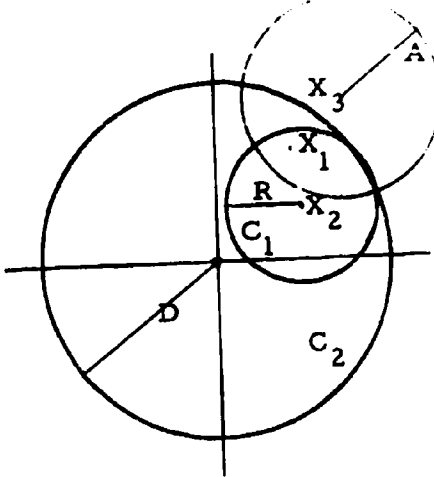


FIG. 3. Big bomb detonates at X_3 , bomblet at X_1 .
Target is at X_2 .

Finally, the probability that the target will be captured no matter where it is located is

$$\int_{C_2} h(X_2) g(X_2) dX_2$$

where C_2 is the region $x_{21}^2 + x_{22}^2 \leq D^2$ and

$$g(X_2) = \frac{1}{\pi D^2}, \quad x_{21}^2 + x_{22}^2 \leq D^2 \\ = 0, \quad \text{otherwise.}$$

This problem will be discussed further in a later section.

To generalize the above result let X_3 = the impact point of the big bomb, $F_3(X_3)$ = the distribution function of X_3 , X_1 = impact point of

a bomblet, $F_{13}(X_1 | X_3)$ = conditional distribution of X_1 given X_3 , the same for each of the N bomblets with all N impact points being independently distributed, X_2 = position of target when the bomblets impact, $G(X_2)$ = distribution function of the point target, $P_1(X_1, X_2)$ = probability of destroying the target for given values of X_1 and X_2 , P_S = probability of capturing the target for any one bomblet given X_3 and X_2 . Then

$$P_S = \int_{-\infty}^{\infty} P_1(X_1, X_2) dF_{13}(X_1 | X_3)$$

and

$$(10) \quad P(\cdot) = \int_{-\infty}^{\infty} \int_{-\infty}^{\infty} [1 - (1-P_S)^N] dF_3(X_3) dG(X_2)$$

is the probability of destroying the target. Expanding the binomial under the integral in (10) leads to the alternate form

$$(11) \quad P(\cdot) = \sum_{k=1}^N (-1)^{k+1} \binom{N}{k} \int_{-\infty}^{\infty} \int_{-\infty}^{\infty} P_S^k dF_3(X_3) dG(X_2).$$

We will define an n -dimensional coverage problem as the evaluation of a probability of the type given by (10) or (11).

If X_3 has density

$$(12) \quad f_3(X_3) = 1, \quad X_3 = B \text{ (a fixed point)} \\ = 0, \quad \text{otherwise}$$

then (10) reduces to

$$(13) \quad P(\cdot) = \int_{-\infty}^{\infty} [1 - (1-P_S)^N] dG(X_2)$$

where $X_3 = B$ in P_S . Formula (13) yields $P(\cdot)$ for N shots aimed independently at B (at the origin if $B = 0$). Further if $N = 1$, (13) becomes

$$\int_{-\infty}^{\infty} \int_{-\infty}^{\infty} P_1(X_1, X_2) dF(X_1) dG(X_2),$$

the single shot formula (where $F(X_1) = F_{13}(X_1 | B)$).

SOME SPECIAL CASES OF FORMULA (13).

Big Bomb Hits Origin with Probability 1, Zero-One Damage Function

Assume that aiming errors of the big bomb are governed by the p.d.f. of (12) with $B = 0$ and that X_2 is uniformly distributed over a sphere of radius D centered at the origin, that is, has p.d.f.

$$(14) \quad g(X_2) = [V(D)]^{-1}, \quad \sum_{i=1}^n x_{2i}^2 \leq D^2 \text{ (region } C_2) \\ = 0, \quad \text{otherwise}$$

where $V(D)$ is the volume of sphere of radius D . We will also assume that the density of X_1 given X_3 is

$$(15) \quad f_{13}(X_1 | X_3) = [(2\pi)^{\frac{1}{2}n} \frac{n}{\pi} \sigma_{1i}]^{-1} \exp[-\frac{1}{2} \sum_{i=1}^n (x_{1i} - x_{3i})^2 / \sigma_{1i}^2]$$

with $\sigma_{1i} = \sigma$, $i=1, 2, \dots, n$ and where $x_{3i} = 0$, $i=1, 2, \dots, n$ because the big bomb hits the origin with probability 1. Then

$$P_S = \int_{C_1} dF_{13}(x_1 | 0)$$

where C_1 is the region $\sum_{i=1}^n (x_{1i} - x_{2i})^2 \leq R^2$. It is well known that this integral has the value

$$(16) \quad P_S = H\left(\frac{R^2}{\sigma^2}; n, \frac{r^2}{\sigma^2}\right)$$

where $r^2 = \sum_{i=1}^n x_{2i}^2$. Hence

$$\begin{aligned} P(\cdot) &= P\left(\frac{R}{\sigma}, \frac{D}{\sigma}\right) = \int_{C_2} \left\{ 1 - [1 - H\left(\frac{R^2}{\sigma^2}; n, \frac{r^2}{\sigma^2}\right)]^N \right\} \frac{1}{V(D)} dX_2 \\ &= \sum_{k=1}^N (-1)^{k+1} \binom{N}{k} \int_0^D [H\left(\frac{R^2}{\sigma^2}; n, \frac{r^2}{\sigma^2}\right)]^k \frac{nr^{n-1}}{D^n} dr. \end{aligned}$$

The multiple integral converts to a single integral by virtue of the result on page 248 of [1]. We know from Formula (9) that the single integral in (17) can be expressed in terms of H functions for $k = 1$. A corresponding result for $k \geq 2$ may be possible but it is unknown at the present time.

For the case $n=2$, Jarnagin [6] has prepared tables of (17) for $R/\sigma = .005(.005), .05(.01), .10(.02), .20(.05)1(.1)2(.2)4(.5)10$, $D/\sigma = .05, 1, (.1)4(.5)12$, $N = 1(1)20$. Also included is an inverse table giving the number of bomblets N required to make $P(\cdot) = .05(.05), .95$ for the range of D/σ given above and with R/σ ranging over values required to make N go from 1 to 999.

Big Bomb Hits at Point B with Probability 1, Exponential Damage Function

Assume that the damage function is

$$(18) \quad P_1(X_1, X_2) = \exp\left[-\frac{1}{2} \sum_{i=1}^n (x_{2i} - x_{1i})^2 / \lambda^2\right]$$

and that the p. d. f. of X_1 given $X_3 = B$ is given by (15) with $x_{3i} = b_i$, $i=1, 2, \dots, n$. Then an easy integration yields

$$P_S = \frac{\lambda^n}{\pi \sum_{i=1}^n (\sigma_{1i}^2 + \lambda^2)^{\frac{1}{2}}} \exp\left[-\frac{1}{2} \sum_{i=1}^n (x_{2i} - b_i)^2 / (\sigma_{1i}^2 + \lambda^2)\right].$$

Expanding the binomial in (13) we can write

$$(19) \quad P(\cdot) = \sum_{k=1}^N (-1)^{k+1} \binom{N}{k} \int_{-\infty}^{\infty} \frac{\lambda^{nk}}{\pi \sum_{i=1}^n (\sigma_{1i}^2 + \lambda^2)^{\frac{1}{2}k}} \exp\left[\left(-\frac{k}{2}\right) \sum_{i=1}^n \frac{(x_{2i} - b_i)^2}{(\sigma_{1i}^2 + \lambda^2)}\right] dG(X_2).$$

First assume that X_2 is uniformly distributed over an ellipsoid whose center is at the origin and whose axes are parallel to the coordinate axes. Then

$$g(X_2) = [V(C_2)]^{-1}, \quad \sum_{i=1}^n (x_{2i}/a_i)^2 \leq 1 \quad (\text{the region } C_2) \\ = 0, \quad \text{otherwise}$$

where $V(C_2)$ is the volume of C_2 . Then if we let $k^{\frac{1}{2}}(x_{2i} - b_i)/(\sigma_{1i}^2 + \lambda^2)^{\frac{1}{2}} = y_i$, the probability (19) becomes

$$(20) \quad P(\cdot) = \sum_{k=1}^N \frac{(-1)^{k+1} \binom{N}{k} \lambda^{nk} (2\pi)^{\frac{1}{2}n}}{V(C_2) k^{\frac{1}{2}n} \prod_{i=1}^n (\sigma_{ii}^2 + \lambda^2)^{\frac{1}{2}(k-1)}} J_k$$

where

$$J_k = \int_{C_{2k}} f_0(Y) dY,$$

$f_0(Y)$ is the standard normal density in n dimensions, and C_{2k} is the region

$$\sum_{i=1}^n \frac{\left(y_i + \frac{b_i \sqrt{k}}{(\sigma_{ii}^2 + \lambda^2)^{\frac{1}{2}}} \right)^2}{k^2 / a_i^2 (\sigma_{ii}^2 + \lambda^2)} \leq 1.$$

Tables from which J_k can be obtained when $n=2$ have been prepared by Germond [7], DiDonato and Jarnagin [8], Lowe [9], and Rosenthal and Rodden [10]. If $b_1 = b_2 = 0$ so that the ellipse is centered at the origin, then J_k can be evaluated from the tables published by Esperti [11], Harter [12], DiDonato and Jarnagin [13], and Marsaglia [14]. All the above tables are described by Guenther and Terragno [1]. Groves [15] derived (20) for the case $n = 2$ and includes a 16 page table of J_k for this case (with $b_1 = b_2 = 0$) in his report.

If all $\sigma_{ii} = \sigma$, and $a_i = D$, then

$$J_k = H \left[\frac{k^2}{D^2 (\sigma^2 + \lambda^2)} ; n, r^2 \right]$$

where

$$r^2 = \frac{k}{\sigma^2 + \lambda^2} \quad \sum_{i=1}^n b_i^2 .$$

Further if $B = 0$, then J_k reduces to a central chi-square probability.

For both the latter two cases many tables are available and a description of these tables is found in Section 1 of [1].

If in (19) we take $B = 0$, $\sigma_{1i} = \sigma$ and assume that $G(X_2)$ gives equal weight to each point on the sphere $\sum_{i=1}^n x_{2i}^2 = D^2$, then (19) reduces to

$$(21) \quad P(\cdot) = \sum_{k=1}^N (-1)^{k+1} \binom{N}{k} \frac{\lambda^{nk}}{(\sigma^2 + \lambda^2)^{nk/2}} \exp\left[\frac{kD^2}{2(\sigma^2 + \lambda^2)}\right]$$

since everything comes out in front of the multiple integral except $dG(X_2)$ which when integrated over the whole space yields 1. For a $G(X_2)$ so chosen, X_2 picks its position at random on the surface of the sphere. The answer is the same, of course, no matter how $G(X_2)$ assigns probability on the surface of the sphere but uniform assignment is the most realistic model.

As one further model let us assume that $B = 0$ and X_2 has p.d.f.

$$(22) \quad g(X_2) = [(2\pi)^{\frac{1}{2}n} \frac{n}{\pi} \sigma_{2i}]^{-1} \exp\left[-\frac{1}{2} \sum_{i=1}^n (x_{2i}/\sigma_{2i})^2\right]$$

Then (19) readily reduces to

$$P(\cdot) = \sum_{k=1}^N (-1)^{k+1} \binom{N}{k} \frac{\lambda^{nk}}{\frac{n}{\pi} [(\sigma_{1i}^2 + \lambda^2)^{(k-1)} (k\sigma_{2i}^2 + \sigma_{1i}^2 + \lambda^2)]^{\frac{1}{2}}}$$

SOME SPECIAL CASES OF FORMULA (10).

The Jarnagin-DiDonato Model

Let us return to the example which we used to introduce multiple shot coverage problems but generalize the discussion to n-dimensions.

Then X_1 given X_3 is uniformly distributed over a sphere of radius A centered at X_1 so that

$$f_{13}(X_1 | X_3) = [V(A)]^{-1}, \quad \sum_{i=1}^n (x_{1i} - x_{3i})^2 \leq A^2 \text{ (region } C_3) \\ = 0, \quad \text{otherwise,}$$

X_2 is uniformly distributed over a sphere of radius D centered at the origin so that it has the p. d. f. given by (14), and

$$(23) \quad f_3(X_3) = [(2\pi)^{\frac{1}{2}} n \pi^{\frac{n}{2}} \sigma_{3i}]^{-1} \exp[-\frac{1}{2} \sum_{i=1}^n (x_{3i}/\sigma_{3i})^2].$$

Here $V(A)$ is the volume of a sphere of radius A . We will assume that $\sigma_{3i} = \sigma$, $i=1, 2, \dots, n$ and for convenience (as DiDonato and Jarnagin have done) we will take $\sigma = 1$ which means all distances are expressed in standard units. The damage function is

$$P_1(X_1, X_2) = 1, \quad \sum_{i=1}^n (x_{1i} - x_{2i})^2 \leq R^2. \quad (\text{region } C_1)$$

Then

$$P_S = \int_{C_1} \frac{1}{V(A)} dX_1 = \frac{V(t^2)}{V(A)}$$

where $t^2 = \sum_{i=1}^n (x_{2i} - x_{3i})^2$ and $V(t^2)$ is the volume common to C_1 and C_3 .

Hence, since all functions appearing in (10) are known, the $2n$ -fold integral could be written down with the integrand expressed in terms of X_2 and X_3 .

Some simplification is possible. We seek $E[u(t^2)]$ where $u(t^2) = 1 - (1-P_S)^N$. If the density of t^2 were known, then $P(\cdot)$ could be expressed as a single integral with integrand in t^2 . We know from working with single shot coverage problems that the density of t^2 given $r^2 = \sum_{i=1}^n x_{2i}^2$ is non-central chi-square with non-centrality parameter r^2 . This is

$$(24) \quad h(t^2; n, r^2) = \frac{1}{2} \left(\frac{t^2}{r^2} \right)^{(n-2)/2} \exp\left[-\frac{1}{2}(t^2+r^2)\right] I_{(n-2)/2}(tr)$$

where $I_{(n-2)/2}(x)$ is the modified Bessel function of order $(n-2)/2$. The density function of r^2 (see [1], p. 248 for the density of r) is

$$g(r^2) = \frac{n(r^2)^{(n-2)/2}}{2D^n}, \quad 0 \leq r^2 \leq D^2$$

$$= 0 \quad \text{otherwise.}$$

Hence the joint distribution of t^2 and r^2 is $h(t^2; n, r^2) g(r^2)$ and

$$(25) \quad P(\cdot) = \int_0^{(A+R)^2} \int_0^{D^2} u(t^2) h(t^2; n, r^2) g(r^2) dr^2 dt^2,$$

a double integral.

For the 2-dimensional case a further simplification is possible since (24) is then symmetric in t^2 and r^2 . Thus, in (25) the integration of r^2 yields $H(D^2; 2, t^2)$ so that

$$(26) \quad P(\cdot) = \int_0^{(A+R)^2} \frac{u(t^2)}{D^2} H(D^2; 2, t^2) dt^2.$$

The Jarnagin and DiDonato report includes over 100 pages of graphs which yield the $P(\cdot)$ of (26). Two cases are considered. For Case I, $R < A$ and $20 \leq N \leq 500$ for various values of D , A , and πR^2 . For Case II, $R > A$ and $1 \leq N \leq 20$ for selected values of R , D , A . The Case I graphs give $\pi D^2 P(\cdot)$ while the set for Case II give $P(\cdot)$ directly. Various approximations to $P(\cdot)$ are discussed.

From a practical point of view the most interesting case is $R < A$. For this situation it is immediately apparent that bounds on the $P(\cdot)$ of (26) are

$$(27) \quad \left[1 - \left(1 - \frac{R^2}{2}\right) \frac{N}{A}\right] \int_0^{(A-R)^2} \frac{1}{D^2} H(D^2; 2, t^2) dt^2 < P(\cdot)$$

$$\left[1 - \left(1 - \frac{R^2}{2}\right) \frac{N}{A}\right] \int_0^{(A+R)^2} \frac{1}{D^2} H(D^2; 2, t^2) dt^2 .$$

Both integrals appearing in (27) can be expressed in terms of H functions by using (9). The H functions in turn can be evaluated by using the tables of Hayman, Govindarajulu, and Leone [4]. Of course, the smaller the R the closer the bounds will be.

EXPONENTIAL DAMAGE FUNCTION, DETONATION POINTS OF BIG AND LITTLE BOMBS NORMALLY DISTRIBUTED. Assume that the damage function is given by (18), the density of X_1 given X_3 by (15), and the density of X_3 by (23). Then a straight forward evaluation yields

$$P_S = \int_{-\infty}^{\infty} P_1(X_1, X_2) f_{13}(X_1 | X_3) dX_1$$

$$= \frac{\lambda^n}{\frac{n}{\pi} (\sigma_{11}^2 + \lambda^2)^{\frac{n}{2}}} \exp \left[-\frac{1}{2} \sum_{i=1}^n (x_{3i} - x_{2i})^2 / (\sigma_{11}^2 + \lambda^2) \right] .$$

The same kind of evaluation next gives

$$(28) \quad \int_{-\infty}^{\infty} P_S^k f_3(x_3) dx_3 = \frac{\lambda^{kn} \exp\left[\left(\frac{-k}{2}\right) \sum_{i=1}^n x_{2i}^2 / (k\sigma_{3i}^2 + \sigma_{1i}^2 + \lambda^2)\right]}{\pi^{\frac{n}{2}} \left[(\sigma_{1i}^2 + \lambda^2)^{(k-1)} (k\sigma_{3i}^2 + \sigma_{1i}^2 + \lambda^2)\right]^{\frac{n}{2}}}$$

To write down $P(\cdot)$ as given by (10) we need finally to integrate (28) over the range of X_2 .

For several distributions of X_2 $P(\cdot)$ is obtained very quickly. We will consider:

Case I: $\sigma_{3i} = \sigma_3$, $\sigma_{1i} = \sigma_1$ and $G(X_2)$ gives equal weight to each point on the sphere $\sum_{i=1}^n x_{2i}^2 = D^2$. Then with the same reasoning used to obtain (21) we get

$$(29) \quad P(\cdot) = \sum_{k=1}^N (-1)^{k+1} \binom{N}{k} \frac{\lambda^{kn} \exp[-kD^2/2(k\sigma_3^2 + \sigma_1^2 + \lambda^2)]}{[(\sigma_1^2 + \lambda^2)^{(k-1)} (k\sigma_3^2 + \sigma_1^2 + \lambda^2)]^{n/2}}$$

Case II: The density of X_2 is given by (14). Letting

$$y_i = \frac{\sqrt{k} x_{2i}}{\sqrt{k\sigma_{3i}^2 + \sigma_{1i}^2 + \lambda^2}}$$

and recalling that

$$V(D) = \pi^{n/2} D^n / \Gamma(\frac{n+2}{2})$$

we get

$$(30) \quad P(\cdot) = \sum_{k=1}^N (-1)^{k+1} \binom{N}{k} \frac{\lambda^{kn} I\left(\frac{n+2}{2}\right) 2^{n/2}}{D^n k^{n/2} \prod_{i=1}^n (\sigma_{1i}^2 + \lambda^2)^{(k-1)/2}} \int_{C_1} \frac{1}{(2\pi)^{n/2}} \exp\left[\frac{1}{2} \sum_{i=1}^n y_i^2\right] dy_1 \dots dy_n$$

where C_1 is the region $\sum_{i=1}^n (k\sigma_{3i}^2 + \sigma_{1i}^2 + \lambda^2) y_i^2 / k \leq D^2$. The evaluation of standard normal integrals over ellipsoidal and spherical regions is discussed in Section 1.3 of [1].

Case III. The density of X_2 is given by (22). A routine integration yields

$$(31) \quad P(\cdot) = \sum_{k=1}^N (-1)^{k+1} \binom{N}{k} \frac{\lambda^{kn}}{\prod_{i=1}^n [(\sigma_{1i}^2 + \lambda^2)^{(k-1)} (\sigma_{1i}^2 + k\sigma_{2i}^2 + k\sigma_{3i}^2 + \lambda^2)]^{1/2}}$$

CONCLUDING REMARKS. Although the definition of a coverage problem which we have given can be further generalized, many of the interesting models which have received attention are special cases of the definition as we have given it. Certainly there are models which may be of interest other than those covered in the Guenther-Terragno review and in this paper.

In this review we have considered only the zero-one damage function and the exponential damage function given by (18). Many others have been proposed. For example, another possibility that has some merit is

$$(32) \quad \begin{aligned} P_1(X_1, X_2) &= 1, & \sum_{i=1}^n (x_{1i} - x_{2i})^2 &\leq R^2 \\ &= \exp \left\{ -\frac{1}{2} \left[\sum_{i=1}^n (x_{1i} - x_{2i})^2 - R^2 \right] / \lambda^2 \right\}, & \sum_{i=1}^n (x_{1i} - x_{2i})^2 &> R^2. \end{aligned}$$

The damage function (32) is found in [1] but the topic is not pursued. Other damage functions are mentioned in [16] and [17].

The first step for a potential researcher in the field of coverage problems is to select a useful and realistic model. Having made that choice, the remainder of the task confronting an investigator is mainly numerical. It is possible that most or all of the computation required is already available in the literature if one knows where to look. Even if no such results are in existence, chances are excellent that probabilities of interest can be evaluated if one is clever enough in handling special functions and computers.

Work on target coverage problems has suffered from a mass duplication of effort. This is in part due to (a) some company publications being difficult if not impossible to obtain, (b) results having been published not only in obscure publications but also in many different journals so that it is difficult to keep current in the field, and (c) some papers being difficult to read unless one has background in both probability and target coverage.

REFERENCES

1. William C. Guenther and Paul J. Terragno, "A Review of the Literature on a Class of Coverage Problems," The Annals of Mathematical Statistics 35, 232-260 (1964).
2. George W. Morganthaler, "Some Target Coverage Problems," Biometrika 48, 313-324 (1961).
3. G. E. Haynam, Z. Govindarajulu, and F. C. Leone, "Tables of the Cumulative Non-Central Chi-Square Distribution," AD 426 500 Office of Technical Service, U. S. Department of Commerce, Washington, D. C. 20230 (1962).
5. M. P. Jarnagin, Jr. and A. R. DiDonato, "Expected Damage to a Circular Target by a Multiple Warhead," NWL Report No. 1936, U. S. Naval Weapons Laboratory, Dahlgren, Virginia (1964).
6. M. P. Jarnagin, Jr., "Expected Coverage of a Circular Target by Bombs all Aimed at the Center," NWL Report No. 1941, U. S. Naval Weapons Laboratory, Dahlgren, Virginia (1965).

7. H. H. Germond, "Integration of the Gaussian Distribution over an Offset Ellipse," Rand Report No. P-94, The Rand Corporation, Santa Monica, California (1949).
8. A. R. DiDonato and M. P. Jarnagin, Jr., "Integration of the General Bivariate Gaussian Distribution over an Offset Ellipse," NWL Report No. 1710, U. S. Naval Weapons Laboratory, Dahlgren, Virginia (1960).
9. J. R. Lowe, "A Table of the Integral of the Bivariate Normal Distribution over an Offset Circle," Journal of the Royal Statistical Society, Series B 22, 177-187 (1960).
10. G. W. Rosenthal and I. J. Rodden, "Tables of the Integral of the Elliptical Bivariate Normal Distribution over Offset Circles," Lockheed Report No. IMSD-800619, Sunnyvale, California (1961).
11. R. V. Esperti, "Tables of the Elliptical Normal Probability Function," Defense Systems Division, General Motors Corporation, Detroit, Michigan (1960).
12. H. Leon Harter, "Circular Error Probabilities," Journal of the American Statistical Association 55, 723-731 (1960).
13. A. R. DiDonato and M. P. Jarnagin, Jr., "A Method for Computing the Generalized Circular Error Function and Circular Coverage Function," NWL Report No. 1768, U. S. Naval Weapons Laboratory, Dahlgren, Virginia (1962).
14. George Marsaglia, "Tables of the Distribution of Quadratic Forms of Ranks Two and Three," Boeing Scientific Research Laboratories Report No. Dl-82-0015-1, Seattle, Washington (1960).
15. Arthur D. Groves, "A Method for Hand-Computing the Expected Fractional Kill of an Area Target with a Salvo of Area Kill Weapons," Ballistic Research Laboratories Memorandum Report No. 1544, Aberdeen Proving Ground, Maryland (1964).
16. Operations Evaluation Group, "Probability-of-Damage Problems of Frequent Occurrence," OEG Study 626, Office of the Chief of Naval Operations, Washington, D. C. (1959).
17. Frank McNulty, "Kill Probability When Lethal Effect is Variable," Operations Research 13, 478-482 (1965).

MAXIMUM LIKELIHOOD ESTIMATION FOR
UNBALANCED FACTORIAL DATA*

H. O. Hartley
Institute of Statistics
Texas A&M University

1. INTRODUCTION. The statistical literature is abundant with results concerning the design and analysis of factorial experiments. Most of these results relate to design experiments whose intricate balance usually provides orthogonal contrasts for the estimation of parameter functions for which inferences are desired. The consequences of such designs are statistical efficiency of estimation with exactness of estimation theory and simplicity of computational procedures thrown in as 'fringe benefits'.

Unfortunately, however, in basic and operation research there are many situations where the scientist is forced to draw inferences from data which have not arisen from carefully balanced factorial experiments mainly because part of the origin of his data is beyond his control. Thus we may be concerned with an analysis of operational data in a chemical plant attempting to relate the quality and yield of the output to various types and sources of input materials, to different types of catalysts, to various modes of operating the plant such as temperature-and pressure levels and running times. Even if it is possible to control the change in the various input factors it will often not be possible to conduct balanced experiments. Again in genetical research concerned with heritability studies we may study certain traits of the progeny resulting from the mating of a number of sires each to a different set of dames. We may try to arrange for the 'breeding pens' of the progeny trail to have an equal number of dames in each but the progeny resulting from each mating is beyond the control of the experimenter, resulting in an 'unequal number nested classification' of data. Again, in medical research we may wish to compare the follow-up of patients who have received different treatments. Such follow-up data are often classified with regard to numerous concomitant characteristics concerning the medical history, environmental and genetical background of patients resulting in data arranged in completely unbalanced factorial patterns. There is clearly no possibility of a designed experiment here.

*This paper gives only a summary of some of the results derived in more detail by Hartley, H. O. and Rao, J. N. K. "Maximum Likelihood Estimation for the Mixed Analysis of Variance Model" submitted for publication in Biometrika.

We do not need to add further examples of this kind; indeed it is generally recognized that they will outnumber, by far, the situations of data from balanced experiments.

In the case of balanced designs the estimation problem for the constants and variances involved in the linear model theory of the experimental data has been extensively treated: Confining ourselves to just one reference on variance estimation, optimality properties of the classical analysis of variance procedures have already been demonstrated for various balanced designs (see e.g., Graybill (1961)). However, results for unbalanced factorial and nested data are much more restricted: Henderson (1953) has suggested a method of unbiased estimation of variance components for the unbalanced two-way classification but his method is computationally cumbersome for a mixed model and when the numbers of classes is large. Searle and Henderson (1961) have suggested a simpler method also for the unbalanced two way classification with one fixed factor containing a moderate number of levels and a random factor permitted to have quite a large number of levels. Bush and Anderson (1963) have investigated for the two-way classification random model the relative efficiency of Henderson's (1953) method and two other methods, A and B, based on the respective methods of fitting constants and weighted squares of means described by Yates (1934) for experiments based on a fixed effects model which also provide unbiased estimates of variance components. Possibilities of generalizations are indicated. In all the above methods the estimates of any constants in the model are computed from the 'Aitken Type' weighted least squares estimators based on the exact variance-covariance matrix of the experimental responses which involves the unknown variance ratios. The estimation of the latter is then based on various unbiased procedures so that little is known about any optimality properties of any of the resulting estimators. However, all these methods reduce to the well known procedures based on minimal sufficient statistics in the special cases of balanced designs.

The method of maximum likelihood estimation here developed differs from the above in that maximum likelihood equations are used and solved for both the estimates of constants and variances. This method has apparently not been used by the above authors (and is indeed 'rejected' by Bush and Anderson, 1963) because the computational effort is not (in their view) warranted by the known properties of maximum likelihood estimation. This point is well taken. However, we have nevertheless undertaken to develop this theory on the following grounds:

- (a) Within reason and with the help of suitable numerical techniques the argument of computational labor loses its stigma with the progress in computer technology.
- (b) Our technique of maximum likelihood estimation provides a numerical analysis for the completely general mixed model and does not require the development of new devices whenever a more involved situation of unbalanced factorial data arises. Moreover, it provides the basis for a completely general 'analysis of variance test' procedure in the form of 'likelihood--ratio tests'.
- (c) We have established large sample optimality properties and it is already apparent that for small experiments the amount of computational labor is quite comparable with that involved in alternatives. Here our technique will permit Monte Carlo evaluations of small sample variances (on the lines made by Bush and Anderson) for the maximum likelihood estimators. For really large experiments (such as arise with certain genetical problems) the large sample optimality properties of maximum likelihood estimators should provide a clear justification of additional computer time (if any).
- (d) Recent researches in identifying minimal sufficient statistics for the estimation of the parameters (see e.g., Hultquist and Graybill, (1965) Furukawa (1960)) is at this time confined to several special designs. Since a universal method of identifying such statistics when they exist is not available it is a considerable (small sample) advantage of maximum likelihood estimators that they will automatically be functions of such statistics whenever they exist.
- (e) Our estimates of variance components are always > 0 (see section 4) and whilst the alternative estimators could be modified to also be > 0 they would thereby lose the property of unbiasedness which is the main justification of their use.

2. **SPECIFICATION OF THE GENERAL MIXED MODEL.** The specification of the general mixed model will be sufficiently general to cover most of the situations of unbalanced factorial data arising in practice.

On the other hand, it utilizes certain specific features which distinguish analysis of variance models from a completely general linear model involving both 'constants' as well as random variables.

The linear model here treated is given by

$$(1) \quad y = X\alpha + U_1 b_1 + \dots + U_c b_c + e$$

where

X is an $n \times k$ matrix of known fixed numbers

U_i is an $n \times m_i$ matrix of known fixed numbers

α is a $k \times 1$ vector of unknown constants

b_i is an $m_i \times 1$ vector of independent variables from $N(0, \sigma_i^2)$

e is an $n \times 1$ vector of independent variables from $N(0, \sigma^2)$.

The random vectors b_1, b_2, \dots, b_c , and e are mutually independent and y is given by (1).

We assume that the design matrices X and U_i are all of full rank i.e., the rank of X is k and the rank of U_i is m_i . In terms of analysis of variance terminology the vector of constants α comprises in its elements all levels of all fixed factors, i.e., the levels of all fixed main effects and interactions appropriately re-parameterised so that the design matrix X has full rank. For the c random factors we are keeping the components separate since all elements of b_i have the same unknown variance σ_i^2 . Usually (with analysis of variance models) each y is associated with precisely one level of the i^{th} random factor so that the design matrix U_i will have in each row precisely one 1 and the remaining $m_i - 1$ elements zero. We therefore assume that the U_i have this property which implies that all $m_i \times m_i$ matrices $U_i' U_i$ are diagonal.

One additional important assumption must be made about the design matrices which may be described as a condition for estimability of the a and σ_i^2 : Denote by

$$(2) \quad m = \sum_{i=1}^c m_i$$

the total number of levels in all random components. Then the adjoined $n \times (k+m)$ matrix

$$(3) \quad M = (X \mid U_1 \mid \dots \mid U_c)$$

is assumed to have as a base an $n \times r$ matrix W of the form

$$(4) \quad W = (X \mid U^*)$$

where the $n \times (r-k)$ matrix U^* must contain at least one column from each U_i so that

$$(5) \quad k + c \leq r \leq k + m.$$

3. THE LIKELIHOOD EQUATIONS. From (1) it is obvious that y follows a multivariate normal distribution with variance-covariance matrix

$$(6) \quad \sigma^2 H = \sigma^2 \{ I_n + \gamma_1 U_1 U_1' + \dots + \gamma_c U_c U_c' \}$$

where

$$(7) \quad \gamma_i = \sigma_i^2 / \sigma^2$$

Hence the likelihood of y is given by

$$(8) \quad L = (2\pi)^{-\frac{1}{2}n} \sigma^{-n} |H|^{-\frac{1}{2}} \exp \{ -(y - Xa)' H^{-1} (y - Xa) / 2\sigma^2 \}.$$

The differentiation of the log likelihood

(9) $\lambda = \text{Log } L$

with regard to a , σ and γ_i yields the equations

(10) $\frac{\partial \lambda}{\partial a} = \sigma^{-2} \{ X' H^{-1} y - (X' H^{-1} X)a \} = 0$

(11) $\frac{\partial \lambda}{\partial \sigma} = -\frac{n}{\sigma} + \frac{1}{\sigma^3} (y - Xa)' H^{-1} (y - Xa) = 0$

and

$$\begin{aligned}
 (12) \quad \frac{\partial \lambda}{\partial \gamma_i} &= -\frac{1}{2} \text{tr} \left\{ H^{-1} \frac{\partial H}{\partial \gamma_i} \right\} - \frac{1}{2\sigma^2} (y - Xa)' \frac{\partial H^{-1}}{\partial \gamma_i} (y - Xa) \\
 &= -\frac{1}{2} \text{tr} \{ H^{-1} U_i U_i' \} + \frac{1}{2\sigma^2} (y - Xa)' H^{-1} U_i U_i' H^{-1} (y - Xa).
 \end{aligned}$$

Whilst it has long been recognized that equations (10) and (11) readily yield the maximum likelihood estimates a and σ^2 as functions of the γ_i involved in H , the solution of equations (12) i.e., $\frac{\partial \lambda}{\partial \gamma_i} = 0$ has not been attempted in the past. We give in the next section a numerical procedure of solving the simultaneous equation (10), (11), and $\frac{\partial \lambda}{\partial \gamma_i} = 0$ given by (12).

4. SOLUTION OF THE MAXIMUM LIKELIHOOD EQUATIONS BY STEEPEST ASCENT. As mentioned in 3. the equations (10) and (11) are readily solved for a and σ^2 in terms of the γ_i : -- We obtain the familiar answers for 'weighted least squares'

(13) $\tilde{a} = (X' H^{-1} X)^{-1} (X' H^{-1} y)$

and

(14) $n \tilde{\sigma}^2 = y' H^{-1} y - (X' H^{-1} y)' (X' H^{-1} X)^{-1} (X' H^{-1} y)$.

Equations (13) and (14) yield \tilde{a} and $\tilde{\sigma}^2$ in terms of the y and γ_i . We require symbols for this functional relationship and write in place of (13) and (14)

$$(15) \quad a = \tilde{a}(\gamma_i)$$

and

$$(16) \quad \sigma = \tilde{\sigma}(\gamma_i) .$$

Substitution of (15) and (16) in (12) and equating to zero would yield c simultaneous equations for the c values of γ_i . The solutions of these equations are now obtained as the asymptotic limits of a system of c simultaneous differential equations, namely the equations of steepest ascent given by

$$(17) \quad \frac{dy_i}{dt} = \frac{\partial \lambda}{\partial \gamma_i} (\tilde{a}(\gamma_i), \tilde{\sigma}(\gamma_i), \gamma_i)$$

where the $k + l + c$ argument function $\frac{\partial \lambda}{\partial \gamma_i} (a, \sigma, \gamma_i)$ is given by the right hand side of (12) and (15) and (16) are substituted for a and σ .

The variable of integration, t , in (17) is auxiliary and the numerical integration of (17) commences at initial trial values $_{0}\gamma_i$ (usually chosen as consistent estimators) so that

$$(18) \quad \gamma_i = _0\gamma_i \text{ at } t = 0.$$

It can now be shown that as $t \rightarrow \infty$

$$(19) \quad \lim_{t \rightarrow \infty} \gamma_i(t) = \tilde{\gamma}_i \text{ (say)}$$

and

$$(20) \quad \lim_{t \rightarrow \infty} \frac{\partial \lambda}{\partial \gamma_i} (\tilde{a}(\gamma_i), \tilde{\sigma}(\gamma_i), \gamma_i) = 0 .$$

Therefore, $\tilde{\gamma}_i$ together with $\tilde{a}(\tilde{\gamma}_i)$, $\tilde{\sigma}(\tilde{\gamma}_i)$ represent a solution of the maximum likelihood equations (10), (11), and $\frac{\partial \lambda}{\partial \gamma_i} = 0$ given by (12). It should be noted that although the limit along a specific path of integration is unique as $t \rightarrow \infty$ it does not follow that there is only one solution of the maximum likelihood equations since a change in the starting point $_{0\gamma_i}$ may give rise to a different path of integration.

Finally we should comment on a modification of our steepest ascent integration which ensures that $\gamma_i = 0$ along the path: First observe that the log likelihood is a differentiable function of $\tau_i = \gamma_i^{\frac{1}{2}}$ which is symmetrical at $\tau_i = 0$. It follows that if τ_i is used as a parameter in place of γ_i we have

$$(21) \quad \frac{\partial \lambda}{\partial \tau_i} = \frac{\partial \lambda}{\partial \gamma_i} \cdot 2\tau_i.$$

Therefore, the steepest ascent differential equations (17) can be replaced by

$$(22) \quad \frac{d\tau_i}{dt} = 2\tau_i \frac{\partial \lambda}{\partial \gamma_i} (\tilde{a}(\gamma_i), \tilde{\sigma}(\gamma_i), \gamma_i).$$

The integration would commence at positive values $_{0\gamma_i}$ but should the path of integration reach a point where one or several of the $\tau_i = 0$, a new integration would be started at that point and the one or several τ_i would be held at $\tau_i = 0$ for the rest of the integration path. The limit as $t \rightarrow \infty$ will again be a solution of the likelihood equations

$$(23) \quad \frac{\partial \lambda}{\partial \tau_i} = 0, \quad \frac{\partial \lambda}{\partial a} = 0, \quad \frac{\partial \lambda}{\partial \sigma} = 0.$$

This procedure ignores and avoids any possible solutions of the likelihood equations with $\gamma_i < 0$.

It would carry us to far afield if we were to discuss in this paper computational details of solving the system of c ordinary first order differential equations (17) or (22). It suffices to state that a large step (high order) Runge-Kutta procedure (see e.g., Henrici (1962)) is found to be quite serviceable. For large n (i.e., $n > 50$) numerical inversion of the $n \times n$ matrix H involved in (12), (13), and (14) can be completely avoided by reducing this task to operations involving only matrix inversions of order $m \times m$ where $m = \sum m_i$ on lines similar to Henderson et al (1959). The relevant equation is

$$(24) \quad H^{-1} = I - Z (Z'Z + I)^{-1} Z'$$

where

$$(25) \quad Z \text{ is the adjoined } n \times m \text{ matrix}$$

$$Z = (\sqrt{\gamma_1} U_1 \mid \dots \mid \sqrt{\gamma_c} U_c)$$

With the help of (24) the computational work is quite manageable on high speed computers and a program is in preparation covering data for which $n \leq 500$, $c \leq 5$, $k \leq 150$, $m \leq 150$. The computer time on the IBM 7094 is estimated to range between 5 minutes and 2 hours largely depending on the magnitudes of m and k .

REFERENCES

- Bush, N. and Anderson, R. L. (1963). "A Comparison of Three Different Procedures for Estimating Variance Components." Technometrics, 5, 421-40.
- Furukawa, N. (1960). "The Point Estimation of the Parameters in the Mixed Model." Kumamoto J. Sci. A, 5, 1-43.
- Graybill, F. A. (1961). An Introduction to Linear Statistical Models, Vol. 1. McGraw-Hill Book Company, Inc.
- Graybill, F. A., Martin, F. and Godfrey, G. (1956). "Confidence Intervals for Variance Ratios Specifying Genetic Heritability." Biometrics, 12, 99-109.

- Henderson, C. R. (1953). "Estimation of Variance and Covariance Components." Biometrics, 9, 226-52.
- Henderson, C. R., Kempthorne, O., Searle, S. R. and Von Krosigk, C. M. (1959). "The Estimation of Environmental and Genetic Trends from Records Subject to Culling." Biometrics, 15, 192-218.
- Henrici, P. (1962). Discrete Variable Methods in Ordinary Differential Equations. John Wiley & Sons, Inc.
- Hultquist, R. A. and Graybill, F. A. (1965). "Minimal Sufficient Statistics for the Two-Way Classification Mixed Model Design." J. Amer. Stat. Assoc. 60, 182-92.
- Searle, S. R. and Henderson, C. R. (1961). "Computing Procedures for Estimating Components of Variance in the Two-Way Classification Mixed Model." Biometrics, 17, 607-16.
- Yates, F. (1934). "The Analysis of Multiple Classifications with Unequal Numbers in the Different Classes." J. Amer. Stat. Assoc. 29, 51-66.

LIST OF ATTENDEES

Alley, Bernard	US Army Missile Command
Anctil, Albert A.	Army Materials Research Agency
Anderson, Virgil L.	Purdue University
Atkinson, John C.	Edgewood Arsenal
Bailey, Milton	US Naval Supply Res & Dev Facility
Barksdale, Thomas H.	Fort Detrick
Barnett, Bruce D.	Picatinny Arsenal
Bechhofer, Robert	Cornell University
Bell, Raymond	BRL, Aberdeen Proving Ground, Md.
Biser, Erwin	Fort Monmouth
Bohidar, Neeti R.	Fort Detrick
Boldridge, A.	TECOM
Bombara, E. L.	Marshall Space Flight Center
Brown, George A.	Thiokol Chemical Corp., Denville, NJ
Brown, William A.	Dugway Proving Ground
Bruce, C.	RAC
Bruno, O. P.	BRL, Aberdeen Proving Ground, Md.
Bulfinch, Alonzo	Picatinny Arsenal
Cameron, Joseph M.	National Bureau of Standards
Carrillo, J. V.	White Sands Missile Range, New Mexico
Carter, F. L.	Fort Detrick
Chernack, Gilbert	Thiokol Chemical Corp., Denville, NJ
Chrepta, M. M.	Fort Monmouth
Ciuchta, Henry P.	Edgewood Arsenal
Cohen, A. C.	University of Georgia
Couington, George F.	Picatinny Arsenal
Cousin, Thomas	BRL, Aberdeen Proving Ground, Md.
Cox, Paul C.	White Sands Missile Range, New Mexico
Curtis, William E.	Picatinny Arsenal
D'Andrea, Mark M.	US Army Material Research Agency
DeCicco, Henry	US Army Munitions Command
Dick, John S.	US Army
Dressel, F. G.	Army Research Office-Durham
Duff, James B.	Fort Belvoir
Dutoit, Eugene	Picatinny Arsenal
Dziobko, John	Picatinny Arsenal
Ehrenfeld, Sylvain	New York University
Eisenhart, Churchill	National Bureau of Standards
Fetters, William B.	Naval Propellant Plant, Indian Head, Md.
Fontana, W.	US Army Electronics Laboratory
Foohey, Sean P.	Research Analysis Corporation

LIST OF ATTENDEES (cont'd)

Foster, Walter D.
Futterer, Arnold T.
Galbraith, A. S.
Geshner, John A.
Groenewoud, Cornelius
Grubbs, Frank E.
Guenther, William C.
Gupta, Shanti S.
Hall, Charles A.
Hanson, Fred S.
Harris, Bernard
Harshbarger, Boyd
Hartley, H. O.
Hassell, Louis D.
Heacock, Frederick E.
Hecht, Edward C.
Helvig, T. N.
Howard, B. A.
Hunter, J. Stuart
Jacobus, David P.
James, Peter G.
Jenkins, Andrew H.
Jessup, Gordon L.
John, Frank J.
Kirby, William
Kocornik, Richard W.
Kolodny, Samuel
Krueger, Albert C.
Landerman, J.
Lavin, George I.
Lawrence, Myron C.
Lehnigk, Siegfried H.
Levy, Hugh B.
Little, Robert E.
Lucas, H. L.
Lum, Harry S.
Lum, Mary D.
Macy, Donald M.
Mandelson, Joseph
Mann, H. B.
Mannello, Edmund L.
Manthei, James H.
Fort Detrick
Edgewood Arsenal
Army Research Office-Durham
Picatinny Arsenal
Cornell Aeronautical Lab., Buffalo, N. Y.
BRL, Aberdeen Proving Ground
University of Wyoming
Purdue University
White Sands Missile Range
White Sands Missile Range
University of Wisconsin
Virginia Polytechnic Institute
Texas University
Picatinny Arsenal
LOH Field Office, St. Louis, Missouri
Picatinny Arsenal
Honeywell, Inc.
US Army Weapons Command
Princeton University
WRAIR
Bureau of Medicine, FDA
Redstone Arsenal
Fort Detrick
Watervliet Arsenal
BRL, Aberdeen Proving Ground
Picatinny Arsenal
Harry Diamond Labs.
Picatinny Arsenal
ONR
BRL, Aberdeen Proving Ground
USAF, Ops. Analysis Ofc., Wash., D.C.
Redstone Arsenal
Picatinny Arsenal
University of Michigan
North Carolina State University
Fort Detrick
Wright-Patterson Air Force Base
US Army Aviation Materiel Command
Edgewood Arsenal
University of Wisconsin, Math Res Center
Picatinny Arsenal
Edgewood Arsenal

LIST OF ATTENDEES (cont'd)

609

Margolin, Barry H.
Masaitis, Cesiovas
Mazzio, Vincent J.
McBroom, C. W. O.
McKeague, Robert L.
McLaughlen, G.
McLean, Robert A.
McMains, Forest
McMullen, W. C.
Miller
Miller, Morton
Mioduski, Robert
Moore, James R.
Mowchan, Walter
Nagorniy, George W.
Nelson, Harold
Nickel, J. A.
Olivieri, Peter G.
Orleans, B. S.
Osiecki, Charles H.
Palmer, J. D.
Parks, Albert
Parrish, Gene B.
Pell, William H.
Pliml, James R.
Provost, Robert G.
Revusky, Samuel H.
Riggs, Charles W.
Rinkel, Richard C.
Rose, Carol D. (Mr.)
Rosenthal, Arnold J.
Rosenblatt, Joan R.
Rothman, David
Rotkin, I.
Saboe, John C.
Sarakwash, Michael
Schlenker, George J.
Schmidt, Th. W.
Scholten, Roger W.
Selig, Seymour M.
Selman, Jerry H.

Fort Monmouth
Ballistic Research Laboratories
US Army Natick Laboratories
Walter Reed Hospital
USA Ammunition Procurement & Supply Agcy.
NRB
University of Tennessee
Picatinny Arsenal
Naval Supply, R&D
Picatinny Arsenal
Scherring RC
BRL, Aberdeen Proving Ground
BRL, Aberdeen Proving Ground
BRL, Aberdeen Proving Ground
Naval Base, Philadelphia, Pa.
Hercules Power Co.
University of Oklahoma
Nuc Rel Div, QAD, Dover, N.J.
BU Ships
Picatinny Arsenal
University of Oklahoma
Harry Diamond Laboratories
Army Research Office-Durham
National Science Foundation
LOH Field Office, St. Louis, Missouri
U. S. Army Missile Command
Fort Knox, Kentucky
Fort Detrick
Research Analysis Corporation
US Army Tank-Automotive Center
Celanese Corporation of America
National Bureau of Standards
Rocketdyne, A Division of NAA
Harry Diamond Laboratories
International Resist. Co.
Thickol Chemical Corporation
U. S. Army Weapons Command
Army Research Office-Durham
The Boeing Company
Office of Naval Research
U. S. Army Munitions Command

LIST OF ATTENDEES (cont'd)

Sloane, Harry S.
Slutter, Carl G.
Smoot, Perry R.
Solomon, Herbert
Somody, Edward V.
Starr, Selig
Strauch, R.
Tang, Douglas B.
Tilden, Donald A.
Tingey, H. B.
Uherka, David J.
Vick, James A.
Walner, Arthur W.
Webb, S. R.
Webster, Robert D.
Weinstein, Joseph
Weintraub, Gertrude
Wiesenfeld, Louis
Williams, Burton L.
Willoughby, Weldon
Youden, W. J.

Dugway Proving Ground
Picatinny Arsenal
AMRA, Watertown, Mass.
Stanford University
Aberdeen Proving Ground
Army Research Office-Washington
Vitro Laboratory
Walter Reed Army Institute of Research
Picatinny Arsenal
University of Delaware
U. S. Army Natick Laboratories
Edgewood Arsenal
US Naval Applied Science Laboratory
Rocketdyne, A Division of NAA
Picatinny Arsenal
Fort Monmouth
Picatinny Arsenal
Picatinny Arsenal
White Sands Missile Range
BRL, Aberdeen Proving Ground
George Washington University